Aus der
Klinik und Poliklinik für Psychiatrie und Psychotherapie
Klinik der Universität München
Direktor: Prof. Dr. Peter Falkai

The Serine/Threonine Kinase
Thousand and One Amino Acid Kinase 2 (TAOK2)
Regulates Hippo/YAP Signaling and Synaptic Activity

Dissertation
zum Erwerb des Doktorgrades der Medizin
an der Medizinischen Fakultät
der Ludwig-Maximilians-Universität zu München

vorgelegt von
Madalina Wernigg

aus
Suceava

Jahr
2025

Berichterstatter: PD Dr. Michael Wehr

Mitberichterstatter: Prof. Dr. Dr. Anna-Sophia Wahl

PD Dr. Swetlana Sirko

Mitbetreuung durch den
promovierten Mitarbeiter:

Dekan: Prof. Dr. med. Thomas Gudermann

Tag der mündlichen Prüfung: 23.01.2025

Table of contents

Abstract (German)

Psychiatrische Erkrankungen sind genetisch komplexe und stress-assoziierte Erkrankungen mit erheblichen gesellschaftlichen Auswirkungen, die bei genetischer Prädisposition durch Umweltfaktoren begünstigt werden und sich oft bereits im jungen Erwachsenenalter manifestieren. Es wird angenommen, dass psychisch beeinträchtigte Menschen genetische Mutationen aufweisen, die subtile Veränderungen in der Aktivität von Schlüsselsignalwegen verursachen. Im Gegenzug manifestieren sich diese Aktivitätsveränderungen der Signalwege durch klinische Symptome. Vor diesem Hintergrund werden psychiatrische Erkrankungen daher auch als Störungen von Signalwegen angesehen.

Auf neurobiologischer Ebene wird über die Integration von Stresssignalen eine Vielzahl von zellulären Signalkaskaden aktiviert, die zu krankheitsfördernden Veränderungen der neuronalen Plastizität und der synaptischen Übertragungsprozesse führen. Über die geregelte Aktivierung und Inaktivierung von Signalmolekülen, z.B. durch Phosphorylierung von Kinasen, können in Zellen unterschiedlichste Prozesse, wie die Differenzierung oder Proliferation von Zellen, vermittelt werden. Dadurch wird u.a. die neuronale Reifung und Ausbildung funktionaler Synapsen reguliert. Zu den Stress-assoziierten Signalwegen gehört auch der Hippo-Signalweg, der neben homöostatischen Zellstoffwechselprozessen das Aufrechterhalten zellulärer Polarität und die Dynamik des Aktin-Zytoskeletts kontrolliert. Der Hippo-Signalweg ist hauptsächlich als Tumorsuppressor-Weg bekannt, dessen Effektoren jedoch sowohl tumorsupprimierende als auch protoonkogene Funktionen vermitteln. Es wurde bisher gezeigt, dass der Hippo-Signalweg mit zahlreichen anderen Signalwegen interagiert, die mit verschiedenen neuropsychiatrischen und onkologischen Erkrankungen assoziiert wurden.

Die Serin/Threonin-Kinase Thousand And One Amino Acid Protein Kinase 2 (TAOK2) gehört neben TAOK1 und TAOK3 zur Familie der MAP-Kinase-Kinase-Kinasen (MAP3K) und wurde 2014 anhand von Daten aus der größten genomweiten Assoziationsstudie (genome-wide association study, GWAS) als Schizophrenie-Risikogen klassifiziert. Nachdem in bisherigen Studien eine Aktivierung des Hippo-Signalweges durch TAOK1 und TAOK3, jedoch nicht durch TAOK2 gezeigt wurde, liegt der Fokus dieser Arbeit auf den Regulationsmechanismus von TAOK2 in HEK293-Zellen und primären Neuronen.

Des Weiteren werden TAOK2-vermittelte Protein-Interaktionen, die vor dieser Arbeit in einem fokussierten Protein-Protein-Interaktionsscreen von potenziellen Modulatoren des Hippo-Signalweges identifiziert wurden, mittels biochemischer Methoden in HEK293 Zellen validiert. Dabei ist eine starke Interaktion zwischen TAOK2 und large tumor suppressor kinase 1 (LATS1) zu beobachten. In Zellen mit überexprimiertem TAOK2 wird eine verstärkte Phosphorylierung von LATS1 und Yes-associated protein 1 (YAP1) gezeigt. Ebenso werden Proteinmengen verschiedener Mitglieder des Hippo-Signalwegs zu unterschiedlichen Lysis-Zeitpunkten, unter nährstoffreichen bzw. nähr-stoffarmen Serumkonditionen sowie unter Stressinduktion durch Zugabe von 2-Deoxy-D-glucose untersucht.

In primären Neuronen wurde der Einfluss von TAOK2 auf die synaptische Aktivität mittels eines multiparametrischen Screenings (pathwayProfiler, Systasy Bioscience GmbH) untersucht und durch den E-SARE-Assay, einem Assay zur Bestimmung der synaptischen Aktivität, validiert. Neuronen mit TAOK2-knockdown weisen eine vermehrte Aktivität von synaptischen Sensoren auf, die mit dem MAPK/ERK1/2 Signalweg in Zusammenhang stehen und an der Regulation von neuronaler Aktivität und zellulärem Stress beteiligt sind.

Abstract (English)

Psychiatric disorders are genetically complex and stress-associated disorders with great impact on society. Their manifestation occurs during early adulthood in genetically predisposed individuals who are exposed to adverse environmental factors. Genetic mutations that are present in patients suffering from mental disorders are believed to cause subtle changes in the activity of key signaling pathways. In turn, these changes in pathway activity manifest as clinical symptoms. Therefore, psychiatric disorders are also viewed as pathway diseases, leading to pathogenic changes in synaptic transmission, neural plasticity, and the manifestation of disease symptoms.

Signaling molecules are activated or deactivated through phosphorylation or dephosphorylation and mediate pro- respectively anti-apoptotic processes regulating neural maturation and formation of functional synapses. A well investigated cellular stress pathway is the Hippo signaling pathway which modulates fundamental homeostatic cellular events such as the maintenance of cellular polarity and actin cytoskeleton dynamics. It is mainly known as a tumor suppressor pathway, mediating both tumor suppressor and proto-oncogenic functions. Previous research works have shown interactions between the Hippo signaling network and other pathways associated to neuro-psychiatric and oncologic diseases.

The serine/threonine kinase Thousand and One Amino Acid Protein Kinase 2 (TAOK2) belongs, as well as TAOK1 and TAOK3, to the TAOK family, a MAP-Kinase-Kinase-Kinase family (MAP3K) and was classified as a schizophrenia risk gene based on data from the 2014 large-scale genome-wide association study (GWAS). Previous studies showed an activation of the Hippo Pathway by TAOK1 and TAOK3, but not by TAOK2. This thesis investigates the regulatory mechanism of TAOK2 from a molecular and cell biological perspective in heterologous cells (e.g. HEK293) und primary neurons.

Further, TAOK2-mediated protein interactions previously identified in a focused protein-protein interaction screening of Hippo modulators were biochemically validated in HEK293 cells. In the process, a strong interaction between TAOK2 and large tumor suppressor kinase 1 (LATS1) was identified. Overexpression of TAOK2 led to increased phosphorylation of LATS1 and Yes-associated protein 1 (YAP1). Also, protein levels of several Hippo pathway components were investigated at different lysis timepoints, under serum stimulation respectively deprivation conditions as well as under 2-Deoxy-D-glucose-induced cellular stress.

In primary neurons, the influence of TAOK2 on synaptic activity was assessed by using a multiparametric assay (pathwayProfiler, Systasy Bioscience GmbH) which was then validated by an E-SARE assay, an assay to monitor synaptic activity signaling. The results showed a strong increase in synaptic activity in TAOK2 depleted cells, indicated by the enhanced activity of several sensors involved in MAPK/ERK1/2 signaling pathways, which are associated with neural activity and cellular stress.

List of figures

List of tables

List of abbreviations

4-AP	4-aminopyridine
AMOT	Angiomotin
AAV	adeno-associated virus
AP-1	activating protein 1
Arc	activity-regulated cytoskeleton associated protein
ASD	autism spectrum disorder
BD	bipolar disorder
BDNF	brain-derived neurotrophic factor
BIC	bicuculline
BME	Base Modified Eagle Medium
BMP2	Bone morphogenic protein 2
BRAF	proto-oncogene B-Raf
BSA	bovine serum albumin
CaMK	calmodulin kinase
CaRE	calcium response element
CCK-8	Cell Counting Kit-8
cDNA	complementary DNA
CMV	Cytomegalovirus
CNS	central nervous system
CNV	copy number variations
CREB	Ca^{2+}/ cAMP response element-binding protein
CTEV	C-terminal moiety of the TEV protease
CTGF	connective tissue growth factor
CYR61	cysteine-rich angiogenic protein 61
DISC1	disrupted in schizophrenia 1
DIV	day in vitro
DMEM	Dulbecco's Modified Eagle Medium

DMSO	dimethyl sulfoxide
DNA	deoxyribonucleic acid
DTT	Dithiothreitol
ECM	extracellular matrix
EDTA	ethylenediaminetetraacetic acid
EGFR	epidermal growth factor receptor
EGR1p	promotor of the Immediate Early Gene And Transcription Factor EGR1
EGTA	egtazic acid
EMT	epithelial mesenchymal transition
ERK	extracellular signal-regulated kinase
E-SARE	enhanced synaptic activity-responsive element
FBS	fetal bovine serum
Fluc	firefly luciferase
fMRI	functional magnetic resonance imaging
FOSBp	promotor of the FosB Proto-Oncogene
FOXO	fork-head transcription factors of the O class
GABA	γ-aminobutyric acid
GAD	glutamic acid decarboxylase
GPCR	G protein-coupled receptor
GTP	Guanosine triphosphate
GWAS	genome-wide association study
HBSS	Hanks' Balanced Salt Solution
HCl	hydrochloric acid
HEK	human embryonic kidney
HEPES	2-(4-(2-Hydroxyethyl)piperazin-1-yl)ethanesulphonic acid
HLH	helix-loop-helix
HRP	Horseradish peroxidase
Hsp	heat shock protein

HTS	high-throughput screening
IEG	immediate early genes
INF	interferon
IPSC	induced pluripotent stem cells
JNK	Jun amino-terminal kinases
KIBRA	kidney and brain expressed protein
LATS1/2	large tumor suppressor kinases 1/2
LDS	Lithium dodecyl sulfate
LTD	long-term depression
LTP	long-term potentiation
MAPK/MEK	mitogen-activated protein kinase
MAPKK	mitogen-activated protein kinase kinase
MAPKKK	mitogen-activated protein kinase kinase kinase
MEF2	myocyte enhancer factor 2
MHC	major histocompatibility complex
MLP	major late promoter
MMP-9	Matrix metalloproteinase-9
MOB1	Mats homolog 1
MOI	multiplicity of infection
mRNA	messenger RNA
MSK	mitogen- and stress-activated kinases
MST1/2	mammalian STE20-like 1/2
mTOR	mammalian/mechanistic target of rapamycin
NaCl	sodium chloride
NDMA	N-methyl-D-aspartate
NF2	Moesin-Ezrin-Radixin Like (MERLIN) Tumor Suppressor
NF-κB	nuclear factor kappa B
NGRN	Neurogranin

NO	nitric oxide
NR4Ap	promoter of the Nuclear Receptor Subfamily 4 Group A Member 1
NSC	neural stem cells
NTEV	N-terminal moiety of the TEV protease
OD	Optical density
PBS	phosphate buffered saline
PEI	polyethylenimine
PCP	phencyclidine
PCR	polymerase chain reaction
PDL	poly-D-lysine
PDZ	PSD-95/DLG/ZO-1
PFC	prefrontal cortex
PKC	protein kinase C
PLB	passive lysis buffer
PLL	poly-L-lysine
PPI	Protein–protein interactions
PV	parvalbumin
PVDF	polyvinylidine fluoride
qRT-PCR	quantitative real-time PCR
RAS	rat sarcoma
RNA	ribonucleic acid
RT	room temperature
RSK	ribosomal protein S6 kinases
SAPK	stress-activated protein kinases
SARAH	Salvador/Rassf/Hpo
SARE	synaptic activity-responsive element
SAV	Salvador
SDS	Sodium dodecyl sulfate

SEM	standard error of the mean
SEPT7	Septin-7
sgRNA	single guide RNA
shRNA	short hairpin RNA
SNP	single-nucleotide polymorphism
SNV	single-nucleotide variants
SRF	serum response factor
STE20	sterile 20 protein
STK3/4	Serine/Threonine Kinase 3/4
SST	somatostatin
SZ	schizophrenia
TAOK	Thousand and one kinase
TAZ	transcriptional coactivator with PDZ-binding motif
TBS	tris buffered saline
TBS-T	tris-buffered saline with tween20
TCF4	Transcription-factor 4
TEAD	TEA domain transcription factor
TEV	Tobacco Etch Virus
TNF	Tumor Necrosis Factor
TNIK	Traf2- and Nck-Interacting Kinase
VIP	vasoactive intestinal protein
WHO	World Health Organization
WPRE	Woodchuck hepatitis virus (WHV) posttranscriptional regulatory element
WWC1	WW domain-containing protein 1
YAP1	Yes-associated protein 1

1. Introduction

1.1 Understanding psychiatric disorders: From phenomenology to neurobiology

Modern psychiatry is a dynamic medical discipline aiming to combine clinical practice with insights from biological psychiatry research to find appropriate treatments for mental disorders. The World Health Organization (WHO) counts depression, bipolar disorder, dementia, autism and schizophrenia spectrum disorders among the most severe mental illnesses with significant social and economic impacts [1]. Despite several decades of intense research, the exact causes are mainly unknown and are best attributed to a mixture of genetic, psychosocial, and contextual factors. The complexity of mental disorders requires highly intertwined interdisciplinary approaches to translate clinical symptoms into neurobiological and genetical correlates. Furthermore, understanding basic mechanisms such as cellular stress responses can lead to a better predictability of psychiatric disorders and facilitate early prevention strategies.

Having a long tradition in German-speaking areas, the phenomenology of psychiatric disorders has been precisely described over the past century. In 1911, Swiss psychiatrist Eugen Bleuler established the term *schizophrenia* after observing a splitting of different psychological functions in psychotic patients [2]. However, the symptomatic level alone does not capture the severity of physical and psychological complaints presented by so many patients. Therefore, therapists and researchers are obliged to zoom in closer to better understand the underlying (patho-) physiological processes. Today, schizophrenia is classified as a highly heritable and polygenic disorder, associated with neurodevelopmental disorders like cognitive impairment and autism spectrum disorders[3].

1.1.1 Stress-induced changes in brain micro- and macro-architecture

Many of the major psychiatric diseases emerge in late adolescence and early adulthood, an especially vulnerable period in brain development [4]. Research works show that intense stress is a key contributor to the onset of psychotic and mood disorders, impairing the individual's resilience and compensatory mechanisms [5]. Given the complex interaction between genetic predisposition and environmental influences in psychiatric disorders, stress reshapes the brain through several subtle mechanisms and leads to micro- and macrostructural changes that can be observed in the long run.

The timing and recurrence of stress exposure across the lifespan leave their mark in particularly stress-susceptible brain areas including the prefrontal cortex (PFC), hippocampus and amygdala, contributing to the development of emotional and cognitive deficits [6–9]. Alterations in volume and function of these regions detected by fMRI studies indicated that large-scale structural modifications might be linked to molecular processes, which drives further investigation at a cytoarchitectural level [10,11]. In spite of limitations regarding the transferability of findings to human psychopathology, pre-clinical rodent models represent an important tool in examining essential brain functions and the contribution of specific stress effects to psychiatric-like phenotypes [5].

Several studies have shown impaired connectivity patterns especially in the PFC and the hippocampus, as these regions are rich in excitatory (glutamatergic) pyramidal neurons that indicate a loss of dendritic spines when exposed to chronic stress [12–15]. Evidence from clinical and postmortem human cohorts indicates that remodeling of excitatory circuits triggered by stress is a significant factor in the onset of depression [16,17], schizophrenia [18,19] and bipolar disorder [20]. Reductions in mature dendritic spines adversely affect the integrative functions of the PFC and the top-down regulation of other brain areas, which may contribute to common psychiatric symptoms like cognitive and emotional deficits [21]. Otherwise, the amygdala reacts with dendritic hypertrophy and therefore increased activity in response to corticosterone administration reflected by anxiety-like behavior in rats [22,23].

1.1.2   Influence of inhibitory neurons on the excitation-inhibition balance

Furthermore, experimental studies have demonstrated that stress significantly influences GABAergic neurons, leading to depression-like symptoms (e.g. anhedonia, decreased social interaction), behavioral and cognitive impairments [24]. These are categorized depending on the presence of distinct calcium binding proteins (e.g. parvalbumin [PV] and calbindin) and neuropeptides (e.g. vasoactive intestinal protein [VIP], neuropeptide Y and somatostatin [SST]) [25]. They create various micro-networks to diminish signal transmission across brain regions. In these networks, interneurons that express PV largely modulate suppression of adjacent interneurons and pyramidal cells.

Various studies have investigated the impact of modifications in the network of inhibitory interneurons on the excitation/inhibition imbalance in psychiatric disorders. On the one hand, cases of schizophrenia and major depression display a reduced number of inhibitory neurons and GABA synthesizing enzyme (GAD-67) [26–28]. On the other hand, evidence also supports the hypothesis of over-inhibition by the GABAergic system in the PFC, leading to hypoactivity of glutamatergic neurons which is associated with emotional and intellectual dysfunction [29]. Alterations in GABAergic neural circuits were identified as the only

consistent pattern in post-mortem analyses of patients with schizophrenia [30]. Spiny projection neurons, a distinct type of striatal GABA interneurons, were recently associated with schizophrenia, independently of cortical interneurons and glutamatergic pyramidal cells. This suggests cell-specific effects in the pathogenesis of schizophrenia [31,32].

Further, the cortical distribution of SST- and PV-expressing interneurons shows a negatively correlated spatial gradient with influence on the balance of inhibitory control. More precisely, the highest relative SST expression was identified in orbitofrontal and medial PFC, anterior insula and the temporal lobe, while PV-expressing interneurons displayed a posterior gradient in somato-motor, visual and parietal cortices [33]. Fast-spiking PV interneurons regulate the homeostasis of targeted pyramidal neurons and maintenance of gamma oscillation, an indicator for synaptic integrity which was found significantly deficient in schizophrenia [34,35]. The E/I balance shifts across different brain areas throughout different stages of brain development, especially during early-life or adolescence, and depends on stress timing as a particular important factor.

1.1.3 Synapse-to-Nucleus Signaling

Synaptic activity is coupled to nuclear signaling by a range of synapse-to-nucleus messengers, converting signals received at synapses into transcriptional activities that are crucial for cognitive, emotional and memory functions. Activated NMDA receptors (NMDARs) mediate calcium entry into dendritic spines and induce the transfer of several synaptic factors (e.g., NF-kB, CaMKII and ERK) to the nucleus [36] (**Fig. 1**). Malfunction of these factors is associated with neuropsychiatric disorders, leading to impaired synaptic plasticity, dendritic degeneration and excitotoxicity [37].

Stimulation and depolarization in glutamatergic neurons induce CaMKII-dependent, cyto-nuclear translocation of Calmodulin (CaM). In the nucleus, it regulates CREB-mediated gene transcription, a significant process for neuronal plasticity and learning in mice [38,39]. *CaMKII* mutations are linked to severe intellectual and episodic memory deficits in humans [40,41], while various CaMKII pathway genes (e.g. CREB, calcium channels) are linked to mental disorders such as depression, ASD and schizophrenia [42,43]. MAPK/ERK represents another glutamate-dependent mediator of excitation-transcription coupling, which is phosphorylated during long-term potentiation and activates the downstream transcriptional regulators Elk-1 and CREB [44]. This signaling pathway regulates a wide range of homeostatic and neurodegenerative mechanisms. For example, ERK1/2 facilitates tau phosphorylation induced by Amyloid-β, which accumulates in Alzheimer's disease [45,46] or induces neuroprotection as shown by an animal model of Huntington's disease [47]. Recent

studies link MAPK/ERK signaling to aberrant synaptic plasticity in mood and stress disorders including depression, bipolar disorder and addiction [48–50].
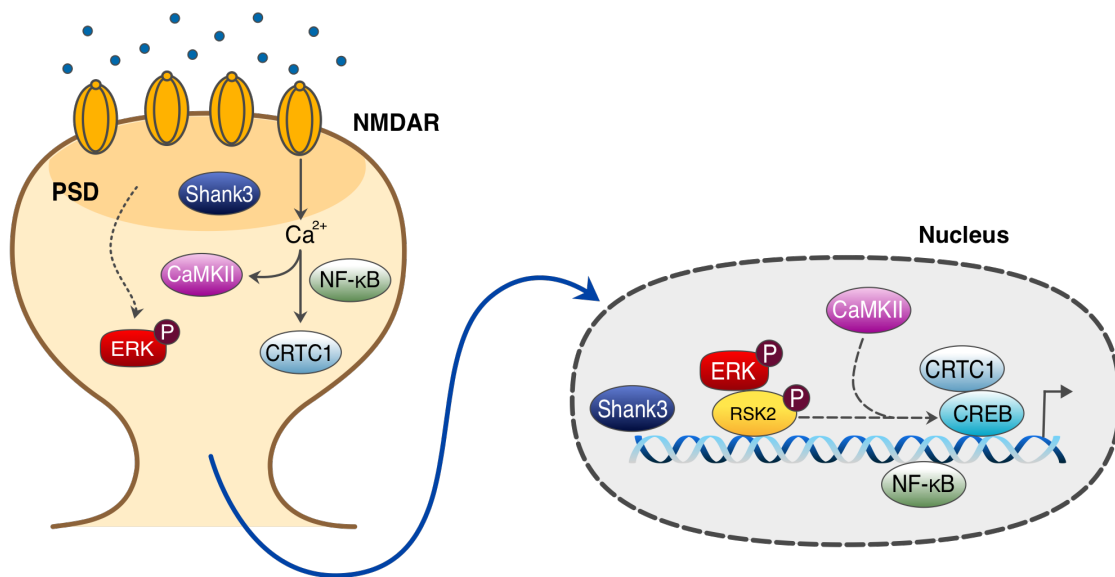
Fig. 1. Regulation of Synaptic Plasticity and Gene Expression through Synapse-to-Nucleus Signaling.

A multitude of synaptic elements, including ERK, CRTC1, NF-kB, Shank3 and CaMKII, are triggered by synaptic stimulation at apical dendrites. These elements then move to the nucleus to modulate CREB-mediated transcription. The illustration depicts the flow of signals from dendritic spines towards the nucleus, controlling gene expression. PSD, postsynaptic density region; NMDAR, N-methyl-D-aspartate receptor; ERK, extracellular signal-regulated kinase; P, phosphorylation; CREB, cAMP-response element binding protein; CRTC1, CREB- regulated transcription coactivator-1; NF-kB, nuclear factor kappa-light-chain-enhancer of activated B cells; Shank3, SH3 and multiple ankyrin repeat domains 3; CaMKII, calcium/calmodulin-dependent protein kinase II (adapted from Parra-Damas&Saura, 2019).

How do brain cells respond to stress at the molecular and cellular level? Increasing knowledge about the mechanisms that underlie stress responses will lay the foundation for identifying new therapeutic targets and preventive strategies. In the following, the central focus lies on signaling pathways activated by cellular stress signals and their importance for cell homeostasis and development of functional neural networks.

1.2   MAPK/ERK signaling: regulation of cellular growth, gene expression, and synaptic activity

The human genome contains over 500 protein kinases which contribute to the proper formation and functioning of the central nervous system [51]. They regulate cellular processes by transferring a phosphate group on multiple sites of their amino acid substrates (e. g. serine, threonine), thereby initiating signaling events with impact on cell migration, axon guidance, synaptogenesis and plasticity [51–54].

Mitogen-activated protein kinases (MAPK) are key components within a strongly interconnected network of signaling molecules which integrate and transduce stimuli from cell surface to the nucleus, allowing the cells to adapt to environmental changes [55]. Eukaryotic cells contain three major branches of MAPKs: ERK 1/2, JNK and p38 MAPK (**Fig. 2B**). While ERK is activated by growth-related extracellular stimuli (e.g. serum, nerve growth factor, hormones), the other two members, JNK and p38 MAPK, are triggered by various environmental and cellular stress signals such as ultraviolet radiation, inflammatory cytokines, osmotic shock and NO [56]. MAP Kinases are organized in a canonical module of three kinases, starting with the activation of a MAPKKK (e.g., Raf) in response to intra- and extracellular signals detected by G-protein-coupled-receptors (GPCRs) and receptor tyrosine kinases (RTKs), e. g. epidermal growth factor receptor (EGFR) [57,58]. In the following, a MAPKK (e.g., MEK) is activated through phosphorylation and in turn phosphorylates and activates a MAPK (e.g., ERK) [59] (**Fig. 2A**). This MAPKKK-MAPKK-MAPK cascade translates extracellular stimuli into cellular responses and affects gene expression through phosphorylation of transcription factors, thereby regulating cellular growth, proliferation, differentiation, and apoptosis.

The ability of cells to adequately respond to environmental or internal stress is crucial for maintaining cell homeostasis and is therefore regulated by evolutionarily highly conserved responses. Exposure of cells to heat and oxidative stress, toxic substances and glucose deprivation leads to a variety of responses ranging from activating survival pathways to inducing programmed cell death in strongly damaged cells [60]. Heat, for example, leads to induction of heat shock proteins (Hsp 27, Hsp 70) which prevent premature aggregation of unfolded proteins inhibiting apoptosis and promoting cell survival [61]. Further, oxidative stress or DNA lesions activate pro-apoptotic molecules (e.g. NF-κB, p53, JNK, or MAPK/ERK) that can initiate cell death pathways [60].

A
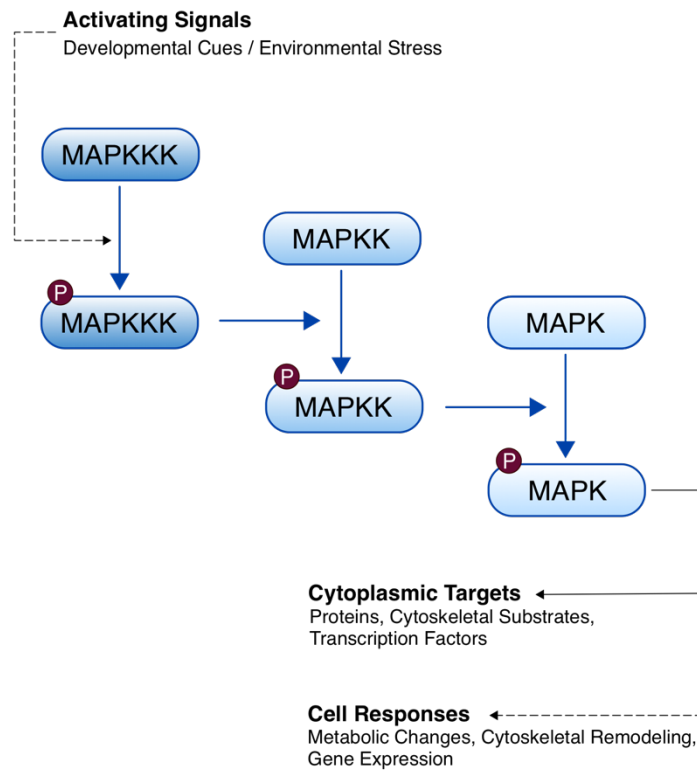
B
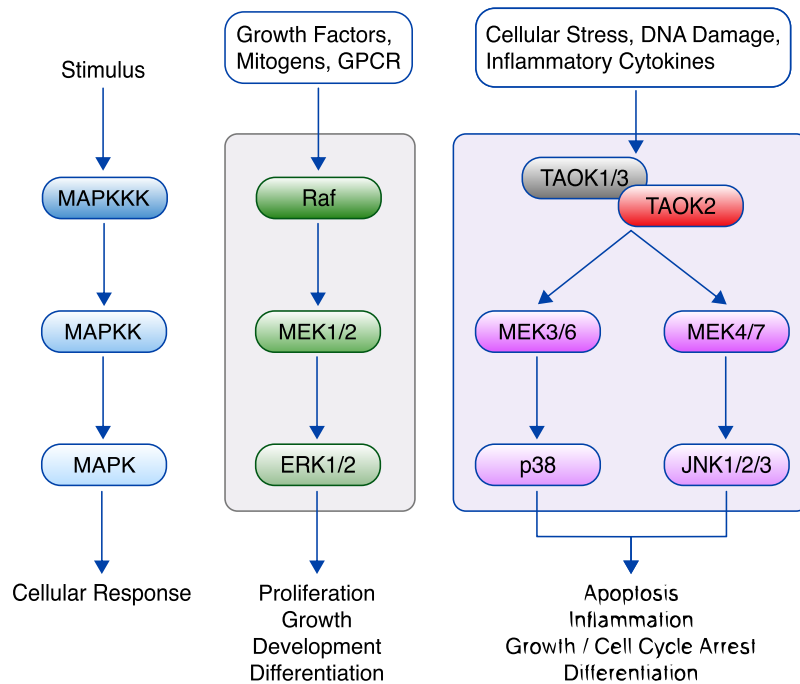
Fig. 2. The MAP Kinase Cascade.

(**A**) Schematic representation of the MAPK cascade. (**B**) The three major branches of MAPK cascades with the effectors ERK1/2, p38 and JNK1/2/3 (adapted from Jagodzik et al., 2018). GPCR: G-Protein-Coupled Receptor

Being an extensively studied signaling pathway, MAP Kinases (especially ERK1/2 and p38) are implicated in numerous health-disease activities related to the central nervous system, including cognitive and anxiety-related functions, addiction behavior, neurotoxicity, neurodegeneration, and integrating synaptic activity signaling in general [62].

ERK1/2 are known to control proliferation and differentiation in several cell types, but interestingly, they also display high expression in mature and terminally differentiated neurons [63]. Further evidence pointed to neuronal ERK1/2 activation prompted by excitatory glutamatergic stimulation, which in turn phosphorylate targets such as ribosomal protein S6 kinases (RSKs) and mitogen- and stress-activated kinases (MSKs), then translocating to the nucleus. Activated ERK1/2 and their substrates phosphorylate nuclear transcription factors, e. g. CREB, thereby mediating synaptic plasticity and neuronal function [63]. Studies have shown that p38 promotes long-term depression (LTD) by regulating glutamate neurotransmission at post-synaptic neurons, downstream of NMDA glutamate receptors. Elevated glutamate levels lead to excitotoxicity, a complex phenomenon mediated by calcium- and Rho GTPase- mediated activation of p38, promoting cell death in neuron cultures.

Another modulator of glutamatergic signaling and cognitive processes is the Traf2- and Nck-Interacting Kinase (TNIK), a MAP4K and member of the sterile 20 (Ste20)-like kinase family. It shows a high expression at the postsynaptic density throughout the adult mouse brain [64–66]. Mice lacking TNIK have exhibited cognitive impairments and synaptic alterations [67]. Furthermore, TNIK has been linked to mental illnesses such as bipolar disorder and schizophrenia [68].

Despite substantial progress in comprehending the role of kinases in this field, further research regarding the influence of related upstream and downstream signaling pathways is needed.

1.3 Thousand-and-one-amino-acid (TAO) kinases

1.3.1 Biology, structure and function

Thousand-and-one-amino-acid (TAO) kinases are mammalian orthologs of the Ste20-kinase of Saccharomyces cerevisiae, which mediates between a heterotrimeric G Protein and the MAPK cascade of the yeast pheromone response pathway [69,70]. Three members of this family, TAOK1, TAOK2, and TAOK3 exist in mammals (**Fig. 3**). The name "thousand and one" comes from the first kinase identified in the rat, TAOK1, comprising 1001 amino acids transcribed by the *TAOK1* gene [71]. In humans, the *TAOK1* gene is situated on chromosome 17p at position 11.2. Its similar counterparts, *TAOK2* and *TAOK3,* are located on 16p11.2 and 12q24.23, respectively. Interestingly, microduplication of the chromosomal locus 16p11.2 is associated with a 14.5-fold increased risk of developing schizophrenia [72], while both microduplication and microdeletion of this region have been strongly linked to autism spectrum disorders [73–75]. TAO kinases are serine/threonine-protein kinases with an N-terminal kinase domain and a serine rich domain, being expressed throughout most tissues, especially in the brain and testes [76,77]. Their highly conserved protein structure include a catalytic domain, a central domain, and a regulatory domain, each gene having two isoforms (except TAOK2 with three isoforms) with different biological functions [78].

Fig. 3. Schematic structure of TAO kinases 1/2/3.

TAO kinases 1/2/3 are highly conserved in humans and consist of a catalytic domain, a central domain, and a regulatory domain. Each gene has two isoforms (α and β, except TAO2 with an additional γ isoform) with different lengths between 853 and 1235 amino acids (adapted from Hu et al., 2021).

TAO kinases (TAOKs) play a pivotal role in physiological regulation processes, signal transduction, protein-protein interaction and pathogenesis of cancer, neurodegenerative and inflammatory diseases [79]. Acting as MAPKKKs, TAOKs activate the p38 MAPK, the Stress-activated protein kinases (SAPK)/Jun amino-terminal kinases (JNK) cascades and the Hippo Signaling pathway as a reaction to harmful stimuli and DNA impairment [59,80–82]. Previous studies showed an activation of Hippo Pathway components by TAO kinases [83,84], a subject discussed in detail in chapter **1.5**.

1.3.2 TAOK2 as a regulator of synaptic plasticity and neural excitability

The serine-threonine kinase TAOK2 is among the 29 protein-coding genes situated in the 16p11.2 genomic region, which is linked to various neurodevelopmental and psychiatric conditions [85]. It is localized to dendritic spines and promotes their maturation by binding to *Septin-7* (SEPT7)[85]. Dendritic spines are tiny extensions from neuronal dendrites serving as postsynaptic locations for the majority of excitatory synapses in the brains of mammals [86]. Their morphology is highly dynamic and can be described in four groups: stubby (without a visible neck), thin (long neck, small and bulbous head), mushroom-shaped and filopodial in early development stages [87,88].

Dendrite plasticity is modulated by synaptic activity, providing the basis for key learning mechanisms, such as long-term potentiation (LTP) and long-term depression (LTD), through calcium compartmentalization [89–92]. Phosphorylated SEPT7 is found in the spine, where it supports the scaffolding protein *Postsynaptic Density Protein 95* (PSD95). Subsequently, PSD95 associates with glutamate receptors and cell adhesion molecules to create functional synapses [85,93]. Earlier reports showed that TAOK2 is crucial for dendrite morphogenesis by regulating membrane and cytoskeleton dynamics [94]. TAOK2 function regulates dendritic filopodia and excitatory synapse structure. Loss of TAOK2 function leads to a substantial reduction in mature, mushroom-like spines and to an increase in synaptic spines with thin, immature filopodial protrusions [54,85,95,96]. According to Yadav et al., neurons with impaired TAOK2 function developed synapses along the dendritic shaft instead of being located on dendritic protrusions [85]. Another essential function attributed to dendritic spines, calcium compartmentalization, was also impaired due to synaptic mislocation and led to a defective NDMA receptor-mediated calcium signaling. To better understand how TAOK2 modulates synaptic plasticity, protein-protein interaction studies between TAOK2 and proteins of the postsynaptic density need to be further analyzed.

1.3.3 Clinical relevance and implications for schizophrenia as a risk gene

As a genetically complex disorder, schizophrenia can be caused the accumulation of multiple single nucleotide polymorphisms (SNPs), which are common, but have a small effect, or by copy number variations (CNVs), which occur rarely, but have a large effect [97]. TAOK2 is associated with SZ both thorugh SNPs and the CNV 16p11.2. Due to its genetic association with CNV 16p11.2 and the implication into the regulation of synptic activity, TAOK2 represents an interesting research target on the path to better understand the genetic architecture of schizophrenia (**Fig. 4**). Alterations in the form of deletions and duplications within the multigenic 16p11.2 copy number variant (CNV) region have been connected to a range of brain-related conditions such as intellectual disability, bipolar disorder, schizophrenia, autism spectrum disorder (ASD) and obesity [98–100].
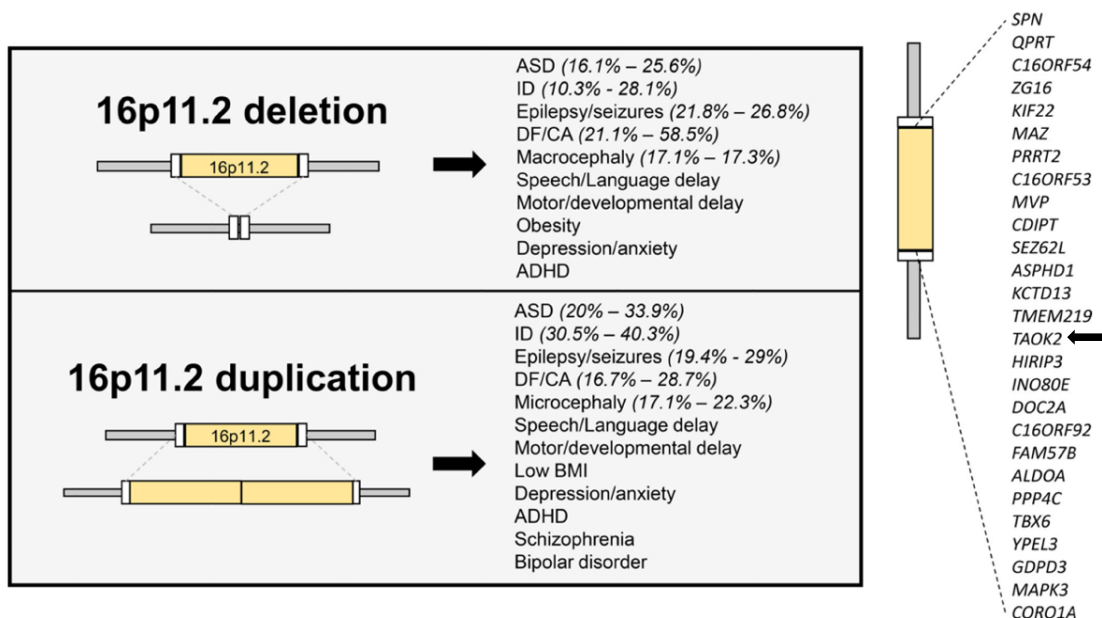
Fig. 4. Typical characteristics in individuals with 16p11.2 copy number variations (CNVs).

Individuals with duplications or deletions in the 16p11.2 region face a significantly increased risk of intellectual disability (ID), autism spectrum disorder (ASD), epilepsy/ seizures, and dysmorphic features/congenital anomalies (DF/CA) with a high degree of penetrance. The numbers in parentheses represent the variability in penetrance reported across cohorts of patients with 16p11.2 CNVs. Inset: List of genes situated in the human 16p11.2 region (Rein et al., 2020).

Numerous genetic epidemiological twin and family studies have well established a contribution of genetic factors to the development of schizophrenia, indicating an estimated heritability of approximately 80-85% [101,102]. The complex and polygenic nature of schizophrenia requires large-scale international collaboration to collect samples of sufficiently high power and enable further genomic discoveries.

Earlier landmark discoveries of recurring mutations in the major histocompatibility complex (MHC) and markers in *NRGN* (Neurogranin) and *TCF4* (Transcription-factor 4) pointed out impaired brain development and cognition as relevant pathophysiologic processes [103]. In 2014, a comprehensive genome-wide association study (GWAS) classified 108 distinct loci linked to schizophrenia [104]. Genotype data from 36.989 cases und 113.075 controls were analyzed and provided ground-breaking insights into associations between enriched gene expression and disease-relevant factors such as the immune system, glutamatergic transmission, and synaptic plasticity. Owen et al. identified genetic loci that exhibit high pleiotropy, featuring common alleles with minor individual effects but significant collective impact, involving hundreds of such loci [105]. Additional research on rare mutations, such as copy number variants (CNVs) and single-nucleotide variants (SNVs), has highlighted genes that produce a wide array of synaptic proteins. These are either located at the post-synaptic density or are members of the voltage-gated calcium channel protein family.

The latest two-stage GWAS from 2022, including up to 76.755 individuals with schizophrenia and 243.649 control participants, identified associations with common variants at 287 separate genomic locations. This study is the most extensive GWAS conducted on schizophrenia to date [106]. Based on the GWAS-derived data, it appears that many schizophrenia risk genes can be attributed to elements that play a crucial role in synaptic plasticity. Notably, schizophrenia relevant SNPs are associated with the *TAOK2* gene, making it a schizophrenia risk gene [106]. Decreased activity of TAOK2 during neural development is linked to dendritic spine abnormalities [85] as well as autism-related cognitive, emotional and social impairments [107]. The central focus of this thesis lies on the function of TAOK2 and its interactions with the Hippo signaling pathway, a pathway with growing evidence to impact on neurobiological functions including memory formation and psychiatric disorders [108,109].

1.4   The Hippo signaling pathway

The Hippo pathway is a highly conserved signaling network with over 30 components. It was originally identified in *Drosophila melanogaster* as a crucial regulator of tissue development. In the past two decades, a multitude of studies investigated the role of Hippo signaling components in tumorigenesis and cancer development, given their dynamic tumor suppressor and proto-oncogenic functions [110]. Major functions of the pathway are modulation of cell proliferation, differentiation and migration during organ morphogenesis as well as restriction of tissue growth in adults [111–113]. Screenings of loss-of-function variants in Hippo pathway kinase genes showed that gene inactivation leads to massive tissue overgrowth in developing wings and eyes [114]. The functional outputs are mediated by the main effectors and transcriptional co-activators YAP1 and TAZ (also WWTR1), which act as oncogenes when Hippo pathway is dysregulated [110].

1.4.1   The core kinase cassette

The signaling cascade comprises **a module of four kinases** with tumor suppressor properties named after *hpo*, a gene mutation that, if inactivated, leads to "hippopotamus-like" overgrown eyes in *Drosophila* [115,116]. The central components of the Hippo pathway include the mammalian Hpo orthologs Serine/Threonine Kinases 3/4 (**STK3** and **STK4,** also known as MST1 and MST2), which interact with the adapter protein Salvador homolog 1 (SAV1) (**Fig. 5**). These phosphorylate and stimulate large tumor suppressor kinases 1 and 2 (**LATS1** and **LATS2)**, which are scaffolded by the protein MOB1 and subsequently phosphorylate and inactivate Yes-associated protein 1 (YAP1) and TAZ [111]. YAP1 and TAZ are stringently controlled by Hippo pathway activity and dynamically translocate from the nucleus to the cytoplasm [115,117]. In operational mode, the activated LATS kinases phosphorylate YAP1/TAZ, leading to cytoplasmic retention and degradation. Consequently, YAP1 is unable to migrate to the nucleus and associate with its transcriptional coactivator TEAD, resulting in the loss of its transcriptional activity. When Hippo pathway is dormant, YAP1/TAZ stay dephosphorylated and gather in the nucleus. There, they interact with TEAD family transcription factors and other genes that promote growth, such as CTGF or CYR61 [115,118,119]. Together, the anti-apoptotic YAP1/TEAD complex stimulate cell survival and proliferation. Increases in YAP1 activity are also associated with cancer development in several organs such as skin, liver and intestine [120–122].
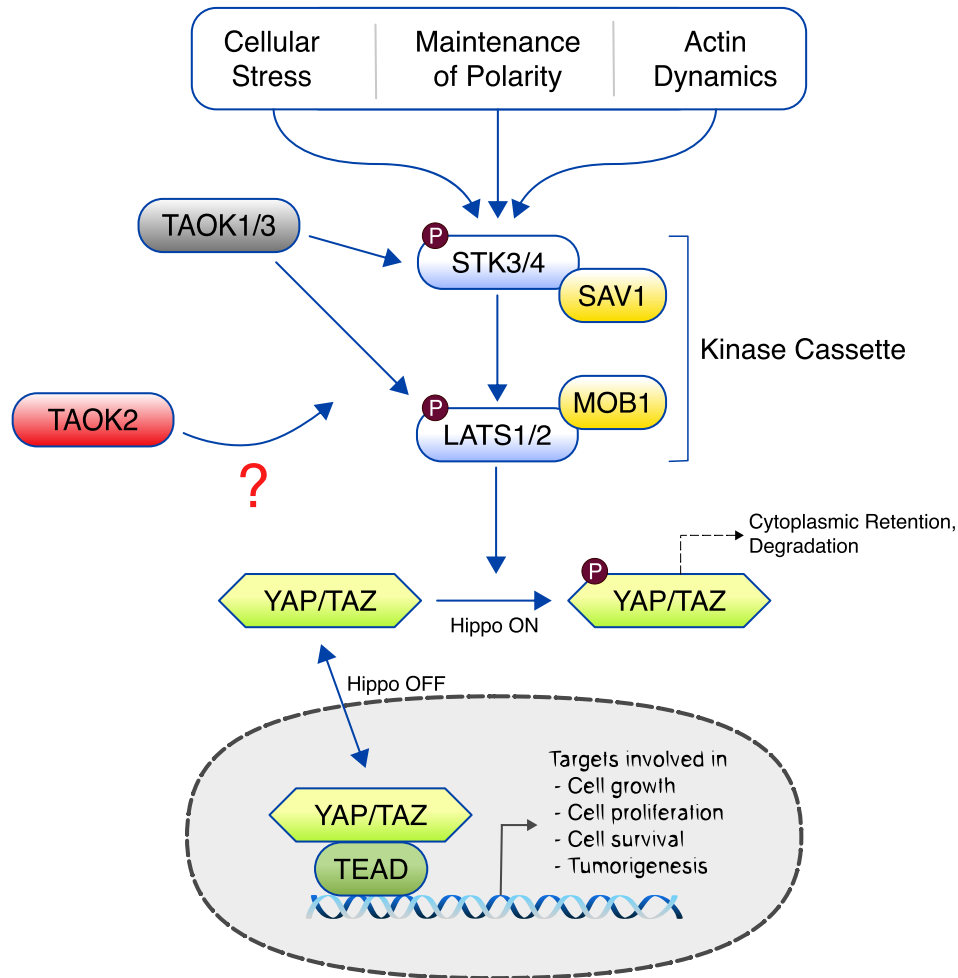
Fig. 5. Schematic representation of the Hippo Signaling Pathway.

The mammalian Hippo signaling pathway primarily regulates the movement of YAP1/TAZ between cytoplasm and nucleus. Pathway activation leads to LATS kinases phosphorylating YAP1/TAZ, which then leads to their retention in the cytoplasm and subsequent degradation. Conversely, in the inactive state, YAP1/TAZ do not get phosphorylated and move to the nucleus. There, complexes with TEADs and additional transcription factors are formed to initiate gene transcription. Nonetheless, the functioning of the Hippo pathway is not strictly binary (ON or OFF). The localization of YAP1 may vary between the cytoplasm and nucleus, contingent upon the relative phosphorylation activity of LATS1/2 kinases on YAP1 (adapted from Ma et. al, 2019).

1.4.2 Upstream signals, mechanotransduction and control of the downstream key mediators YAP1/TAZ

Cell organization in multicellular organisms depends on precisely orchestrated regulatory mechanisms that control tissue development and organ size. Cell fate and behavior are strongly determined by physical and mechanical contacts with surrounding cells and their extracellular matrix [123]. Mechanotransduction starts with the ability of cells to integrate mechanical forces through integrin adhesion complexes and actin cytoskeleton dynamics in order to adjust their tensional homeostasis and modulate physiological cell processes by transducing sensory signals into cellular signaling events [115,116,123].

Rho GTPases are pivotal in detecting alterations in cellular geometry and regulating YAP1/TAZ transcriptional activities through Hippo signaling (**Fig. 6**). Under mechanical stress, STK3/4 and LATS1/2 function is modulated by polarity and adhesive proteins such as Kibra/WWC1, NF2, adherens junctions, and tight junctions [115,124,125]. STK3/4 and LATS1/2 can be directly phosphorylated and activated by TAO kinases and inhibit YAP1/TAZ in parallel [83,84,126]. YAP1/TAZ activity is directly controlled by proteins with influence on cell polarity [127–129], growth factors and hormones acting through several GPCRs [111,118,130] as well as the rigidity of the extracellular matrix (ECM) [115,123]. YAP1/TAZ activity can be regulated in LATS1/2-dependent and independent ways. For example, the junctional adaptor protein Angiomotin (AMOT) inhibits YAP1/TAZ through direct binding and cytoplasmic sequestration. AMOT also stimulates LATS1/2 kinase activity by complexing with and activating NF2, consequently leading to the phosphorylation and inhibition of YAP1/TAZ [115]. YAP1/TAZ are reported to regulate trascription of genes which are particularly involved in matrix remodeling and actin cytoskeleton reorganization.

The exact process by which various mechanical signals regulate YAP1/TAZ remains partially unclear. As main Hippo pathway downstream effectors, YAZ1/TAZ collaborate with several transcription factors, such as DNA binding TEA domain (TEAD) family proteins, p73, ERBB4, and connective tissue growth factor (CTGF). This interaction facilitates the promotion of gene expression, cellular growth, and epithelial mesenchymal transition (EMT) [131–135]. TEADs were cassified as the most relevant YAP1 interacting proteins. Together, they drive the transcription of growth promoting target genes like CTGF and CYR61 [135]. Under osmotic stress, TEADs also associate with p38 MAP kinase and translocate to the cytoplasm, leading to YAP1/TAZ inactivation [136].

Against this background, numerous chemical compounds have been developed for thera-
peutic purposes. Verteporfin, for example, is a small molecule that inhibits the interaction
between YAP1 and TEADs, being used for treating neovascular macular degeneration [137].
Other novel YAP inhibitors with similar properties and potential antitumor drugs are CA3
[138] and narciclasine [139].
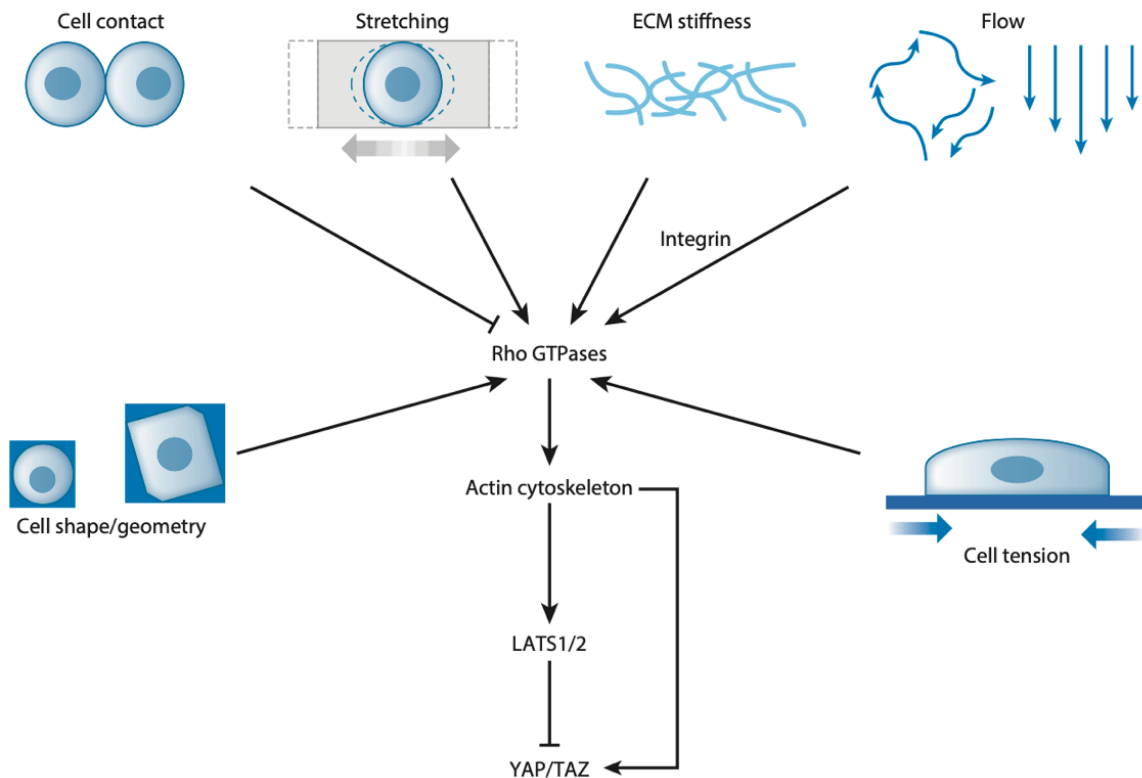
**Fig. 6. Mechanotransduction and regulation of YAP1/TAZ via Rho GTPase and the Hippo
pathway.**

Cellular interaction, tension, extracellular matrix (ECM) stiffness, and changes in cell geometry regulate
activity of Rho GTPases, leading in turn to actin cytoskeleton remodeling. This cytoskeletal rearrangement
can regulate the cytoplasmic-nuclear movement and YAP1/TAZ transcriptional activity via mechanisms both
dependent and independent of LATS1/2 (adapted from Ma et al., 2019).

1.4.3 Hippo signaling and the nervous system

Hippo pathway contributes to maintaining the complex balance between several process-
es in the nervous system, such as the development of nerve cells and their connections
as well as the regulation of their number and distribution [140]. During embryonic brain de-
velopment, neural stem cells (NSCs) are capable of self-renewal and can differentiate into
neurons, glial cells and astrocytes [141]. Differentiation and proliferation of NSCs are regu-
lated by many pathways, e.g., Wnt/β-catenin, Sonic Hedgehog and Notch pathways [142],
but also by increased *YAP1/TEAD1* transcription [143]. YAP1/TEAD1 promote progression

of the cell cycle by inducing Cyclin D1 and inhibit differentiation of NSCs by suppressing the expression of neurogenic b-HLH factor (NeuroM). However, an inhibition of YAP1/TEAD1 can lead to apoptosis of NSCs [144].

With regard to the role of Hippo signaling in synaptic development, *Yap1* conditional knockout mice exhibited impairments in dendritic morphology such as reduced dendritic length, dendritic tree width, and number of dendritic branching points [145]. Central Hippo pathway elements (STK3 and STK4, SAV1, LATS1 and LATS2) are highly expressed in almost every cell type in the brain, including neurons, astrocytes, oligodendrocytes, glia, and endothelial cells. In contrast, YAP1 showed high expression patterns solely in endothelial cells and astrocytes, while displaying reduced expression in neurons and other cell types. Interestingly, TAZ expression is not consistent with YAP1, as it is prominently expressed across all the mentioned cell types. This suggests different functions of YAP1 and TAZ in distinct cells of the nervous system [109]. Murine YAP1 was shown to contribute to neocortical differentiation and proliferation of astrocytes during cerebral development. *Yap1* knockout resulted in a decreased count of neocortical astrocytes and impaired proliferation via the BMP2-YAP1-SMAD1 pathway [146].

Further, STK4 can be activated by oxidative stress and then promotes either YAP1-dependent or YAP1-independent apoptosis via regulating the phosphorylation and nuclear translocation of FOXO transcription factors [122,147,148]. STK4 also activates NFκB/MMP-9 signaling in the context of subarachnoid, causing blood-brain-barrier disruption and promoting inflammation by activating microglia [149]. In general, Hippo signaling is pivotal for neurogenesis by modulating essential cellular mechanisms needed for the appropriate development of the CNS and its physiological conditions [140].

1.4.4 Clinical implications

1.4.4.1 Hippo pathway as a modulator of cellular and immune homeostasis

Hippo pathway components have been identified as modulators of immune functions. Research has demonstrated that STK4 mutations result in immune deficiency in humans and mice, characterized by a decline in naïve T cells, regardless of Hippo pathway mediated regulation of YAP1/TAZ [150–152]. Further experiments in mouse xenograft models showed a rather unexpected role of Hippo pathway in tumor cell immunity. Loss of LATS1/2 in tumor cells lead to increased anti-tumor immune responses by IFN (interferon) stimulation and consequent T cell activation, leading to the apparently paradoxical conclusion that inactivation of the "tumor suppressor" kinases LATS1/2 increases tumor immunogenicity and therefore enhances the tumor vaccine efficacy [153,154]. Notably, inactivation of LATS1/2 and

subsequently increased YAP1/TAZ activity are required to drive cell proliferation in wound healing and tissue regeneration [150]. This has been shown in liver recovery after partial hepatectomy in rat models [155–157], in lung regeneration after pneumectomy in mice [158–161], and in cardiac regeneration [162–164]. Elevated expression levels of YAP1/TAZ in cancers was shown to increase chemotherapy resistance and to treatments aimed at promoting genetic alterations in EGFR, BRAF and RAS [150,165]. Further, YAP1/TAZ also mediates changes in cellular metabolism that contribute to metastasis (e.g., cell cycle, migration, anchorage-independent growth, invasion) [136].

1.4.4.2 Implications of Hippo signaling for neuropsychiatric disorders

Recent studies report interactions between the Hippo signaling network and other pathways associated to various psychiatric and neurologic conditions such as bipolar disorder (BD), schizophrenia (SZ), Alzheimer's disease, glioma proliferation, amyotrophic lateral sclerosis (ALS) and Huntington's disease [122,166–170]. Main molecular and cellular processes that are thought to be involved in the pathophysiology of stress-related neuropsychiatric conditions are modulated by Hippo pathway members. While inhibition of Hippo increases tumorigenesis, activation of the pathway may be implicated in neuronal degeneration by mediating neuronal apoptosis induced by oxidative stress [171].

Genetic studies, among them a genome-wide association study [175], indicate an association between the KIBRA (KIdney and BRAin) gene with episodic memory performance, grey and white matter volume and functional brain activity [171]. Liu and colleagues identified an upregulation and significant enrichment of Hippo pathway genes with a high degree of connectivity in the PPI network, including YAP1, in post-mortem prefrontal cortex of people with BD compared to healthy controls [170]. The authors suggest that the activity of the Hippo pathway could be significant in the pathophysiology of BD, providing a source of new potential therapeutic targets.

1.5 Targeted Interaction Screen of Hippo Pathway modulators using a protein-protein interaction assay based on the split TEV technique

Prior to this work, a focused interaction screen was performed by our group to uncover novel connections between central Hippo pathway members and crucial regulatory proteins (**Fig. 7**)[176]. The split TEV technique, which relies on complementation of TEV protease, was utilized in living cells to quantitatively measure Hippo pathway protein-protein interactions [177]. While confirming previously reported associations among tested components, especially within members of the Hippo kinases and proteins that regulate cell polarity [178–181], novel interactions between TAOK2 and LATS kinases were identified. Within the TAOK family, previous studies have demonstrated that TAOK1 and TAOK3 directly interact with and phosphorylate LATS1/2 and STK3/4, while TAOK2 does not exhibit this interaction [83,84,126]. However, the impact of TAOK2 on the Hippo pathway has never been directly shown. TAOK2 has been associated to Hippo signaling due to its decreased expression in diverse cancer types [182], suggesting that it may regulate YAP1 phosphorylation states and transcriptional activity, cell growth, and cell proliferation, making TAOK2 also an interesting pharmacological target in the treatment of human cancer. Based on this hypothesis, further experiments were conducted in this work to work to elucidate the molecular mechanisms which drive phosphorylation of downstream effectors LATS1/2 and YAP1.
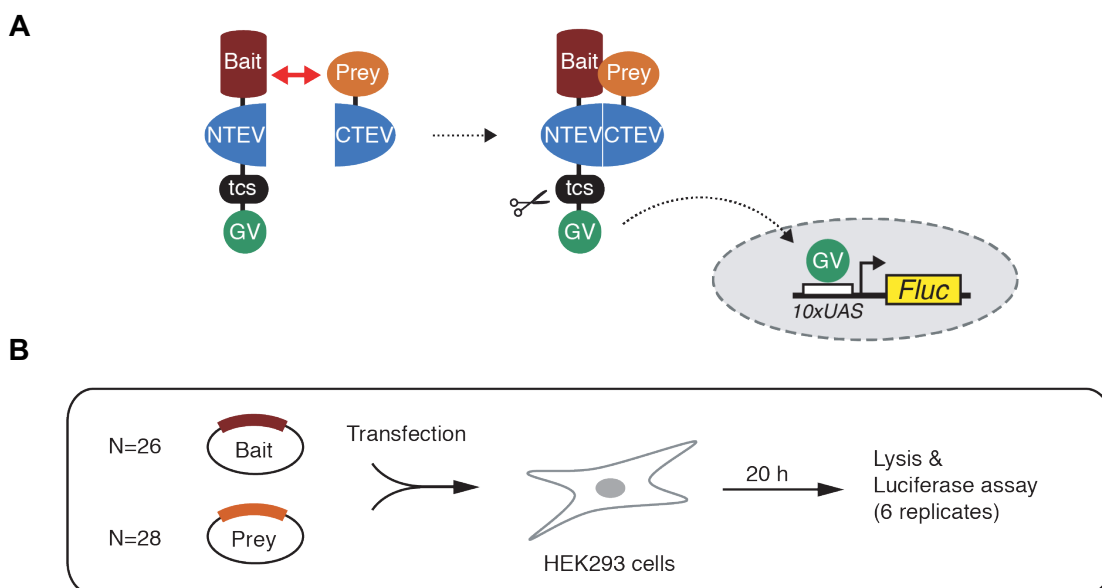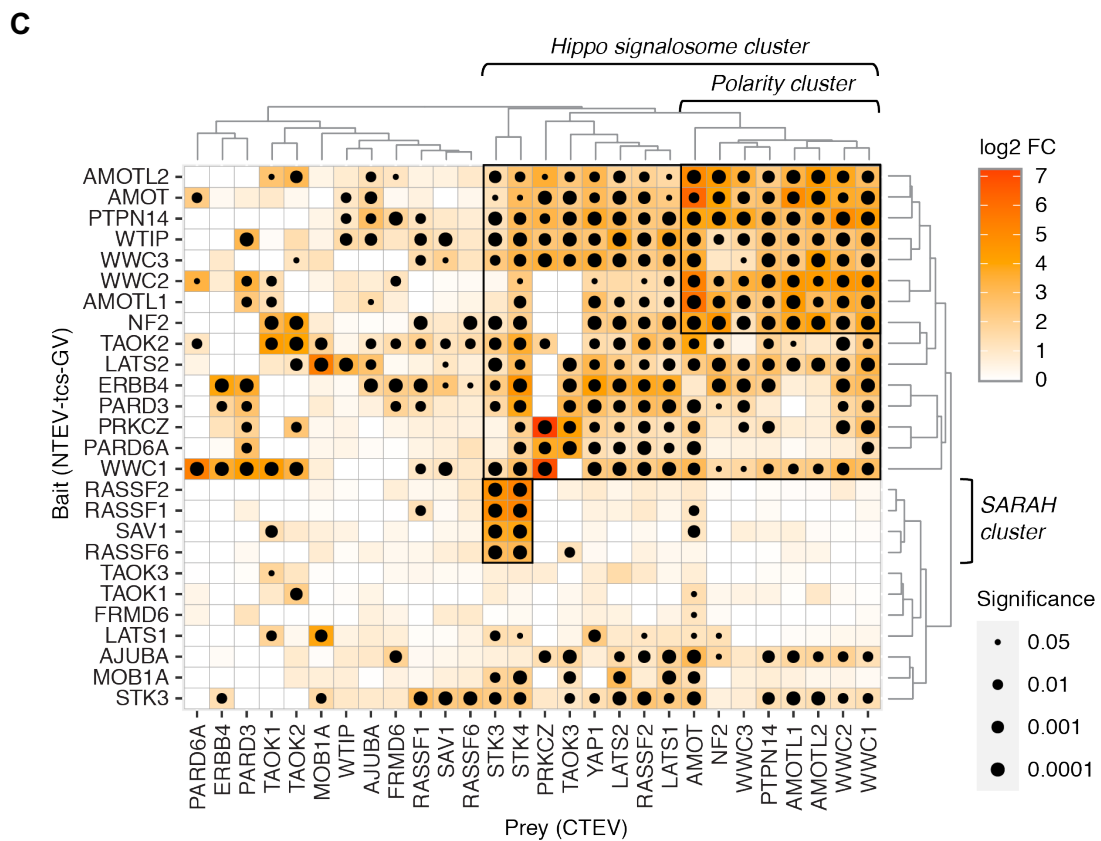
Fig. 7. A targeted protein-protein interaction assay using the split TEV technique reveals previously undiscovered interactions among Hippo pathway components.

(**A**) The split TEV protein-protein interaction assay is based on the following principle: Bait prospects are attached to the N-terminal portion of the TEV protease (NTEV), a TEV protease cleavage site (tcs), and the synthetic co-transcriptional transactivator GAL4-VP16 (GV). The prey proteins are linked to the C-terminal TEV moiety (CTEV). When a bait and a prey protein form a complex, the TEV protease regains functionality, leading to the detachment of GV. The released GV enters the nucleus, where it activates transcription of a firefly luciferase (Fluc) gene by attaching to upstream activating sequences (UAS). (**B**) During the targeted split TEV interaction assay, 26 bait proteins were evaluated versus 28 prey proteins. (**C**) Heatmap displaying orderly structured protein-protein interactions among Hippo pathway components tracked using split TEV. Grouping indicates three primary groups within the Hippo pathway, a cluster comprising polarity proteins, the Hippo signalosome cluster encompassing both core kinases and polarity proteins, and a cluster for the SA-RAH interaction domain. Interactions are depicted as log2-scaled fold changes compared to baseline controls. Black dots represent interactions that are statistically significant (Wehr et al., 2006, Ma et al., 2023).

Also, a previously performed assay in HEK293 cells measuring YAP1 transcriptional and luciferase activity showed a potent inhibition of YAP1 activity, which was significantly higher than the TAOK1- or TAOK3-mediated inhibition (**Fig. 8**).
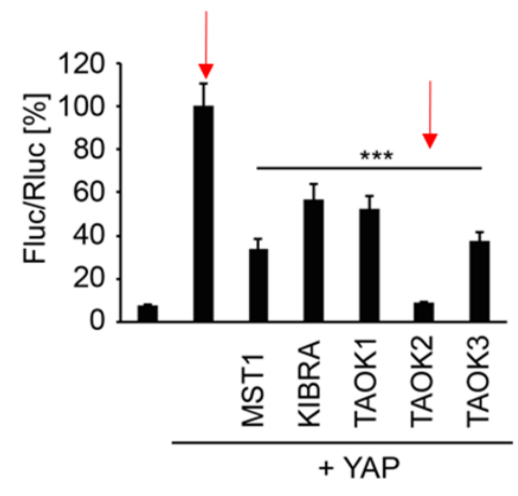
Fig. 8. TAOK2 inhibits YAP transcriptional activity.

HEK293 cells were co-transfected with YAP1 and with plasmids expressing MST1, KIBRA, TAOK1/2/3 and a firefly luciferase reporter to monitor luciferase activity. Significance level: ***, $p < 0.0005$ (Ma et al., 2023).

1.6   Aim of the thesis

The Hippo signaling pathway has been identified as a key controller of tissue growth, cell proliferation, differentiation, and migration during organ development. Further, it controls several processes during neurogenesis, such as differentiation of NSCs into neurons, astrocytes, and glial cells or formation of neural connections.

The serine-threonine kinase TAOK2 has been classified as a modulator of oncogenic pathways, synaptic plasticity, and neural excitability, also being associated with proliferative, neurodevelopmental, and psychiatric diseases. TAOK1 and TAOK3, with the exception of TAOK2, have been demonstrated to bind to STK3/4 and LATS1/2 kinases, thereby activating Hippo signaling. However, a previously conducted protein-protein interaction screen using the split TEV technique identified TAOK2 as central key interacting protein to Hippo pathway core components. Therefore, it is hypothesized that TAOK2 can deliver similar functions as TAOK1 and TAOK3 to regulate Hippo pathway activity by modulating phosphorylation levels of STK3/4 and LATS1/2 kinases (**Fig. 9**).

The focus of this thesis lies on investigating the regulatory mechanism of TAOK2 and its interactions with the Hippo signaling cascade in heterologous cells (e. g., HEK293) and primary neurons. TAOK2-mediated protein interactions to Hippo core components were biochemically validated by co-immunoprecipitation assays. Furthermore, I aimed to determine the most favorable environment for TAOK2 mediated effects on Hippo pathway activity. To do this, experiments were performed in HEK293 cells under different treatment conditions (e.g., serum starvation vs. stimulation, endogenous vs. overexpressed protein levels, different lysis timepoints). To address the influence of TAOK2 on synaptic signaling, the multiparametric profiling tool pathwayProfiler (developed by Systasy Bioscience GmbH) and the E-SARE-fluc assay were used to assess the activity of cellular pathways in primary cortical neurons.
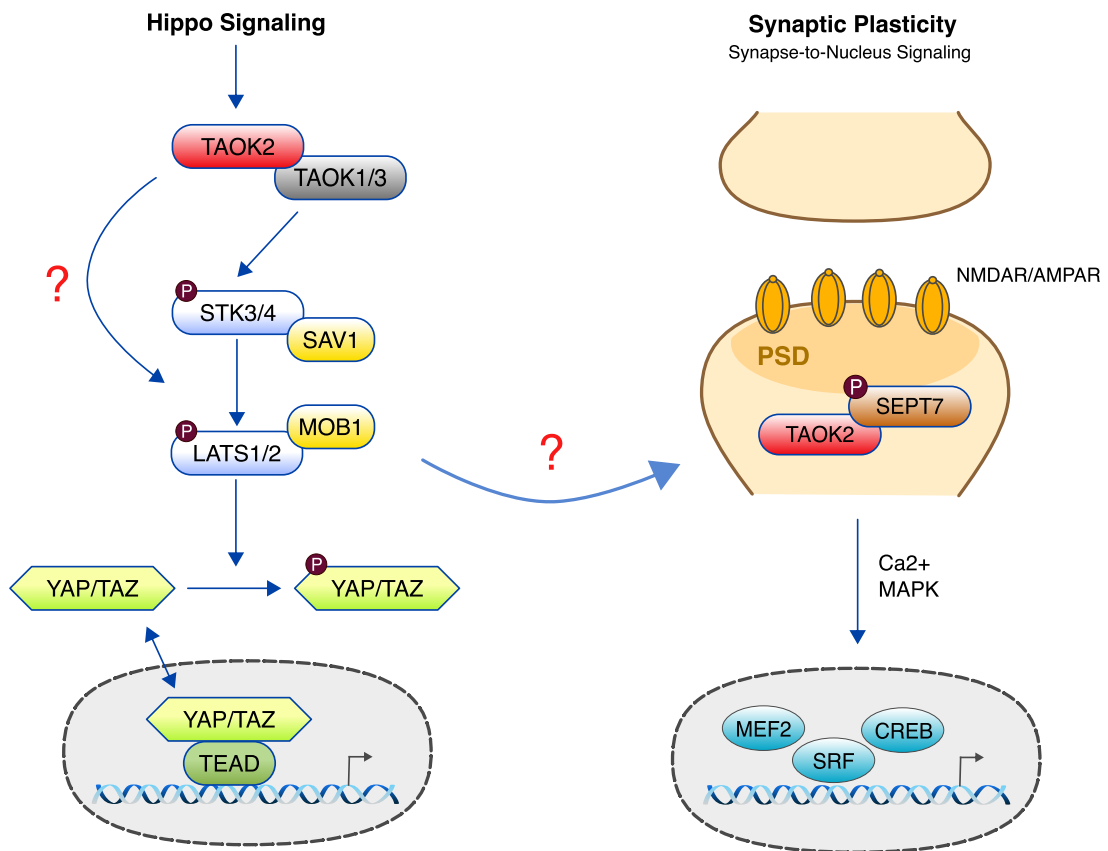
Fig. 9. TAOK2 modulates Hippo signaling and synaptic plasticity.

TAOK1/3, with the exception of TAOK2, were shown to initiate Hippo signaling upstream of STK3/4 and to directly phosphorylate LATS1/2. Interactions between TAOK2 and Hippo components were previously identified in a split TEV protein-protein-interaction screen performed by our group, requiring further investigations about the signaling pathways involved. TAOK2 was reported to have a significant role in modulating synaptic plasticity and formation of functional dendritic spines, being classified as a risk gene for conditions like autism and schizophrenia. As the Hippo signaling network has also been associated to various psychiatric and neurologic conditions, the connections between TAOK2 and Hippo components and their influence on cellular processes represent interesting key aspects addressed in this work.

2. Material and Methods

2.1 Materials

2.1.1 Instruments and consumables

Name	Manufacturer	Serial/ref. no.
CB 210 CO_2 incubator	Binder	90400013
HSP12 Hera Safe workbench	Heraeus Instruments	98104177
Centrifuge 5810 R	Eppendorf	5811AN864288
Universal 32 R Centrifuge Type 1610	Hettich	00625402-00
Microscope Axiovert 40	Zeiss	3825002079
Microscope Axio Observer Z1	Zeiss	1024693549
Microplate Luciferase Reader	Berthold	42-6049
Mithras LB940	Technologies	
BioPhotometer	Eppendorf	613125057
T Professional Thermocycler	Biometra	2103281
StepOnePlus Real-Time PCR System AB	ThermoFisher	2720010558
	Scientific	
Mini Trans-Blot® Cell gel-electrophoresis system	BioRad	153BR
Trans-Blot® Turbo™ Blotting System	BioRad	170-4155
Eppendorf Thermomoxer comfort	Eppendorf	F 1.6 A
ECL ChemoCam Imager	Intas	
Falcon® 48 Well Clear Flat Bottom Plate	Corning	353078
Falcon® 6 Well Clear Flat Bottom Plate	Corning	353046
Cell strainer, 40 µM	BD Falcon	352340

4-15 % Mini-PROTEAN® TGX™ Pre-cast Protein Gels, 10 well, 30 µl	Bio-Rad	4561083
4-15 % Mini-PROTEAN® TGX™ Pre-cast Protein Gels, 12 well, 20 µl	Bio-Rad	4561085
PVDF Transfer Membrane Hybond-P	GE Healthcare	RPN303F
Blotting Roller, 8.6 cm wide	Invitrogen	LC2100
Ultra-15 ml centrifugal filter, PLHK	Amicon	UFC910024
Ultracel-PL Membrane, 100 kDA		
Discardit II Syringe, 10 ml	BD Biosciences	309110
PCR 96-well plate	Biozym	712220
Adhesive plate seals	ThermoFisher Scientific	AB-0580
NucleoSpin® Gel and PCR Clean-up kit	Macherey-Nagel	740609.5
Direct-zol™ RNA MiniPrep	Zymo Research	R2050
High-Capacity cDNA Reverse	ThermoFisher Scientific	4368814
Transcription kit AB		
Bio-Rad Protein Assay Dye Reagent Concentrate	Bio-Rad	5000006

2.1.2 Reagents and chemicals

Name	Manufacturer	Catalog no.
Poly-L-lysine	Sigma-Aldrich	P1274
Poly-D-lysine hydrobromide	Sigma-Aldrich	P7886
NeurobasalTM Medium (1x)	Gibco	21103-049
B-27TM Supplement (50 x), serum-free	Gibco	17504044
Fetal Bovine Serum (FBS), qualified, heat inactivated	Gibco	10500064
DMEM, 4.5 g/l glucose, w/o glutamine	Lonza	BE12-614F

GlutaMAX (100x)	Gibco	35050061
PBS powder	Merck Milli-pore	L182-50
2,5 % Trypsin (10 x)	Gibco	15090-046
OptiMEM (1x) Reduced Serum Medium	Gibco	31985047
Sodium chloride	Roth	3957.1
Tris	Roth	4855.3
Lipofectamine®2000	Invitrogen	11668019
Dimethyl Sulfoxide	Sigma-Aldrich	D4540
Passive Lysis Buffer (PLB) (5x)	Promega	E1941
D-Luciferin, free acid	PJK GmbH	102112
Co-Enzyme A	PJK GmbH	102212
ATP	PJK GmbH	102261
Dithiothreitol (DTT)	PJK GmbH	102252
Coelenterazin	PJK GmbH	102172
Tricine	Sigma-Aldrich	T0377
$(MgCO_3)_4 * Mg(OH)_2 * 5 H_2O$	Sigma-Aldrich	M5671
$MgSO_4 * 7 H_2O$	Roth	T888.2
QIAzol Lysis Reagent	Qiagen	79306
4-aminopyridine	Abcam	ab120122
(-)-Bicuculline methiodide	Abcam	ab120108
Glycine	Abcam	ab120050
Strychnine hydrochloride	Abcam	ab120416
Triton X-100	Roth	66831
EGTA	VWR	437012C
PhosphoStop – Phosphatase Inhibitor Cocktail Tablets	Roche	4906837001

cOmpleteTM, Mini, EDTA-free Protease Inhibitor Cocktail Tablets	Roche	4906837001
Trizoma-Hydrochloride (Tris-HCl)	Sigma-Aldrich	T3253
Lithium dodecyl sulfate (LDS)	Sigma-Aldrich	L9781
Phenol Red	Sigma-Aldrich	P4758
Brilliant Blue G250	Roth	95981
Glycerol	Roth	3783.1
Tween20	Sigma-Aldrich	P1379
Sodium dodecyl sulfate (SDS)	Sigma-Aldrich	L3771
Methanol	Roth	8388.5
Bovine Serum Albumin (BSA)	Sigma-Aldrich	A3059
Milk powder	Roth	T5145.2
SpectraTM Multicolor Broad Range Protein Ladder	ThermoFisher Scientific	26634
PierceTM ECL Plus Western Blotting Substrate	ThermoFisher Scientific	32132

2.1.3 Antibodies

Name	Manufacturer	Antibody Identifier
Mouse monoclonal anti-V5 (D3H8Q)	Cell Signaling Technology	Cat# 13202; RRID: AB_2687461
Mouse monoclonal anti-FLAG (clone M2)	Sigma-Aldrich	Cat# F3165; RRID: AB_259529
Mouse monoclonal anti-FLAG M2 Affinity Gel	Sigma-Aldrich	Cat# A2220; RRID: AB_10063035
Rabbit polyclonal anti-TAOK2	ProteinTech	Cat# 21188-1-AP; RRID: AB_10755293
Rabbit monoclonal anti-p-YAP1 (Ser127) (D9W2I)	Cell Signaling Technology	Cat# 13008; RRID: AB_2650553

Rabbit monoclonal anti-p-YAP1 (S397) (D1E7Y)	Cell Signaling Technology	Cat# 13619; RRID: AB_2650554
Mouse monoclonal anti-YAP1 (M01), clone 2F12	Abnova	Cat# H00010413-M01; RRID: AB_535096
Rabbit monoclonal anti-p-LATS1 (Thr1079) (D57D3)	Cell Signaling Technology	Cat# 8654; RRID: AB_10971635
Rabbit monoclonal anti-LATS1 (C66B5)	Cell Signaling Technology	Cat# 3477; RRID: AB_2133513
Rabbit monoclonal anti-p-MOB1 (Thr35) (D2F10)	Cell Signaling Technology	Cat# 8699; RRID: AB_11139998
Rabbit monoclonal anti-MOB1 (E1N9D)	Cell Signaling Technology	Cat# 13730; RRID: AB_2783010
Rabbit monoclonal anti-p-CREB (Ser133) (87G3)	Cell Signaling Technology	Cat# 9198; RRID: AB_2798359
Rabbit monoclonal anti-CREB (D76D11)	Cell Signaling Technology	Cat# 4820; RRID: AB_1903940
Rabbit polyclonal anti-p-MST1 (Thr183)/pMST2 (Thr180)	Cell Signaling Technology	Cat# 49332, RRID: AB_2799355
Mouse monoclonal anti-STK4/MST1	BD Bioscience	Cat# 611052, RRID: AB_398365
Rabbit monoclonal anti-STK3/MST2 [EP1466Y]	Abcam	Cat# ab52641, RRID: AB_882734
Mouse monoclonal anti-alpha-Tubulin	Sigma-Aldrich	Cat# T5168; RRID: AB_477579
2ndary AB – HRP mouse	Jackson Immuno Research Labs	Cat# 115-035-003, RRID: AB_10015289
2ndary AB – HRP rabbit	Jackson Immuno Research Labs	Cat# 111-036-003, RRID: AB_2337942

2.1.4 Plasmids

For plasmids that are freely available from a repository according to the FAIR principles, an Addgene ID is provided. For other plasmids that have only been used in the host laboratory, an internally used ID is provided.

Name	Manufacturer	ID / alternate ID
pFdelta6	Alexander Herholt (Systasy Bioscience GmbH)	V1739
pRV1	Alexander Herholt (Systasy Bioscience GmbH)	V1740
pH21	Alexander Herholt (Systasy Bioscience GmbH)	V1741
pAAV_4xSARE-ArcMin-luc2_hU6	Alexander Herholt (Systasy Bioscience GmbH)	V1301
pcDNA3.1_nV5-LATS1	Michael Wehr (LMU Munich)	V670 / Hs246
pcDNA3.1_nV5-YAP1-var1	Michael Wehr (LMU Munich)	V598/ Hs194
pCMV7.1_3xFLAG-TAOK1	Michael Wehr (LMU Munich)	Addgene #172991
pCMV7.1_3xFLAG-TAOK2_var1	Michael Wehr (LMU Munich)	Addgene #172992
pCMV7.1_3xFLAG_TAOK2_var2	Michael Wehr (LMU Munich)	V1682 / Hs911
pCMV7.1_3xFLAG-TAOK3	Michael Wehr (LMU Munich)	Addgene #172993
pCMV7.1_3xFLAG-KIBRA-var3	Michael Wehr (LMU Munich)	Addgene #172994
pCMV7.1_3xFLAG-LATS1	Michael Wehr (LMU Munich)	Addgene #172986

pCMV7.1_3xFLAG-LATS2	Michael Wehr (LMU Munich)	Addgene #172987
pCMV7.1_3xFLAG-TAOK2_var1_KD	Michael Wehr (LMU Munich)	Hs 940
pCMV7.1_3xFLAG-MST1	Michael Wehr (LMU Munich)	Addgene #172989
pCMV7.1_3xFLAG-MST2	Michael Wehr (LMU Munich)	Addgene #172990
Tc39_pcDNA3.1_3xMyc-EGFP	Michael Wehr (LMU Munich)	V556

2.1.5 Adeno-associated viruses (AAV)

Name	Manufacturer	ID / alternate ID
pAAV_CAG_EYFP_WPRE	Alexander Herholt (Systasy Biocscience GmbH)	V823
pAAV_shRNA- mTaok2_4_Syn1p_EGFP_Mm114	Michael Wehr (LMU Munich)	V1976
AAV-DJ_cisPRO_v2.4	Alexander Herholt (Systasy Biocscience GmbH)	Plasmid mix (Herholt et al., 2018)

2.1.6 Cell lines

HEK-293	Human Embryonic Kidney wildtype cell line	ATCC	CLS Cat# 300192/p777_HEK293, RRID: CVCL_0045
HEK-293T	Human Embryonic Kidney cell line (fast growing, transfected with the SV40 T antigen)	ATCC	Cat# PTA-5077; RRID: CVCL_6911
Primary cortical neurons	Isolated from C57BL/6 mouse embryos	C57BL/6 mouse in house breeding	

2.1.7 Buffers

Buffer preparation	Indication	Usage
150 mM NaCl, 50 mM Tris-HCl (pH 8.5); stored at 4 °C	AAV lysis buffer	AAV harvest
5mM Tris-HCl buffer (pH 8,5), stored at room temperature	DNA buffer	Solvent for plasmid DNA
20 mM Tricine 1.07 mM (MgCO3)4 * Mg(OH)2 * 5 H2O 2.67 mM MgSO4 * 7 H2O 0.1 mM EDTA 33.3 DTT 270 µM Co-Enzyme A 470 µM D-Luciferin, free acid 530 µM ATP Comment: To solve magnesium carbonate, adjust the pH value using HCl (37%) until the solution gets clear. Then adjust the pH value to 7.8 using 5 M NaOH. Add D-Luciferin and Co-Enzyme A afterwards. Stored at-20°C without light, thaw at room temperature for use.	Fluc assay buffer	Firefly luciferase assays
50 mM Tris pH 7.5 150 mM NaCl 1% Triton X-100 1 mM EGTA Stored at 4 °C.	1 % Triton X lysis buffer	Cell lysis for Western blot
40% Glycerol 564 mM Tris 424 mM Tris-HCl 245 mM LDS 2.5 % (v/v) Phenol Red 7.5% (v/v) Brilliant Blue G250 2 mM EDTA Stored at -20 °C.	4 x loading dye	For preparing protein denaturation buffer
50 mM Tris 15 mM NaCl adjust to pH 7.4 with 37% HCl Dilute 20fold with dH2O before usage. Stored at room temperature	Tris Buffered Saline (TBS) (20 x)	For preparing TBS-T buffer in Western blot
0.1% Tween20 diluted in 1 x TBS Stored at room temperature.	1 x TBS-T	For preparing blocking solutions in Western blot

1.92 M Glycine 0.25 Tris SDS 1% Dilute 10fold with dH2O before usage. Replace if the final pH if it is not within 0.1 pH units of pH 8.3. Stored at room temperature.	10 x Running buffer	SDS-PAGE gel-electrophoresis
1.92 M Glycine 0.25 Tris Dilute 10fold with dH2O before usage and add 20% methanol and 0.2% SDS. Stored at room temperature.	10 x Transfer buffer	Western blotting
5% BSA (for phospho-antibodies) or 5% milk-powder (for normal antibodies) in TBS-T. Stored at 4 °C.	Blocking buffer	Membrane blocking in Western blot

2.1.8 Compounds to influence neuronal activity

Compounds	Indication	Usage
1µM TTX (Stock: 1mM) 100µM AP5 (Stock: 100mM)	Tetrodotoxine (TTX) mix	silencing
50µM BIC (Stock: 7.5mM) 100µM 4AP (Stock: 100mM) 100µM Glycine (Stock: 100mM) 1µM Strychnine (Stock: 20mM)	Bicuculline (BIC) mix	stimulation
BDNF (50 ng/well 2 ml) (Stock 10 µg/ml)	Brain-derived neurotrophic factor	stimulation

2.2 Methods

2.2.1 Cell cultures

2.2.1.1 Isolation, preparation and cultivation of mouse primary cortical neurons

Primary cortical neurons were prepared from 15.5 days old C57BL/6 mouse embryos. To ensure optimal adherence conditions for primary neurons, culture plates were treated with poly-D-lysine (PDL) to enhance cell attachment. PDL provides cationic sites for improved interaction with the negatively charged cell surface, promoting neuron survival and neurite growth. The coating conditions were changed from poly-L-lysine (PLL) to PDL during the optimization of neuron cell culture conditions. Neurons only grew in Neurobasal medium containing PhenolRed, which has estrogen-like activity and can prevent abnormal, epileptiform bursting activities in neurons. Therefore, Neurobasal medium containing PhenolRed was used for neuron cultivation in the experiments.

Before dissection, culture plates were freshly coated with 0.1 mg/ml PDL overnight at room temperature. On the day of dissection, serum-containing plating medium (Neurobasal-PhenolRed/5% Fetal bovine serum (FBS)/2% B27/1% Glutamax) was added to the 6-well plates after washing, and the plates were placed into the incubator (37°C/5% CO2) for at least two hours to warm the media and to adjust the pH. After removing PDL from the plates and rinsing with ddH2O, half of the final volume of plating medium was added to the plates, which were kept in the incubator until dissection. Immediately before dissection, a mix of 2 ml DMEM + 80 μl Papain (20 U/ml) + 80 μl DNaseI + 20 μl L-cysteine was incubated at 37°C (waterbath) to activate Papain.

Mouse cortices were isolated from embryos and dissected in cold HBSS/5 mM HEPES. After slow aspiration of HBSS and addition of 1 ml of activated Papain, the cortices were incubated for 13 min at RT. Papain treatment was stopped by adding 10 ml pre-warmed and pH equilibrated DMEM(4.5 g/l glucose)/10 % FBS. The medium was replaced by 10 ml of fresh pre-warmed and pH equilibrated DMEM(4.5 g/l glucose)/10 % FBS, then 2 ml pre-warmed and pH equilibrated plating medium were added. Cortices were gently triturated using a P1000 pipette. The cell suspension was pipetted through a 40 μm mesh (BD Cell strainer) to remove any cell aggregations. After, cells were counted by diluting 10 μl of the cell suspension with 90 μl medium, using a Neubauer cell counting chamber. Finally, half of the suspension volume was added to culture medium in the cell culture dish. During cultivation, cells were fed by replacing 1/4 of the medium with fresh, warm and pH adjusted Culture medium every 4-5 days. The procedure was carried out according to

the Standard Operation Procedure "Primary Neuron Culture" (SOP104) used in the laboratory and to Alexander Herholts PhD Thesis [183].

2.2.1.2 Cultivation of permanent cell cultures (HEK293 cells)

HEK293 cells are an immortalized, robust, and fast-growing cell line isolated from the kidney of a human embryo. The experiments were mainly performed in wild-type HEK293 cells, while the HEK293-FT cell line was used to generate high titer adeno-associated vectors (AAV). Both cell lines were cultivated in 15 cm petri dishes and maintained in DMEM (with 4.5 g/L glucose), supplemented with 10% FCS, 1% GlutaMAX and 1% penicillin/streptomycin. All cells were incubated at 37°C and 5 % CO_2. They were regularly passaged when reaching a confluence of 80-90% and split into the ratio 1:5 and 1:10. The old medium was removed with a vacuum pump. The cells were washed with 10 ml of phosphate buffered saline (PBS) and then treated with 5 ml trypsin/versene for 3 minutes in the incubator. To stop the reaction, 10 ml of maintenance medium (37°C) was added. The cell mixture was transferred to a tube and centrifuged at 800 rpm for 5 minutes. After removing the supernatant, the cells were mixed with new medium according to the desired ratio. The cell suspension was transferred to a new dish containing 20 ml of pre-warmed maintenance medium and incubated at 37°C and 5% CO_2 until they reached a density of 80-90%.

2.2.2 Viral vectors

2.2.2.1 Production of adeno-associated viral vectors (AAV)

To modify TAOK2 expression in cells and perform E-SARE assays based on firefly (Fluc) luciferase, corresponding viral vectors had first to be established. The production of the AAV vectors was carried out according to the general guideline published by McClure et al. [184], comprising three principal steps: 1. Transfection of HEK293FT cells, 2. AAV harvest (purification and enrichment), and 3. Titer determination by absolute quantitative real-time PCR (qRT-PCR).

2.2.2.2 Transfection of HEK293-FT cells

HEK293-FT cells were seeded onto PLL-coated petri dishes one day before transfection. One hour after medium change to fresh 37 °C pre-warmed HEK maintenance medium, the AAV plasmids (previously cloned by Alexander Herholt) were transfected into the cells using polyethylenimine (PEI) as transfection agent. A mix of four plasmids - 10 µg of pFdelta6 (adenovirus helper plasmid), 3.75 µg of pH21 (containing the Rep and Cap sequences from AAV serotype 1), 3.75 µg of pRV1 (containing the Rep and Cap sequences

from AAV serotype 2) and 4 µg of pAAV_E-SARE-ArcMin_Fluc_WPRE – was diluted in 500 µl OptiMEM. In the following, PEI was added with a DNA-to-PEI ratio of 1:4, the solution was vortexed for 10 seconds and incubated at RT for 10 min. After incubation, the transfection mix was added dropwise to the cells. Four hours after transfection, 15 ml of fresh medium were added, and the cells were incubated for another three days at 37 °C. The combination of two different AAV serotypes for capsid expression (pH21, pRV1) enabled a more efficient infection of neuronal cells compared to the usage of one single serotype.

2.2.2.3 AAV purification and enrichment

The AAV particles were harvested three days post-infection, including purification and enrichment. For purification, the cells were detached by thorough pipetting, transferred into a 50 ml tube, and centrifuged at 1000 rpm for 10 min. After removing the supernatant, the cells were resuspended in 5 ml of AAV lysis buffer (150 mM NaCl, 50 mM Tris-HCl pH 8.5) and lysed by three freeze-thaw cycles between -80 °C and 37 °C. The cells were frozen at -80°C for 20 minutes and afterwards thawed in a water bath at 37 °C, repeating this step twice. To digest the genomic DNA, 1 µl of Benzonase (50 U/ml) was added and incubated at 37 °C for 30 min. The suspension was centrifugated at 1000 rpm for 10 min, followed by collection of the AAV-containing supernatant, which was filtered through a 0.45 µM filter with a syringe. To proceed with the virus enrichment, the supernatant was transferred into an Amicon Ultra-15 centrifugal filter unit (100 kDa membrane cutoff, Millipore), 10 ml of PBS were added and centrifuged at 3000 rpm for 15 min. Subsequently, another 10 ml of PBS were added, repeating the centrifugation until reaching a stock volume between 0.25 ml and 0.5 ml. Aliquots were made and frozen at -80 °C for future use.

2.2.2.4 Titer determination by quantitative real-time PCR (qRT-PCR)

To measure the titer of the AAV stocks, a quantitative real-time PCR (qRT-PCR) was performed. 5 µl of AAV stock were mixed with 84 µl dH2O, 10 µl of Turbo DNase buffer and 1 µl of Turbo DNase (2U/ml) to digest residual plasmid DNA and release cellular DNA. Then, the mix was then incubated at 37 °C for 15 min and the Turbo DNase was inactivated at 95 °C for 10 min. To break open the capsid, 5 µl of proteinase K (10 mg/ml) were added and incubated at 50 °C for 15 min. The released AAV-DNA was purified using the NucleoSpin® Gel and PCR Clean-Up kit (Macherey-Nagel) and eluted in 200 µl elution buffer.

Absolute quantification was carried out on the StepOnePlus Real-Time PCR System Applied Biosystems (AB) by ThermoFisher Scientific using the 2 x Power-UpTM SYBR® Green Master Mix. The PCR master mix for one single approach was obtained by mixing

7.5 µl 2x Power-UpTM SYBR® Green Master Mix with the according volume of the 10 µM concentrated WPRE primers to get a final primer concentration of 0.15 µM. Afterwards, the volume was expanded to 10 µl with dH2O and the DNA samples were diluted at 1:1000. To generate the standard curve, a dilution series with 103-106 copies/µl of a pAAV plasmid plus non-template control were prepared. For performing the RT-PCR, 10 µl of master mix per sample were transferred into a single well of a PCR 96-well plate and 5 µl of the DNA samples or dH2O were accordingly added.

After sealing the PCR 96-well plate, the qRT-PCR was carried out by adjusting the PCR parameters corresponding to the manual instructions for the Power-Up^{TM} SYBR® Green Master Mix AB (ThermoFisher Scientific).

2.2.3 Co-Immunoprecipitation and analysis by Western blotting

HEK293 cells were plated at 6x100.000 cells in 6-well plates and transfected with plasmids using Lipofectamine 3000 (Thermo Fisher Scientific). After 18 h of expression, cells were treated and lysed in a 1% Triton-X lysis buffer supplemented with phosphatase inhibitors (10 mM NaF, 1 mM Na2VO4, 1 mM ZnCl2 and 4.5 mM Na4P2O7) or the Complete Phosphatase Inhibitor Cocktail PhosSTOP (Roche) and cOmplete™ Mini Protease Inhibitor Cocktail (Roche). Protease inhibitors are used to prevent protein degradation, while phosphate inhibitors aim at preserving protein phosphorylation states, which are particularly important in kinase pathways.

To lyse cells, the medium was first removed, and the cells were washed once by adding 1 ml of 1xPBS to each well. After washing the plates, 250 µl of cell lysis buffer was added and the plates were incubated for 10 minutes on ice. The lysates were transferred into centrifugation tubes and centrifuged at 13,000 rpm for 10 minutes at 4 °C to remove the cell debris. 230 µl of the centrifuged lysate samples were transferred into new 1.5 ml centrifugation tubes, 123 µl of protein denaturation buffer was added and then incubated at 70 °C for 10 minutes.

For co-immunoprecipitations, FLAG-tagged proteins were purified using anti-FLAG M2 affinity gel (Sigma) and incubated for 2 h at 4°C. Afterwards, the FLAG immunoprecipitates were washed four times in lysis buffer and denatured for 10min at 70°C. 100 µl aliquots were stored at -20 °C for later use. The remaining lysate samples were used to perform the Bradford assay to check whether the protein content was approximately the same in every lysate. For the assay, the Bio-Rad Protein Assay Dye Reagent Concentrate was diluted at a ratio of 1:5 with dH2O and 1 ml of the dilution was mixed with 2 µl of ly-

sate sample in a cuvette. The OD600 was measured, including a blank sample as a control.

The protein gels for Western blotting were run using the SDS-PAGE gel-electrophoresis system. 10 µl of SpectraTM Multicolor Broad Range Protein Ladder and 16 µl of lysate were applied to 10-well or 12-well 4-15 % Mini-PROTEAN® TGXTM Precast Protein Gels and electrophoresis was run at 100 V for 15 min and at 150 V for another 45 min. Before setting up the Trans-Blot® TurboTM Blotting System (Bio-Rad), four sheets of Whatman paper were soaked in 1 x transfer buffer, while one piece of PVDF (polyvinylidine fluoride)-membrane was activated for 30 seconds in methanol. The membrane and the gel were both equilibrated in 1 x transfer buffer for 15 min.

Afterwards, one cassette unit of the blotting device was removed to build up the blotting sandwich by first placing two sheets of the soaked Whatman paper on the cassette base (anode). The activated and equilibrated PVDF-membrane was placed on top of them, while the gel was placed on top of the membrane and always kept wet. Air bubbles were carefully removed with a mini roller. Finally, the other two sheets of Whatman paper were placed onto the gel. The lid of the cassette (cathode) was placed on the blotting sandwich, locked, and put back into the Trans-Blot® TurboTM Blotting System. The transfer was performed by using the standard Bio-Rad transfer protocol (pre-programmed standard setting: 25 V, 1.0 A, 30 min).

After finishing the transfer, the blot-membranes were blocked for 30 min at RT in either 5 % BSA blocking solution for phospho-antibodies or 5 % milk powder for non-phospho-primary antibodies. Altogether, three cycles of antibody staining were performed. In the first run, BSA-blocked membranes were incubated with the primary Phospho-antibody (e.g., pLATS (Thr1079), pYAP (Ser127), pYAP (Ser397)) diluted at a ratio of 1:1000 in 5 % BSA blocking solution overnight at 4 °C. The membranes were then rinsed twice and washed four times with TBS-T for 5 min each at RT. After, they were incubated with the secondary antibody (Rabbit IgG HRP Linked or Mouse IgG HRP Linked Whole Antibody) diluted at a ratio of 1:5000 in 5 % BSA blocking solution for 90 min at RT. Again, the membranes were rinsed twice and washed four times with TBS-T for 5 min each.

After being washed, the stained proteins were detected by using the PierceTM ECL Plus Western Blotting Substrate, more precisely by a mixture of ECL solution A and ECL solution B at a ratio of 40:1. The ECL solution was dropped onto the membranes, following an incubation time of 1 min. Shortly after, excess substrate was removed, and the blot membranes were placed into transparent plastic folders to continue with the imaging process using the Intas ECL ChemoCam Imager.

In the second round, the membranes were again incubated with the primary antibodies (e.g. LATS-G12, YAP 63.3) at a dilution of 1:1000 in 5 % milk powder blocking buffer and with the secondary antibodies diluted at a ratio of 1:5000 in 5 % milk powder blocking buffer. In the final run, anti-α-Tubulin (mouse) was used as a loading control at a dilution of 1:2000 in 5 % milk powder blocking buffer. To remove membrane bound antibodies between cycles, blot membranes were rinsed once with TBS-T to wash away the ECL solution and incubated with 0.5 M NaOH for 5 min at RT. Subsequently, the membranes were rinsed twice and washed three times with TBS-T for 5 min at RT, preparing the new cycle by blocking the membranes in the appropriate blocking solution. Densitometric analysis of western blots was performed with Image J, following a protocol available on http://www.lukemiller.org.

2.2.4 pathwayProfiler: Pathway profiling in primary neurons

Phenotypic screening assays are used to identify substances or molecules with predefined effects on the phenotype of cells or animal-based models, e.g., the measurement of neural activity in primary neurons. In this work, a multiparametric profiling tool called pathwayProfiler (developed by Systasy Bioscience GmbH) was applied on primary cortical neurons to simultaneously measure relevant signaling events under defined treatment conditions. This method uses 100 barcoded biosensors to address distinct transcription factor activities and distal endpoints of signaling cascades, grouped into seven major signaling clusters including regulation of cellular stress, cell fate, metabolism, immune response, stem cell pluripotency, synaptic activity & calcium signaling, and immediate early gene (IEG) response [185].

Several conditions were tested in this assay. Stimulation of primary neurons with bicuculline (BIC) and 4-aminopyridine (4-AP) or brain-derived neurotrophic factor (BDNF) led to enhancement of the luciferase signal. BIC is a GABA receptor antagonist which, in combination with the antagonizing effect of 4-AP on voltage-gated potassium channels, indirectly enhances synaptic activity [186]. BDNF activates MAPK by binding to tyrosine kinase receptor B (Trk-B) [187]. In contrast, neurons were silenced with tetrodotoxin (TTX), a sodium channel blocker, and (2R)-amino-5-phosphonovaleric acid (APV), a NMDA receptor antagonist [188,189], leading to decreased luciferase signals.

Timeline: On DIV0, primary cortical neurons from E15.5 old mouse embryos were plated on DIV0 onto PLL-coated 6-well plates containing 2000 µl plating medium per well (Neurobasal-PhenolRed/5% FBS/2% B27/1% Glutamax). One day after, the plating medium was exchanged to culture medium (Neurobasal-PhenolRed/2%B27/1%Glutamax). On DIV5, cells were fed by removal of 650 µl old medium and addition of 570 µl fresh cul-

ture medium per well. On DIV6, cells were infected by adding AAV particles diluted in 100µl fresh culture medium (2000 µl total volume/well). Half of the cells were infected with a mix containing the viruses AAV-DJ_cisPRO_v2.4 (barcoded pathwayProfiler sensors) and pAAV_CAG_EYFP_WPRE (EYFP control), while the other half got infected with a mix of AAV-DJ_cisPRO_v2.4 and pAAV_shRNA-mTaok2_4_Syn1p_EGFP_Mm114 for Taok2 depletion. Cells were fed again on DIV 8. 24 hours before lysis, cells were silenced by adding the TTX mix (1 µM/2000 µl). Finally, 2 h before lysis on DIV14, the stimulating compounds BIC mix (50 µM/2000 µl) and BDNF (50 ng/2000 µl) were added. Cells were then lysed with Qiazol (350 µl per 6-well), transfered into Eppis and stored in the freezer at -80°C. Every treatment condition was run in three replicates, with a total number of 36 samples.

Then, qRT-PCR was performed by Karin Neumeier using Dynabeads TMmRNA Direct Kit TM (Thermo fisher) for RNA purification and the High-capacity cDNA reverse Transcription Kit (Applied Biosystems) for cDNA synthesis. The following steps, barcode amplification and sequencing, were carried out according to the protocol described in Alexander Herholt's PhD thesis (Section 4.5 Multiplexed cis-regulatory sensor assay, [183]). Barcodes were amplified after cDNA synthesis by adding 1 µl of cDNA (1/10 dilution) to 20 µl PCR reaction. PCR was performed for 30 cycles at an annealing temperature of 59°C. The PCR product was verified using agarose gel-electrophoresis. In the following PCR, barcodes were fused with the adapter sequences for Ion Torrent sequencing. The PCR was performed using HotStar Taq plus DNA polymerase (Qiagen) and its product was verified using agarose gel-electrophoresis. Barcode libraries were sequenced by an Ion Torrent Proton PGM sequencer with an Ion PI Sequencing 200 v3 kit. Raw data was processed using custom shell and R scripts with support from Dr. Sven Wichert. Finally, the results were presented in a heatmap of log2-transformed fold changes relative to the untreated reference samples.

2.2.5 E-SARE-Fluc assays

To validate the results from the pathwayProfiler assays, E-SARE-Fluc assays were performed. The Synaptic Activity-Responsive Element (SARE) is a conserved promoter region of the immediate-early gene *Arc* (activity regulated cytoskeletal protein) which consists of transcription factor binding sites for CREB (cAMP response element-binding protein), MEF2 (myocyte enhancer factor-2) and SRF (serum response factor) [190]. The *Arc* gene is an activity-dependent regulator of synaptic plasticity and a significant molecular marker for strong synaptic activity [191].

Originally engineered by Kawashima et al. [192], the enhanced SARE element (E-SARE) generated in our laboratory is a cluster of four SARE subregions fused to the proximal *Arc* promoter (ArcMin) and to a firefly luciferase (FLuc) to monitor luciferase activity in primary neuronal cultures (**Fig. 20A**) [193]. This construct was shown to strongly enhance the expression of the firefly luciferase in response to synaptic stimuli, while synaptic inactivity/inhibition led to a low basal expression. Thereby, the changes in synaptic activity measured by the nuclear E-SARE sensor reflect signals from multiple synapse-to-nucleus signaling pathways such as calcium signaling or MAPK signaling. The sensor was integrated into the neuronal genome by adeno-associated virus (AAV)-based transfer vectors containing the E-SARE-luciferase reporter, next to AAV co-infection transferring two types of TAOK2-shRNA, as well as an EYFP (Enhanced Yellow Fluorescent Protein) control.

Timeline: In this work, primary cortical neurons from E15.5 old mouse embryos were plated on DIV0 onto a 48-well plate with a cell density of 40.000 cells/well. The plates were PLL-coated and contained 400 µl plating medium per well (Neurobasal-PhenolRed/5% FBS/2% B27/1% Glutamax). One day after, the plating medium was exchanged to 200 µl culture medium per well (Neurobasal-PhenolRed/2% B27/1% Glutamax). After removal of 40 µl old medium and addition of 50 µl fresh culture medium per well on DIV5, the cells were infected by adding AAV particles diluted in 100µl fresh culture medium (300 µl total volume/well) on DIV6. On DIV8, 100 µl of fresh culture medium were added to each well. The neurons were cultivated until DIV12 to allow sufficient maturation by forming active synapses and spontaneous network activity [193]. To silence neuronal activity on DIV11, a cocktail containing TTX (Tetrodotoxin) was added to the medium and incubated for 24 h. Four hours before cell lysis on DIV12, neuronal activity was stimulated by addition of BDNF and a mix containing Bicuculline (BIC), which inhibits inhibitory neurons, and 4-aminopyridine (4-AP), which delays repolarization. Further mix compounds, glycine, and strychnine, have a positive regulatory effect on glutamatergic transmission. For cell lysis, the medium was removed and 70 µl of Passive Lysis Buffer (PLB) were added per well. Luciferase activity was measured for 2 seconds per well after addition of FLuc Buffer, using a Mithras LB 940 Microplate Reader (Berthold Technologies) and the software MicroWin2000.

2.2.6 Statistical data analysis

Statistical analysis of Western blot data was performed with careful consideration of sample size limitations. In general, three independent experiments were performed for each condition. However, the quality of the Western Blot results was fluctuating due to unstable protein expression or technical problems. Therefore, only the most consistent results are

shown and analysed in this work. Due to the experimental design with typically n=2 replicates per group, non-parametric statistical methods were employed throughout the analysis. While normality testing using methods such as Shapiro-Wilk or Kolmogorov-Smirnov tests is traditionally recommended [194], these tests lack statistical power with such small sample sizes and can lead to unreliable conclusions about data distribution [195] . Therefore, distribution-free methods that make no assumptions about normality appeared to be the best choice.

For comparisons between two experimental groups, the Mann-Whitney-U-test was applied for non-normally distributed data, as it provides robust analysis for small sample sizes and is resistant to outliers [196]. When analyzing experiments involving multiple groups of non-normally distributed data, the Kruskal-Wallis test was implemented as the primary statistical method, followed by Dunn's test for post-hoc comparisons where appropriate. To control for multiple testing in these cases, p-values were adjusted using the Benjamini-Hochberg procedure to maintain an acceptable false discovery rate while preserving statistical power [197]. Statistical significance was denoted as follows: $*p < 0.05$, $**p < 0.01$, and "n.s." for non-significant results.

All quantitative data are presented as mean values with error bars representing the standard error of the mean (SEM). Paired measurements from Western blot bands were processed to calculate relative protein levels, expressed either as arbitrary units (a.u.) for direct ratios or as fold changes (FC) when normalized to control conditions. This statistical approach acknowledges the limitations of small sample sizes while maintaining statistical rigor appropriate for the experimental design.

3.   Results

3.1   The influence of TAOK2 on Hippo pathway activity

3.1.1   TAOK2 associates with Hippo pathway core components

The outcomes of the split TEV-based focused interaction screen conducted by our team revealed novel connections among core components of the Hippo pathway and key regulatory proteins [177]. Of particular interest are the novel interactions between TAOK2 and LATS kinases, which have previously been reported only for TAOK1 and TAOK3 [126,198,199]. The function of Hippo main kinases STK3, STK4, LATS1, LATS2, and the transcriptional output of YAP1 can be modulated by multiple upstream regulators (**Fig. 10A**), such as the polarity proteins KIBRA, AMOT and the tumor suppressor protein NF2 [124,129,180]. To validate the most important findings biochemically, experiments using co-immunoprecipitation followed by Western blotting were performed in HEK293 cells. For these assays, HEK293 cells were transfected in pairs with FLAG-tagged Hippo pathway components and V5-tagged TAOK2. Cell lysis was performed 18 h later, followed by immunoprecipitation of FLAG-tagged proteins, and an occurred interaction between TAOK2 and Hippo pathway core components LATS1, LATS2, STK3, STK4 and modulators PKCzeta and AMOT was identified by blotting for V5-tagged TAOK2 (**Fig. 10B**).
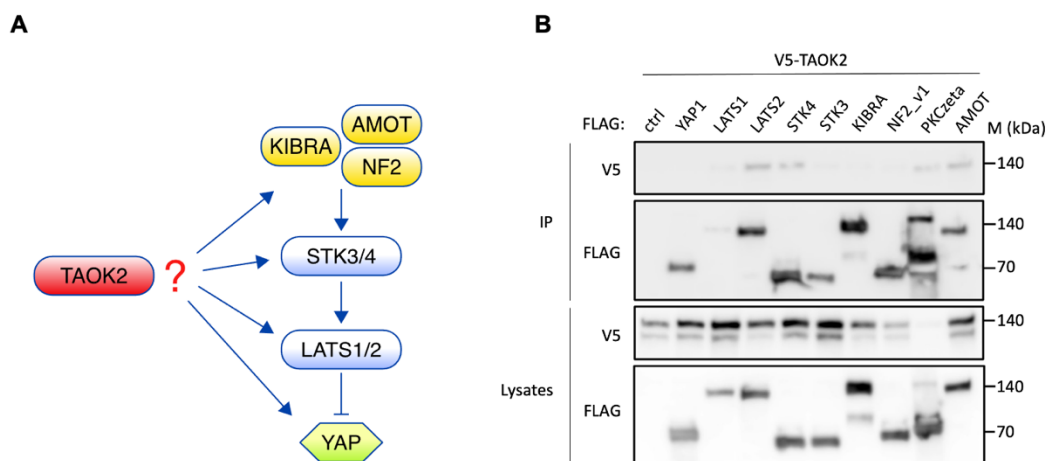
Fig. 10. TAOK2 interacts with Hippo pathway components.

(**A**) Chart illustrating potential TAOK2-Hippo pathway interactions. (**B**) TAOK2 engages with components of the Hippo pathway. TAOK2-overexpressed HEK293 cells were transfected simultaneously with plasmids tagged with FLAG and V5, followed by lysis after 18 h of expression. Lysates underwent FLAG-co-immunoprecipitation and Western blot analysis, using V5-tag and FLAG-tag antibodies. IP indicates FLAG-immunoprecipitates, while lysates imply whole cell lysates.

3.1.2 TAOK2 phosphorylates LATS1

As TAOK2 binds to LATS1/2 kinases, it was next tested by Western Blot whether increased TAOK2 expression in HEK293 cells also modulates phosphorylation of LATS kinases. Indeed, FLAG-tagged TAOK2 co-transfected with V5-tagged LATS1 lead to slightly increased LATS1 phosphorylation (**Fig. 11A, B**). Compared to the effect of co-transfected TAOK2, overexpression of an inactive form of the TAOK2 kinase (TAOK2-KD) did not increase LATS1 phosphorylation (**Fig. 11C, D**), confirming that the kinase activity of TAOK2 is responsible for the phosphorylation of LATS1. Since TAOK2 binds to LATS1 and TAOK2 kinase activity leads to the phosphorylation of LATS1, it can be suggested that TAOK2 directly phosphorylates LATS1.

Further, a time course analysis was performed to determine endogenous LATS1 phosphorylation levels at different lysis timepoints (6 h vs. 12 h post transfection). This method allows to examine how gene expression changes over time and to identify the ideal environment for LATS1-TAOK2 interactions. For TAOK2 overexpression, different amounts of TAOK2 plasmid (10-300ng) were transfected into HEK293 cells, without overexpression of LATS1. Endogenous phospho-LATS1 levels are increased in TAOK2 co-expressed cells, but no significant differences could be observed between samples transfected with 10ng, 30 ng, 100 ng, or 300 ng of TAOK2 plasmid (**Fig. 11E, F**). The results from the 6 h-lysis timepoint are not shown here due to weak expression. Altogether, 12 h incubation time might still not be sufficient for proper protein expression.
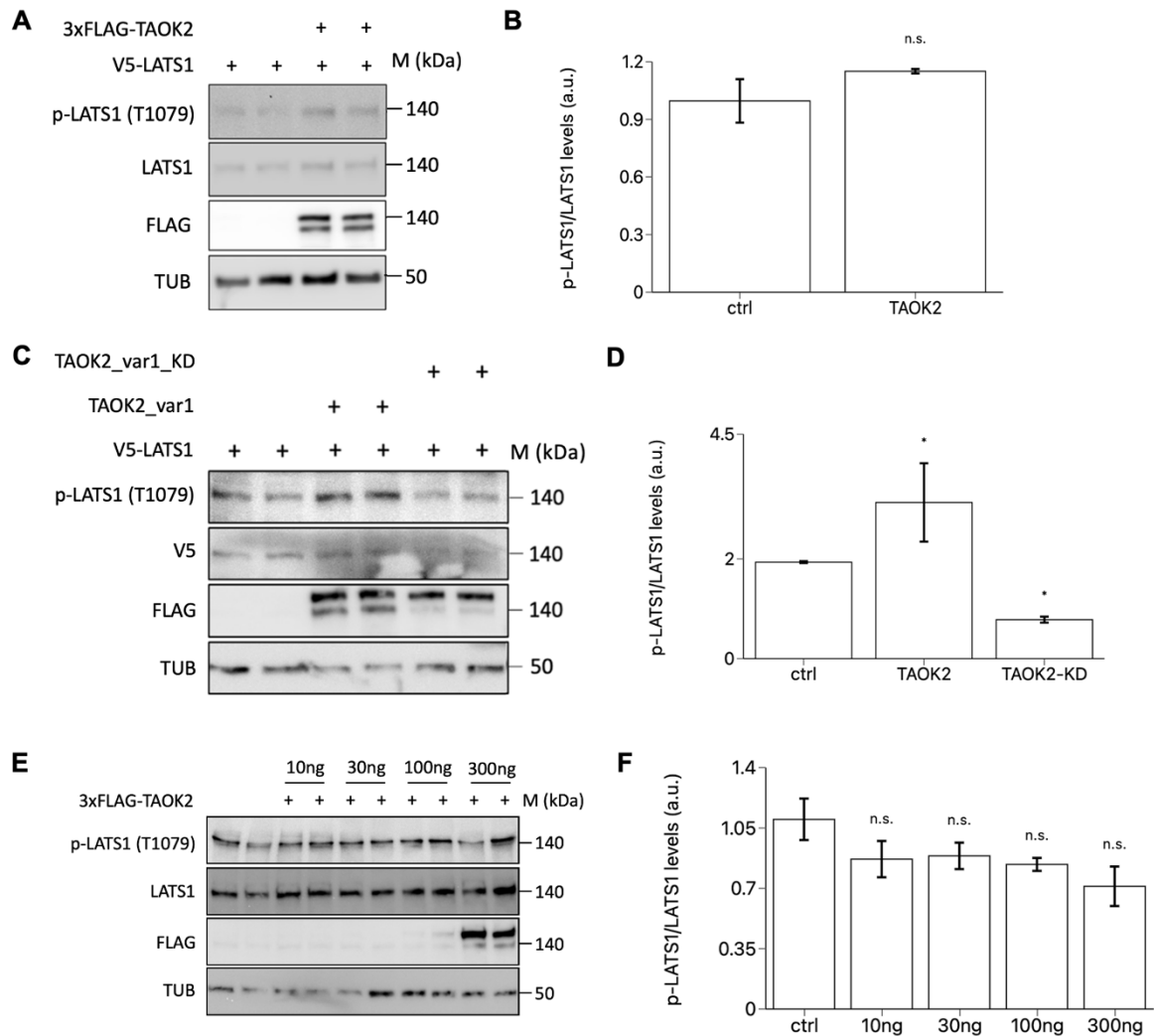
Fig. 11. TAOK2 increases LATS1 phosphorylation in HEK293 cells.

(**A**) TAOK2 upregulates p-LATS1 in HEK293 cells. Plasmids that express TAOK2 and LATS1 (3xFLAG-TAOK2 and V5-LATS) were transfected into HEK293 cells cultivated in medium containing 10% FCS and lysed after 20 h. Western blotting was conducted applying the specified antibodies. (**B**) Quantification of phosphorylated LATS1 shown in (A). (**C**) Co-transfection of an inactive variant of TAOK2 (TAOK2_var1_KD) leads to lower phosphorylation of LATS1 compared to TAOK2 (TAOK2_var1). V5- and FLAG-antibodies were used to detect V5- and FLAG-tagged proteins. (**D**) Quantification of phosphorylated LATS1 depicted in (C). (**E**) Time course analysis of endogenous LATS1 phosphorylation in HEK293 cells. Different amounts of TAOK2 (3xFLAG-TAOK2, 10 ng-300 ng) were transfected into HEK293 cells cultivated in medium containing 10% FCS and lysed after 12 h. (**F**) Quantification of phosphorylated LATS1 depicted in (E). Significance was calculated using a Mann-Whitney-U test in (B) and a Kruskal-Wallis test in (D) and (F), n=2 per group, values represent paired band measurements. Error bars show SEM with *, $P < 0.05$, **, $P < 0.01$, and n. s., not significant.

To compare the effect of the three TAOKs on LATS1 phosphorylation, TAOK1/2/3 were each co-transfected with LATS1 into HEK293 cells and lysed after 20 h incubation time. TAOK1 strongly increased p-LATS1, while TAOK2 and TAOK3 showed a weaker effect (**Fig. 12A, B**).
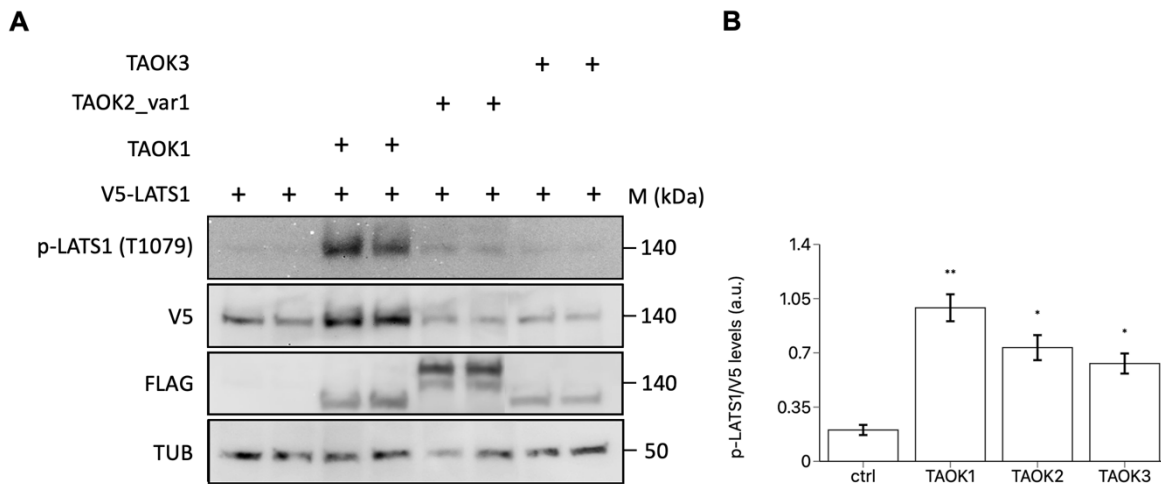
Fig. 12. TAO kinases promote phosphorylation of LATS1.

(**A**) TAO kinases increase phosphorylation of LATS1 in HEK293 cells. Plasmids expressing TAOK1, TAOK2, TAOK3 and V5-tagged LATS1 were simultaneously transfected into HEK293 cells, followed by lysis after 20 h of incubation. V5- and FLAG-antibodies were used to detect V5- and FLAG-tagged proteins. (**B**) Quantification of phosphorylated LATS1 depicted in (A). Significance was calculated using a Kruskal-Wallis test, n=2 per group, values represent paired band measurements. Error bars show SEM with *, $P < 0.05$, **, $P < 0.01$, and n. s., not significant.

3.1.3 TAOK2 increases YAP1 phosphorylation

YAP1 and TAZ serve as the primary transcriptional targets of the Hippo pathway, controlling the expression of genes associated with tissue growth, proliferation, and apoptosis [111]. It is known that TAOK1 and TAOK3 can promote Hippo pathway activity by phosphorylation of STK3/4, which in turn activate LATS1/2. LATS1/2 activation results in the phosphorylation of YAP1 and TAZ, leading to cytoplasmic retention by associating with 14-3-3 protein at YAP phosphorylation site S127 and subsequent ubiquitin-mediated degradation [111,119,132] (**Fig. 13A**). Recent developments indicate that various members of the Hippo pathway, especially LATS1/2 and YAP1/TAZ, are regulated by degradative and non-degradative ubiquitin modifications through the ubiquitin system [200]. Being involved in post-translational modification and mediating various cellular stress responses, E3 ubiquitin ligases form a three-enzyme cascade with ubiquitin activating enzymes (E1) and ubiquitin conjugating enzymes (E2), catalyzing the transfer of ubiquitin to the targeted substrate [201].

To determine possible dose-dependent effects of TAOK2 on YAP1 expression, HEK293 cells were co-transfected with V5-tagged YAP1 and increasing FLAG-tagged TAOK2 plasmid amounts (10 ng, 100 ng and 300 ng). TAOK2 overexpression increased phospho-YAP1 levels at the phosphorylation site S397, facilitating E3 ubiquitin ligase-mediated proteasomal degradation (**Fig. 13B, C**). This effect was observed in a following experiment targeting the YAP1 phosphorylation site S127 associated with cytoplasmic retention (**Fig. 13D, E**). It was also validated using Western blotting, showing an increase in endogenous YAP1 and TAZ phosphorylation levels in TAOK2-co-transfected cells (**Fig. 13J, K, L**).

Further, a time course analysis was performed in analogy to LATS1, following the same procedure as described in chapter 3.1.2. Cells were lysed after 12 h, while the results from the 6 h-lysis timepoint are not shown here due to weak expression. YAP1 expression levels detected by the antibody p-YAP1 (S397) were significantly increased with a peak at co-transfection with TAOK2 100 ng (**Fig. 13F, G**). Another experiment using the antibody p-YAP1 (S127) (**Fig. 13H, I**) showed a significant increase in YAP1 phosphorylation at co-transfection with TAOK2 10ng, 30 ng and 300 ng. However, the irregularity of the bands and the high background on the blots might impose limitations on the qualitative analysis of the effect of TAOK2 on YAP1 phosphorylation.

In summary, the results indicate that TAOK2 indirectly inhibits YAP1 transcriptional activity by phosphorylating and activating LATS1/2, which phosphorylate YAP1 and prevent it from translocating to the nucleus to promote gene expression.
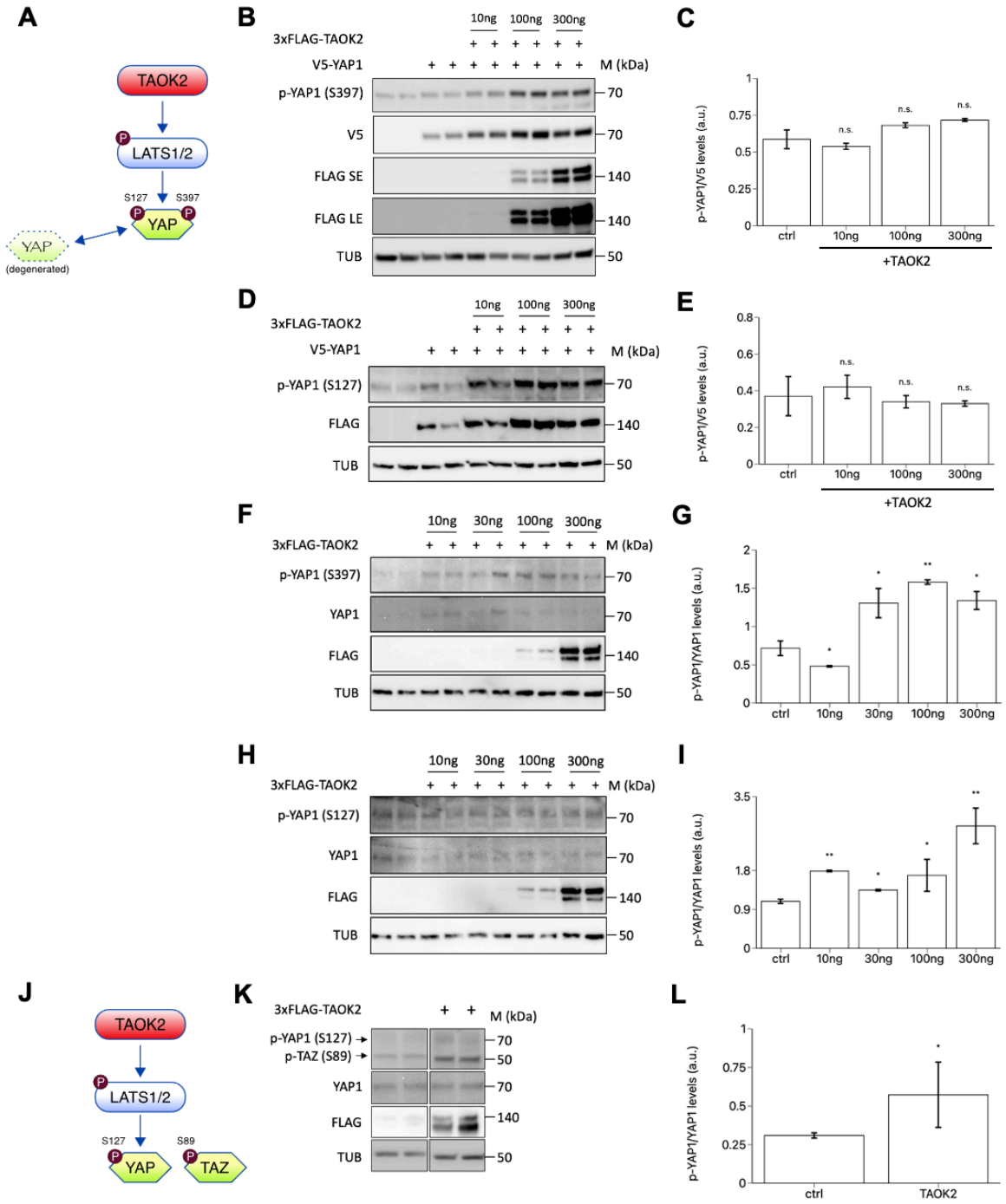
Fig. 13. TAOK2 increases YAP1 phosphorylation.

(**A**) Schematic map of TAOK2-induced phosphorylation of downstream Hippo targets leading to YAP1 degradation. (**B**) TAOK2 overexpression increases p-YAP1 at the phosphorylation site S397, facilitating proteasomal degradation via ubiquitination by E3 ligases. A similar impact of TAOK2 was observed at (**D**) S127, a YAP1 phosphorylation site promoting cytoplasmic retention. Different amounts of TAOK2 (3xFLAG-TAOK2, 10 ng-300 ng) and YAP1 expressing plasmids (V5-YAP) were transfected into HEK293 cells cultivated in medium containing 10% FCS and lysed after 20 h. (**C, E**) Quantification of p-YAP1 (S397) (C) and p-YAP1 (S127) (E) depicted in (B) and (D). (**F, H**) Time course analysis of endogenous YAP1 phosphorylation levels in HEK293 cells. Different amounts of TAOK2 (3xFLAG-TAOK2, 10 ng-300 ng) were transfected into HEK293 cells cultivated in medium containing 10% FCS and lysed after 12 h. TAOK2 upregulates endogenous phospho-YAP levels at the phosphorylation sites S397 (F) and S127 (H). (**G, I**) Quantification of p-YAP1 (S397) (G) and p-YAP1 (S127) (I) depicted in (F) and (H). (**J**) Schematic representation of TAOK2-induced phosphorylation of YAP1 at S127 and TAZ at S89. (**K**) TAOK2 upregulates endogenous p-YAP1 (S127) and p-TAZ (S89) in HEK293 cells. Only TAOK2 was overexpressed by transfection of 3xFLAG-TAOK2 into HEK293 cells (10% FCS). (**L**) Quantification of p-YAP1 (S127) shown in (K). Western blot analyses were performed using the denoted antibodies. Significance was calculated using a Kruskal-Wallis test in (C), (E), (G) and (I), and a Mann-Whitney-U test in (L). n=2 per group, values represent paired band measurements. Error bars show SEM with *, $P < 0.05$, **, $P < 0.01$, and n. s., not significant. FCS: Fetal Calf Serum; S: Serine; SE: Short Exposure, LE: long exposure.

3.1.4 TAOK2 mediated phosphorylation of LATS1 and YAP1 are increased under starvation conditions

The Hippo signaling pathway assimilates numerous environmental cues to regulate cell metabolism and growth. Cellular stress triggered by e.g., nutrient deprivation or toxic stimuli, is registered by GPCRs and leads to interaction of Hippo signaling and KIBRA/WWC1 to suppress YAP1 transcriptional activity and negatively regulate cell proliferation and tissue growth [129,171]. Serum starvation is frequently used method in molecular biology to investigate stress-related signaling pathways (e.g., ERK/JNK pathway, mTOR signaling) and protein degradation effects [202]. To test whether TAOK2 as a stress-responsive kinase has a modulatory effect on Hippo pathway, cells were repeatedly cultivated in medium with low serum concentration (0.1%) and transfected with TAOK2 overexpressing plasmids. As TAOK2 was expressed strongly from the expression plasmid used in previous experiments, only 50% of the plasmid amount were transfected in these serum starvation experiments.

3.1.4.1 TAOK2 variant 2 leads to CREB phosphorylation under starvation conditions

In the first run, HEK293 cells were starved for 8 h, lysed, and tested for endogenous LATS1, YAP1 and CREB phosphorylation levels (**Fig. 14A, B**). The cells were transfected with two plasmid variants for TAOK2 overexpression, TAOK2 variant 1 (TAOK2_var1) and variant 2 (TAOK2_var2). It has been shown that the two TAOK2 gene variants play different roles in dendritic spine development, dependent on the development stage [96,107].

Variant 1 has a molecular weight of 140 kd and contains transmembrane domains, while variant 2 is shorter with a molecular weight of 120 kd. TAOK2_var1 expression levels remains constant during early embryonic development of the cortex, with a significant increase at perinatal and adult time points. In comparison, TAOK2_var2 could not be detected prior to E19 [78,94,203].

Overexpressed TAOK2 lead to increased phospho-YAP1 and phospho-LATS1 levels in HEK293 cells, as a possible response to cellular stress. Interestingly, increased TAOK2 expression (especially induced by TAOK2 variant 2) lead to upregulated CREB phosphorylation as well, suggesting a potential link between TAOK2 and calcium signaling. This has been observed before in hippocampal neurons, where TAOK2-mediated calcium compartmentalization was necessary for dendritic spine maturation [85]. CREB is recognized for its role in the adaptive stress response and its regulation by ERK1 and ERK2 [204,205]. In this case, nutrient deprivation as stressful environment might activate MAPK and TAOK signaling, leading to CREB upregulation and changes in intracellular processes.
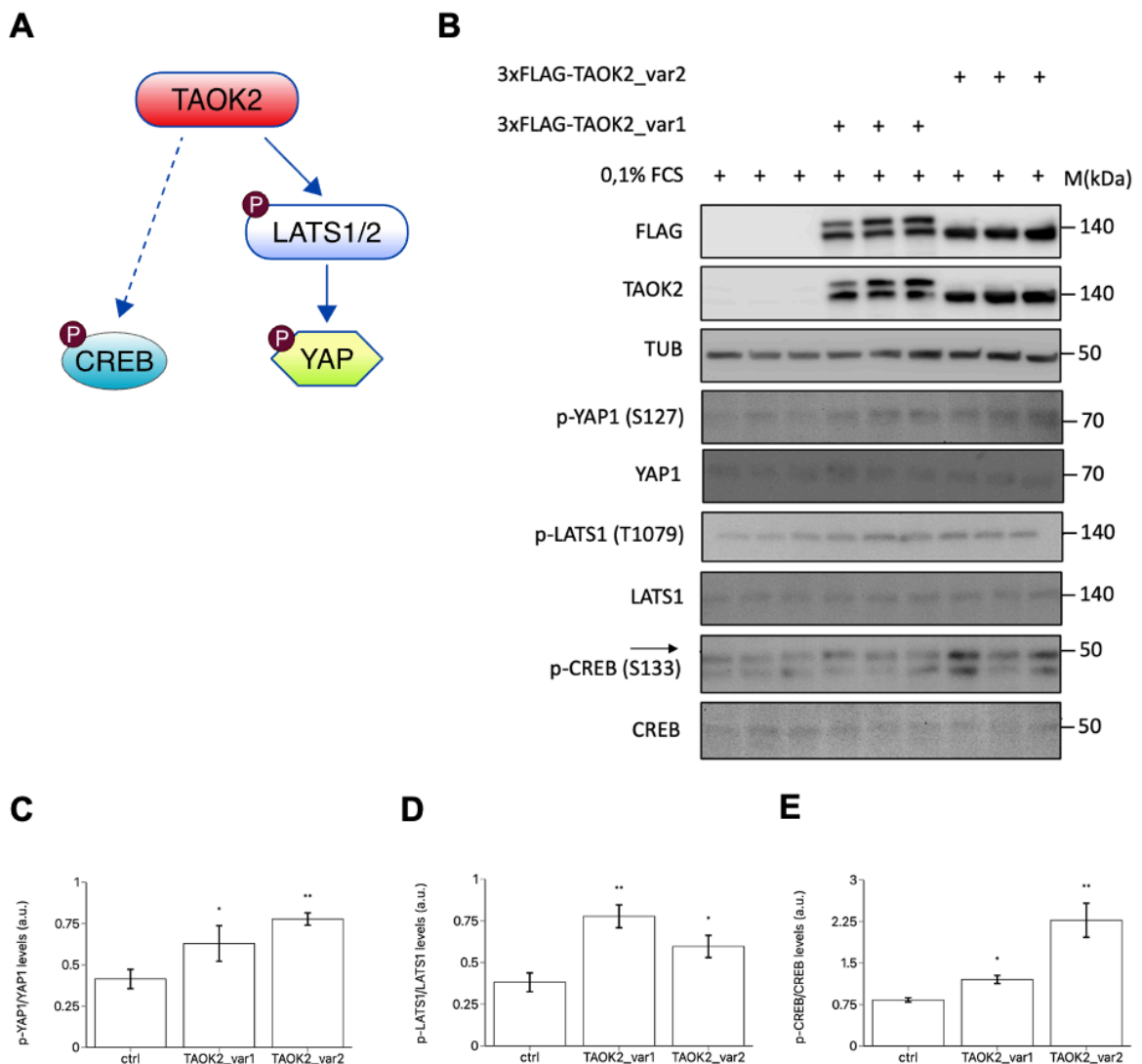
Fig. 14. TAOK2 variant 2, but not variant 1, increases CREB phosphorylation under serum starvation.

(**A**) Schematic map of TAOK2-induced phosphorylation of downstream Hippo targets and CREB. (**B**) Overexpression of TAOK2 variant 1 and variant 2 increases p-YAP1, p-LATS1 and p-CREB levels in HEK293 cells. TAOK2 expressing plasmids (3xFLAG-TAOK2_var1, 3xFLAG-TAOK2_var2) were transfected into HEK293 cells maintained in starvation medium containing 0.1% FCS for 8 h before lysis. Serum starvation is used as a method to induces cellular stress and activate MAPK. Western blot analyses were performed using the denoted antibodies. (**C, D, E**) Quantification of p-YAP1 (C), p-LATS1 (D) and p-CREB (E) shown in (B). Significance was calculated using a Kruskal-Wallis test, n=3 per group, values represent paired band measurements. Error bars show SEM with *, P < 0.05, **, P < 0.01, and n. s., not significant. FCS: Fetal Calf Serum.

3.1.4.2 Starvation: 6 h (0.1% FCS), Stimulation: 30 min (10% FCS)

In the second run, different serum conditions were used: 6 h starvation time at 0.1% FCS and 30 min stimulation time at 10% FCS. The assumption is that Hippo pathway is active under stress at low serum conditions, with increased LATS1 phosphorylation levels. In consequence, high serum conditions would inactivate Hippo pathway (**Fig. 15A**). Phosphorylation of MOB1 by STK3/4 facilitates the activation of LATS1/2, making it a valuable indicator of upstream Hippo pathway activity [206,207]. Starvation alone led to increased p-MOB1 levels. Additional overexpression of TAOK2_var1 further increased MOB1 phosphorylation, while overexpression of TAOK2_var2 showed no effect on MOB1 phosphorylation (**Fig. 15B).** CREB protein levels were upregulated upon stimulation with 10% FCS. Overexpression of TAOK2_var1 and TAOK2_var2 also increased CREB phosphorylation (**Fig. 15D**).
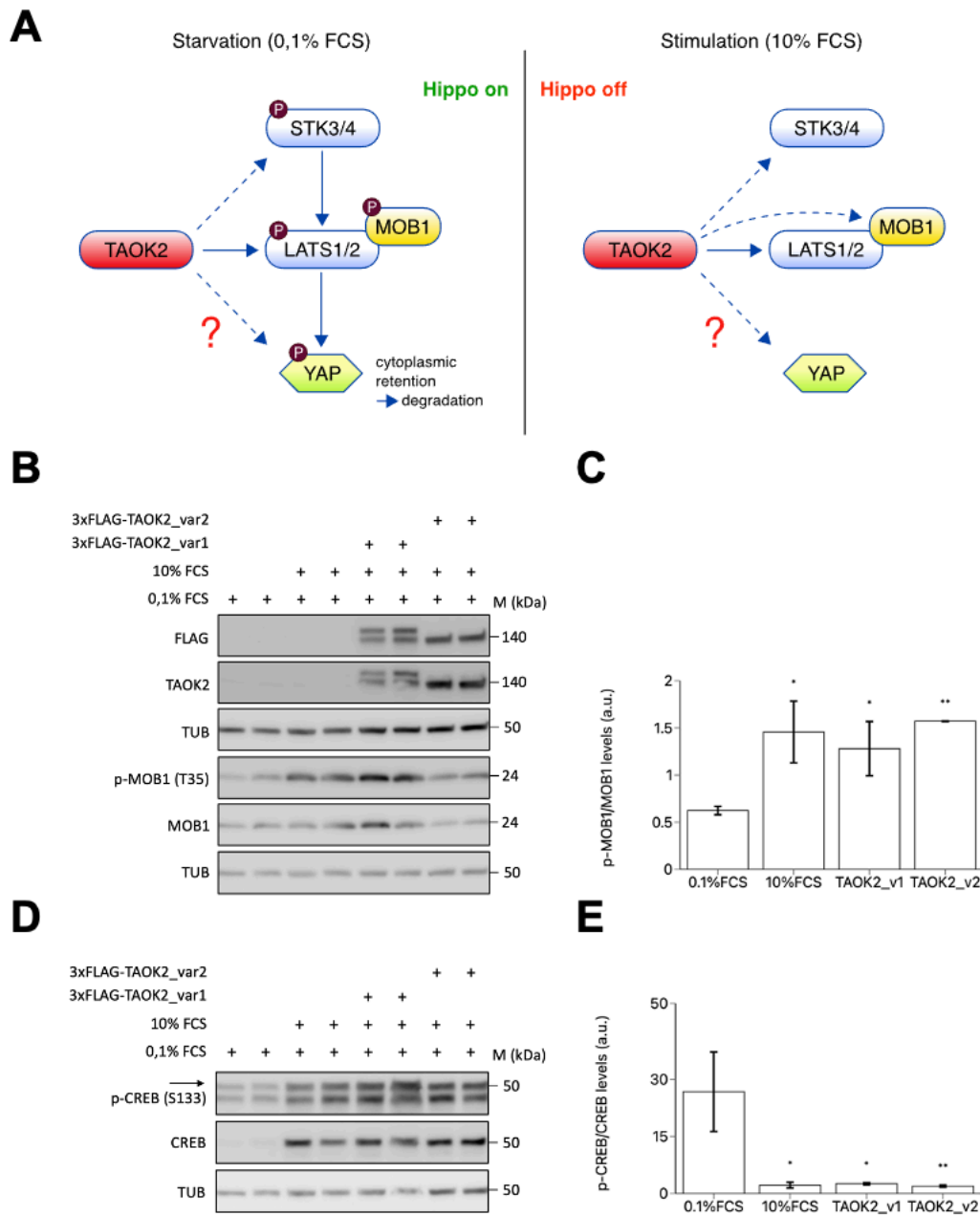
Fig. 15. Serum starvation versus stimulation effects on endogenous YAP1, LATS, MOB1 and CREB.

(**A**) Schematic map of TAOK2-Hippo pathway interactions under different serum conditions. When HEK293 cells are maintained in starvation medium containing 0,1% FCS, Hippo pathway and TAOK2-induced phosphorylation are expected to be activated in response to cellular stress. Under serum stimulation with 10% FCS, Hippo pathway and TAOK2 are expected to be inactive. All cells were starved for 6 h at 0.1% FCS. Two samples serves as control, while the remaining six samples were stimulated for 30 minutes at 10% FCS before lysis. (**B**) TAOK2 has no effect on p-MOB1 levels, displaying a gradient. TAOK2 expressing plasmids (3xFLAG-TAOK2_var1, 3xFLAG-TAOK2_var2) were transfected into HEK293 cells maintained in stimulation medium containing 10% FCS for 30 min before lysis. (**D**) TAOK2 increases p-CREB levels, which are also higher in the stimulated control samples compared to the starved control samples. (**C**, **E**) Quantification of p-MOB1 (C) and p-CREB (E) depictedin (B) and (D). Western blot analyses were performed using the denoted antibodies (TAOK2: Tao2-K16, FLAG: FLAG-M2). Significance was calculated using a Kruskal-Wallis test, n=2 per group, values represent paired band measurements. Error bars show SEM with *, P < 0.05, **, P < 0.01, and n. s., not significant. FCS: Fetal Calf Serum.

3.1.4.3 Starvation: overnight (0.1% FCS), Stimulation: 30 min (10% FCS)

In a following experiment, HEK293 cells were transfected with TAOK2 variant 1 (TAOK2_var1) only and starved over night. Plasmids expressing TAOK2 and YAP1 were introduced into HEK293 cells maintained in starvation medium (0.1% FCS) overnight or in stimulation medium (10% FCS) for 30 min before lysis. TAOK2 increased phosphorylation levels of YAP1 under both serum conditions, with a stronger effect in starved samples (**Fig. 16A, B**). Same procedure was repeated with TAOK2- and LATS1-overexpression, showing an analogous increase in LATS1 phosphorylation levels (**Fig. 16C, D**).
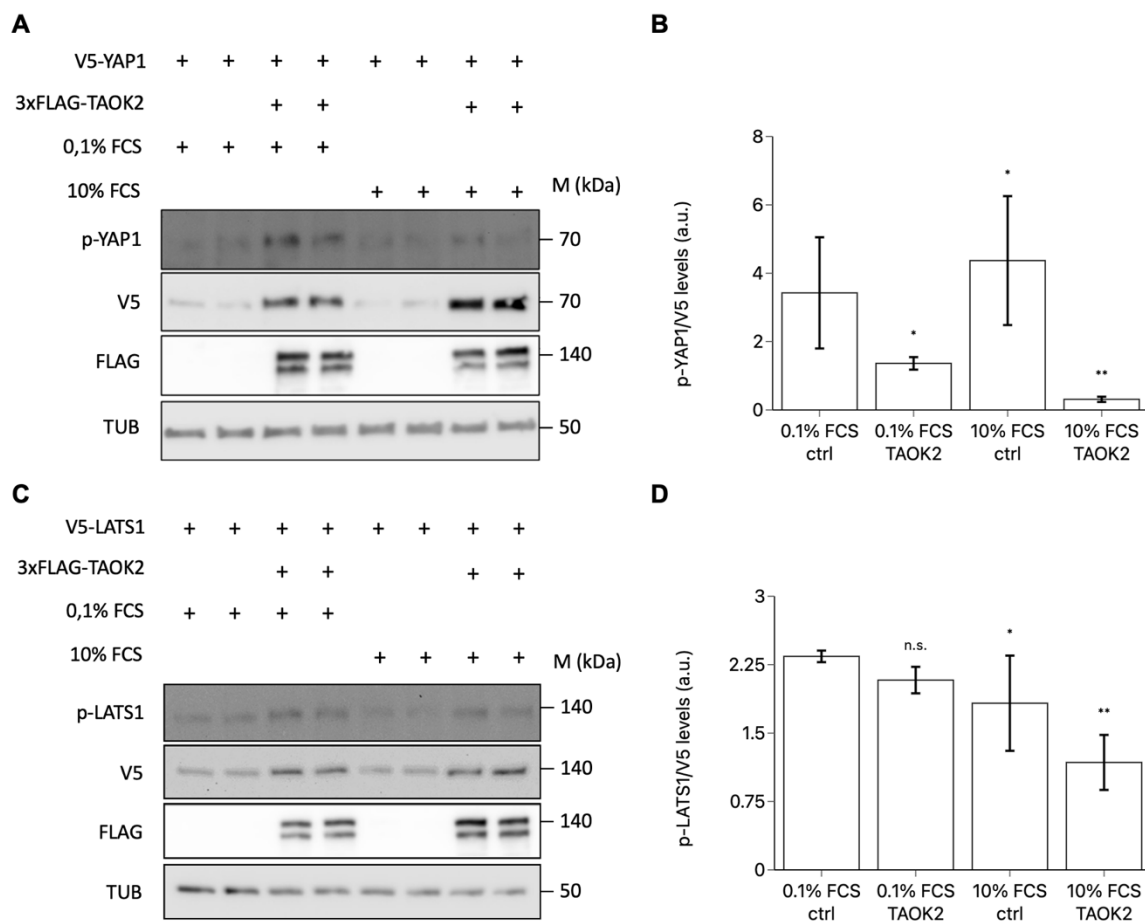
Fig. 16. TAOK2 upregulates phosphorylation levels of overexpressed YAP1 and LATS1 under different serum conditions.

(**A**) TAOK2 increases phosphorylation levels of YAP1 in HEK293 cells. TAOK2- and YAP-expressing plasmids (3xFLAG-TAOK2, V5-YAP1) were transfected into HEK293 cells maintained in starvation medium (0,1% FCS) overnight or in stimulation medium (10% FCS) for 30 min before lysis. (**C**) TAOK2 increases phosphorylation levels of LATS1 in HEK293 cells. Plasmids that express TAOK2 and LATS1 (3xFLAG-TAOK2, V5-LATS1) were transfected into HEK293 cells maintained in starvation medium (0,1% FCS) over night or in stimulation medium (10% FCS) for 30 min before lysis. V5- and FLAG-antibodies were used to detect V5- and FLAG-tagged proteins. (**B**, **D**) Quantification of p-YAP1 (C) and p-LATS1 (D) depicted in (A) and (C). Western blot analyses were performed using the denoted antibodies (TAOK2: Tao2-K16, FLAG: FLAG-M2). Significance was calculated using a Kruskal-Wallis test, n=2 per group, values represent paired band measurements. Error bars show SEM with *, $P < 0.05$, **, $P < 0.01$, and n. s., not significant. FCS: Fetal Calf Serum.

3.2   TAOK2 modulates synaptic activity

TAOK2 and its locus 16p11.2 are linked to neurodevelopmental conditions such as autism and schizophrenia [73,99]. At the molecular level, TAOK2 regulates cytoskeleton dynamics and promotes synaptic development by associating with Myosin Va upon phosphorylation by STK24, which is necessary for its dendritic localization [94,95]. Likewise, it contributes significantly to spine maturation through phosphorylation of the cytoskeletal GTPase *Septin-7* (SEPT7) and consequent stabilization of PSD-95. TAOK2 depletion lead to mislocated synapses established among the dendritic shaft and impaired calcium compartmentalization [85]. Furthermore, a murine model displaying a 16p11.2 deletion showed defective function of synpases and behavioral perturbations (e.g., hyperactivity, impaired habituation) [208]. In summary, these findings suggest that changes in TAOK2 function could disrupt neural connectivity, supporting the hypothesis that TAOK2 contributes to the development of neuropsychiatric disorders. In this context, the following experiment provides insight into TAOK2 function and its influence on synaptic signaling in primary neurons.

3.2.1   TAOK2 depletion results in increased activity of synaptic pathways

To measure the effects of functional versus altered TAOK2 activity on neural signaling, a multiparametric profiling tool called pathwayProfiler was performed in primary cortical neurons from E15.5 old mouse embryos and treated with different stimuli to either enhance (BIC, BDNF) or silence (TTX) synaptic activity (**Fig. 17A, B**). TAOK2 knockdown was performed by using an AAV-mediated delivery of shRNA (**Fig. 17C**), while control neurons were incubated with scrambled shRNA to guarantee a functional TAOK2. The experiment was performed in accordance to the developmental stages of mouse neurons which were sufficiently mature at DIV14 (**Fig. 17D**).
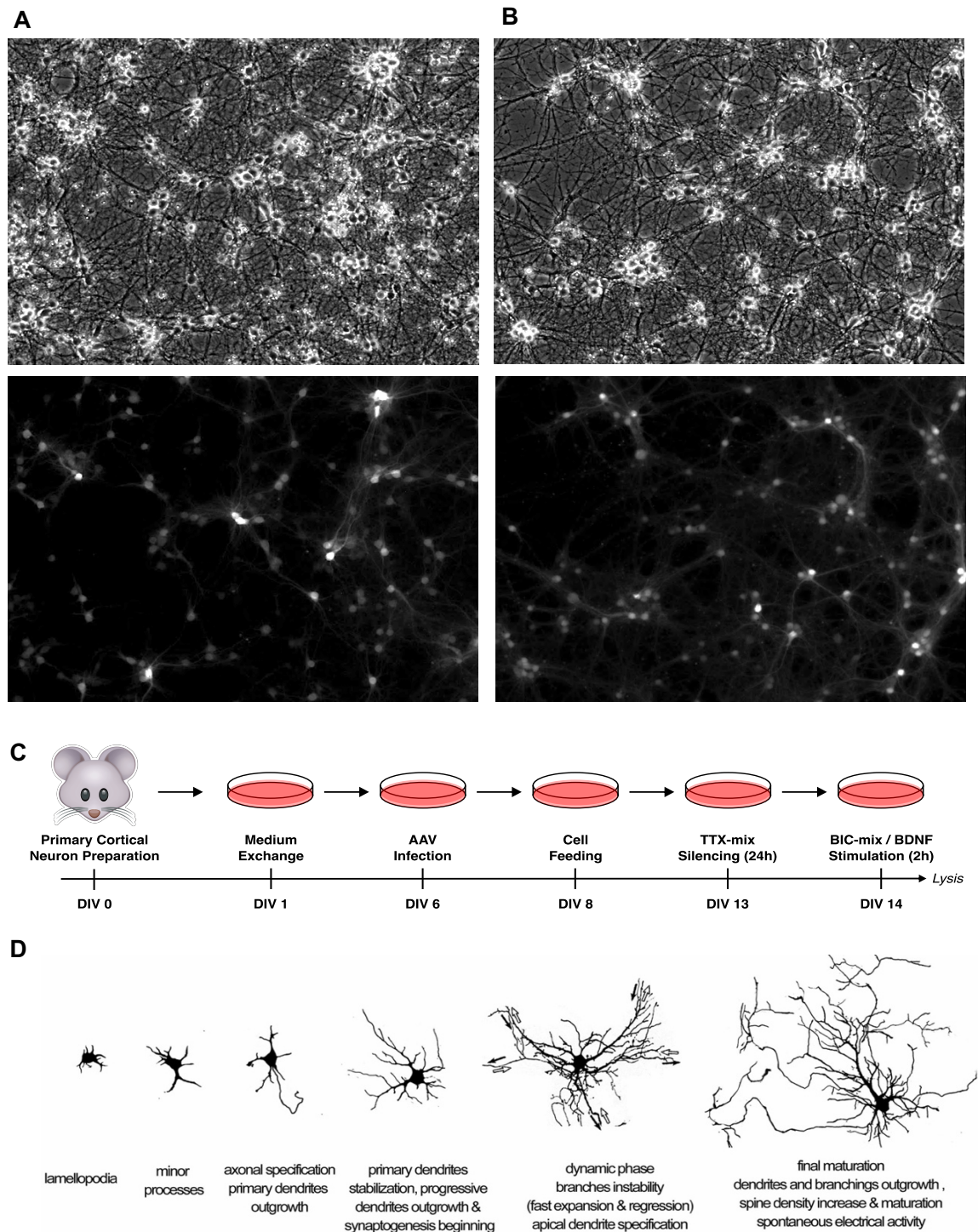
Fig. 17. Experimental workflow for the pathwayProfiler assay in primary cortical neurons.

Control images of GFP expression taken on DIV 12 of the neurons infected with AAV containing (**A**) an EYFP control and (**B**) a TAOK2 shRNA. (**C**) Experimental timeline: Cells were plated on DIV0, the plating medium was exchanged by culture medium on DIV 1. On DIV 6, cells were infected with adenoviral vectors (AAV) to introduce the barcoded Pathway PROFILER sensors, the TAOK2 shRNA and the EYFP control. On DIV8, fresh medium was added to the cells. On DIV13, 24 h before lysis, cells were treated with an inhibiting TTX-mix. On DIV14, the stimulating compounds BIC-mix/BDNF were added and incubated for 2 h, followed by cell lysis and further analysis of the samples. (**D**) Developmental stages of mouse and rat hippocampal neurons in vitro, corresponding to the timeline above (Baj et al., 2014).

To detect simultaneous signaling events, cells were infected with AAV particles containing the pathwayProfiler pool, a library of 52 barcoded sensors (**Figure 18A-D**). The sensors consist of short promoters, clustered transcription factor binding sites or enhancers linked to molecular barcodes and to a luciferase reporter [193].
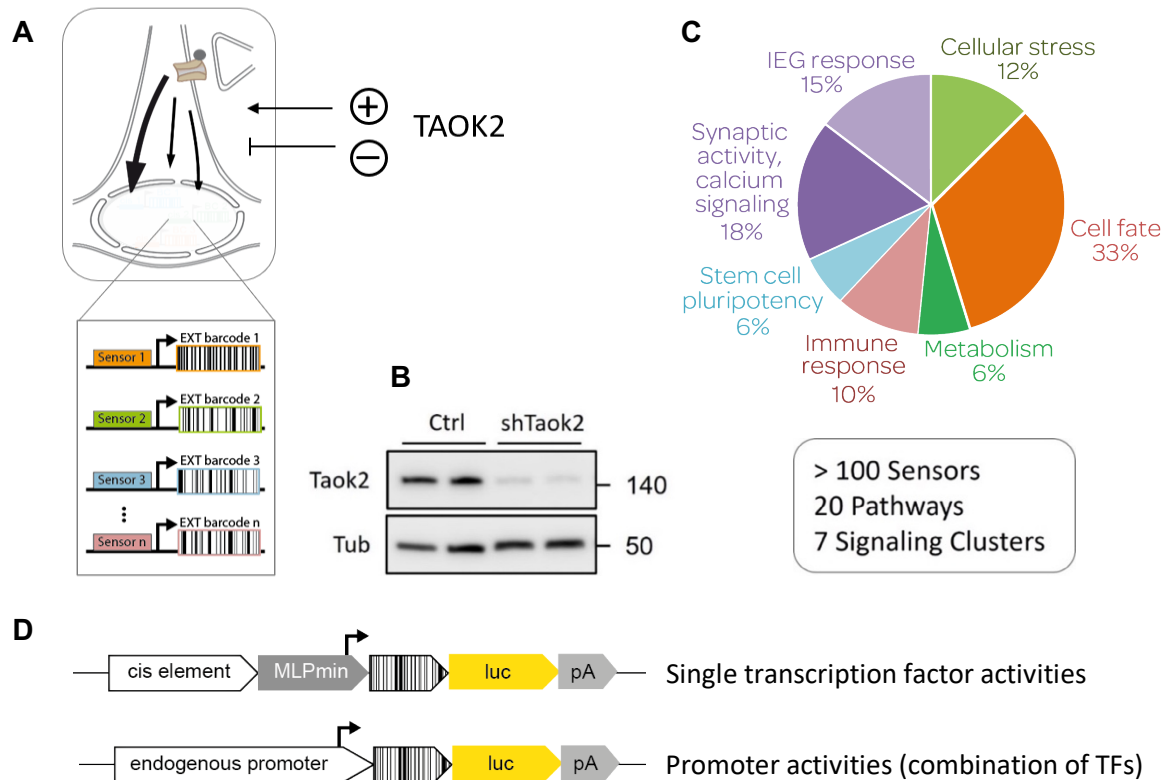
Fig. 18. Principle of the multiparametric pathwayProfiler.

(**A**) Scheme of the multiparametric pathwayProfiler assay consisting of barcoded sensors. (**B**) The assay was performed in cells with functional (ctrl) or depleted TAOK2 (shTaok2), validated by Western Blotting. (**C**) Pie chart and description visualizing the signaling clusters addressed by the pathwayProfiler assay. (**D**) Different types of sensors detecting either single transcription factor activities or promoter activities.

BIC and BDNF stimulation led to increased activities of multiple pathway sensors in both wildtype and TAOK2 depleted samples. However, the BIC-/BDNF-stimulated, TAOK2 depleted samples displayed an even stronger upregulation of in signaling pathways associated with neural activity and cellular stress (**Fig. 19A**). The following sensors showed the strongest response in both *TAOK2* knockdown and wildtype neurons: NR4Ap, EGR1p, FOSp, SARE - MLP and FOSBp. As this profiling assay monitors transcription factor activities as distal endpoints of signaling cascades, increased synaptic activity corresponds with a higher transcriptional output of sensors that respond to synaptic activity, e.g., SARE, EGR1p, and FOSBp. Notably, co-treatment of each BIC and BDNF with TTX resulted in a strong inhibition of upregulated sensor activities. In total, shTAOK2 treated

samples showed a globally higher background, while the genetic effect alone (depletion of TAOK2) was sufficient to increase sensor activity. Remarkably, sensor activity was stronger in untreated shTaok2 samples, compared to BIC- and BDNF- stimulated samples **(Fig. 19B)**. The highlighted sensor containing the SARE region has previously displayed advantages in comparison to other neuronal activity reporters (e.g., higher fold-change activation, well investigated structure) and has therefore been established as main sensor element by our group [193]. The final construct was called E-SARE and used in the following experiment to validate the findings from this profiling assay.

C
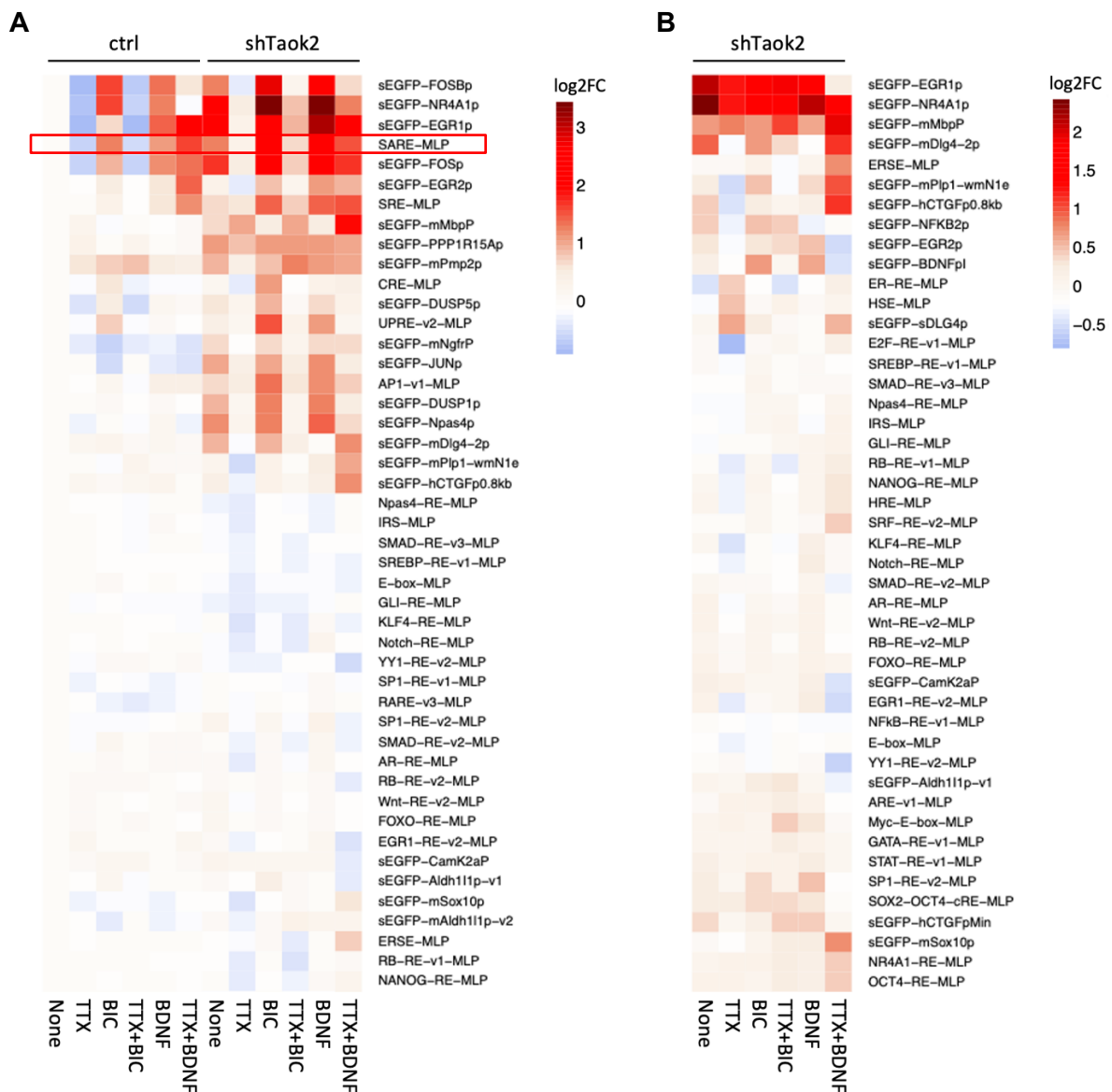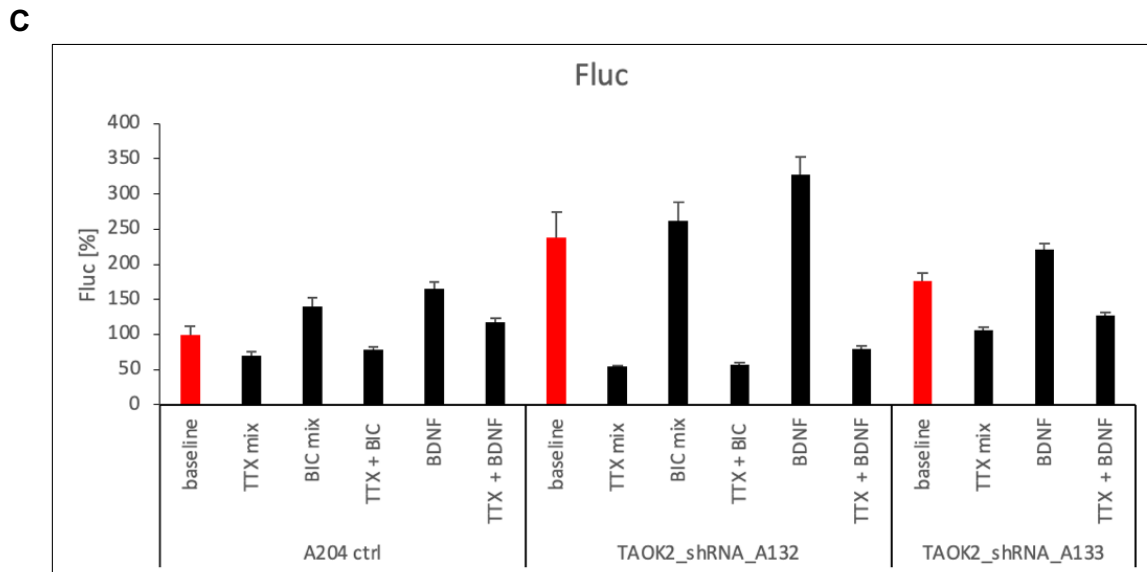
Fig. 19. TAOK2 knockdown increases synaptic activity measured by pathwayProfiler and E-SARE.

(**A**) Heatmap of 52 pathwayProfiler sensor responses in primary neurons (ctrl vs. shTaok2) as log2 fold changes between untreated control (ctrl none) and treated samples (TTX, BIC, TTX+BIC, BDNF, TTX+BDNF) measured by barcode sequencing. Both groups were silenced for 24 h with TTX, while stimulation with BIC or BDNF occurred in the last 2h before lysis. (**B**) Heatmap showing sensor responses in shTaok2 neurons as log2 fold changes, normalized to untreated shTaok2 samples (shTaok2 none). Several pathways associated with neural activity and cellular stress are upregulated in TAOK2 knockdown cells, with the strongest signal in untreated shTaok2 samples. Highlighted in red: the SARE sensor reported high fold-change activation in previous experiments and was established as main neural activity sensor (E-SARE). (**C**) Validation of the pathwayProfiler results using E-SARE. Primary cortical neurons from E15.5 old mouse embryos were infected with AAV introducing E-SARE-luciferase and TAOK2 shRNA into the cells. TAOK2 knockdown neurons showed higher activity levels in the baseline and BIC/BDNF-stimulated samples than in the control group, while TTX strongly reduced neuronal activity. E-SARE: Enhanced Synaptic Activity Responsive Element; BIC: bicuculline; TTX: Tetrodotoxin; BDNF: Brain Derived Neurotrophic Factor; Fluc: firefly luciferase.

3.2.2 TAOK2 regulates E-SARE activity

The E-SARE assay for monitoring synaptic activity was performed to verify the results from the pathwayProfiler. Changes in synaptic activity measured by the nuclear E-SARE sensor reflect signals from multiple synapse-to-nucleus signaling pathways (e.g., calcium signaling, MAPK signaling) (**Fig. 20C**). As described under 2.2.5., the E-SARE sensor was shown to recruit transcription factors such as CREB, MEF2, and SRF in response to synaptic stimuli such as BIC and BDNF, thereby strongly enhancing the expression of the firefly luciferase (**Fig. 20B**). In contrast, synaptic activity was inhibited by treatment with TTX. In this experiment, primary neurons were divided in three groups and infected with a AAV control (A204) and two TAOK2 shRNA AAVs (A132 and A133) to deplete *TAOK2* gene function. Treatment with TTX occurred 24 h before lysis, while BDNF and BIC-mix

were added 4 h before lysis (**Fig. 20D)**. Dynamic changes in E-SARE activity upon stimu-
lation/inhibition of synaptic activity was monitored by live cell luciferase recordings. Com-
pared to the control-baseline, both TAOK2 shRNA treated samples displayed higher base-
line activity (**Fig. 19C**). Treatment with the stimulating compounds BDNF and BIC led to
an increase in luciferase signal (up to 2.5-fold), especially in A132 knockdown samples,
whereas TTX-treated neurons showed decreased synaptic activity and luciferase signal
(up to 5-fold). Addition of BDNF or BIC to TTX led to mild enhancement of the luciferase
signal. In total, the AAV-induced shRNA knockdown of TAOK2 measured by pathwayPro-
filer was validated in this assay.
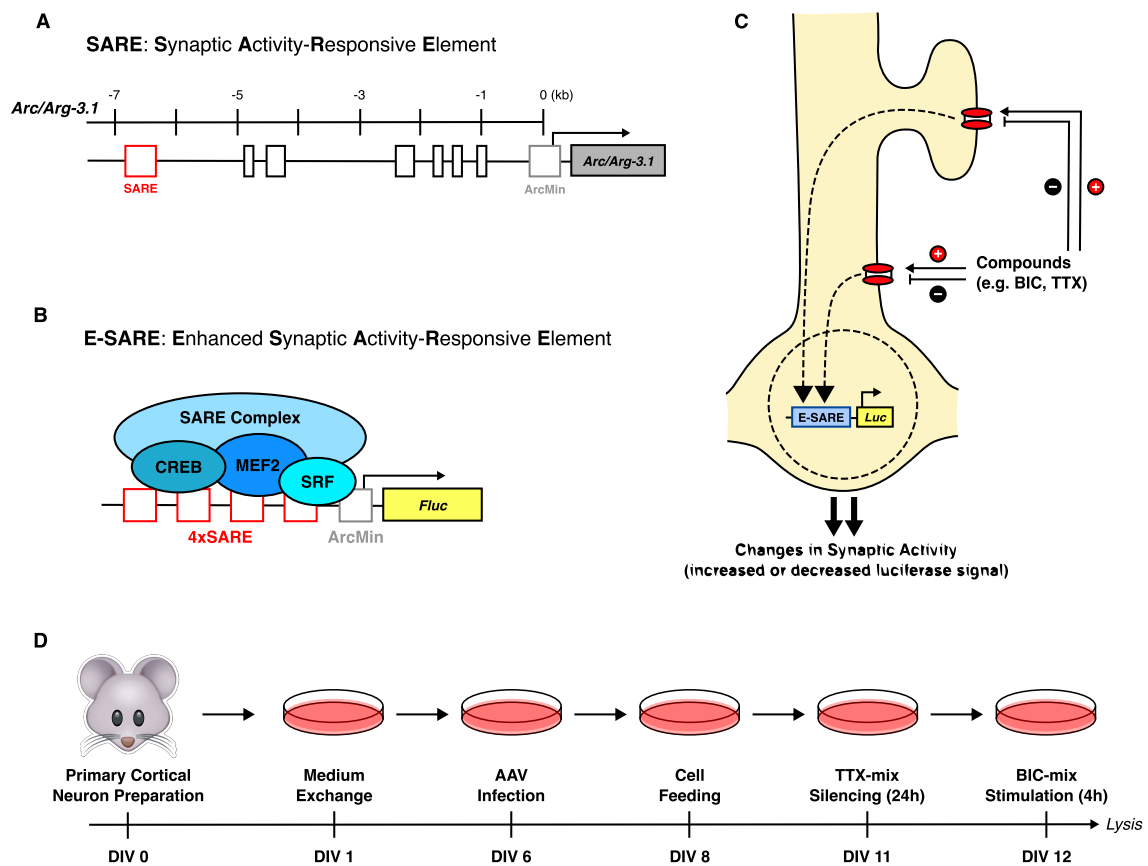
Fig. 20. Experimental workflow for the E-SARE assay in primary cortical neurons.

(**A**) Structure of the *Arc* (activity regulated cytoskeleton protein) gene promoter region containing the con-
served SARE (Synaptic Activity-Responsive Element) region (adapted from Kawashima et al., 2009). (**B**) The
transcription factors CREB, MEF2 and SRF bind to E-SARE (enhanced SARE, 4x clustered SARE elements)
upon synaptic stimulation; Fluc: firefly luciferase. (**C**) Treatment with stimulating compounds like BIC/BDNF
leads to increased luciferase reporter signal, while addition of TTX decreases the signal (scheme adapted and
modified from Marion Maier's Master Thesis, 2017). (**D**) Experimental timeline: Cells were plated on DIV 0, the
plating medium was exchanged by culture medium on DIV1. On DIV6, cells were infected with adenoviral
vectors (AAV) to introduce the TAOK shRNA and the EYFP control. On DIV8, fresh medium was added to the
cells. On DIV11, cells were treated with an inhibiting TTX-mix for 24 h. On DIV12, the stimulating compounds
BIC-mix/BDNF were added and incubated for 4 h, followed by cell lysis and further analysis of the samples.

4.   Discussion

4.1   TAOK2 modulates Hippo pathway activity

Prior to this work, studies indicated that only TAO family kinases TAOK1 and TAOK3 activated Hippo signaling by phosphorylating STK3/4 and LATS 1/2 [83,84,126]. Our group has then identified novel associations between TAOK2 and central members of the Hippo pathway through a split-TEV-based targeted interaction screen. The most important findings were biochemically validated in this thesis using co-immunoprecipitation and Western Blotting, contributing to the paper which was later published by our group [209]. TAOK2 was shown to increase LATS1 and YAP1 phosphorylation levels under different experimental conditions.

4.1.1   TAOK2 increases phosphorylation of LATS1 and YAP1 upon cellular stress

To determine the optimal lysis timepoint, a time course analysis of endogenous LATS1 and YAP1 protein levels was performed in TAOK2 overexpressed HEK293 cells. The results indicated that protein levels were too weak when lysis occurred earlier than 16-18 hours after transfection. Given the interaction between TAOK2 and LATS1, it was tested whether TAOK2 phosphorylates LATS1. Compared to TAOK2 with functioning kinase activity, introduction of an inactive kinase variant of TAOK2 (TAOK2-KD) did not result in increased phosphorylation of endogenous LATS1, indicating that the enzymatic activity of TAOK2 mediates phosphorylation of LATS1. This hypothesis was later verified by our group by carrying out an in vitro assay in HEK293 cells, showing that incubation of precipitated LATS1 with recombinant GST-TAOK2 lead to increased LATS1 phosphorylation in the presence of ATP [209].

The interactions between TAOK2 and other Hippo pathway members, e.g., SAV1 and MOB1, are not as well elucidated as the TAOK2-Hippo core kinase cassette interactions. Western Blot results presented in **Fig. 15B** showed no clear effect of TAOK2 on MOB1 phosphorylation levels. The previously identified interaction between TAOK2 and upstream Hippo pathway kinases STK3/4 was validated using co-immunoprecipitation (**Fig. 10B)**. However, at the time of conducting this research, it remained unclear whether TAOK2 directly phosphorylates STK3/4. Results presented in our paper confirmed showed that the phosphorylation levels of STK3/4 and MOB1 alike were elevated in HEK293 cells that underwent induction of TAOK2 expression with doxycycline [209]. Against this background and with reference to the targeted split-TEV interaction assay depicted in

Fig. 7, it is assumed that TAOK2 binds to LATS kinases via MOB1 phosphorylation. TAOK2 might also bind to the core kinase complex via the STK3/4 adaptor protein, SAV1 (personal communication with M. Wehr).

The activity of Hippo downstream effectors YAP1/TAZ can be regulated respectively inhibited by canonical Hippo signaling cascade-mediated phosphorylation and through several non-canonical mechanisms [210]. Like TAOK2, the angiomotin (AMOT) family proteins were identified as potential tumor suppressors which directly inhibit YAP1 through different mechanisms including cytoplasmic retention, ubiquitin-mediated destabilization of YAP1 and enhanced activation of STK3/4 and LATS1/2 [127,211,212]. With reference to the presented experiments testing the effect of serum starvation vs. stimulation on Hippo signaling and TAOK2, a study indicated that serum starvation induced phosphorylation and activation of LATS1/2, leading to stabilization of the AMOT isoform p130 [211]. Consequently, AMOT promoted ubiquitination and degradation of YAP1 via recruiting the E3 ubiquitin ligase AIP4 (atrophin-1 interacting protein 4)[211]. Interestingly, TAOK2 also bound to AMOT in both the split TEV screen and the biochemical analysis.

To find out more about the regulation of TAOK2 and its association with AMOT, further experiments are needed to study the impact of TAOK2, AMOT protein family members AMOT and AMOT-like proteins AMOT-like 1 and 2 (AMOTL1/2) on LATS1/2 kinases, YAP1, and the YAP1 transcriptional targets *CYR61* and *CTGF* [118,127,135].

4.1.2 Effects of TAOK2 inactivation on Hippo Signaling and cell behavior

Most of the experiments in this thesis investigating TAOK2 and Hippo signaling were conducted using HEK293 cells transfected with TAOK2 plasmids for TAOK2 overexpression. Increased TAOK2 protein levels resulted in elevated phosphorylation levels of YAP1, decreased expression of its targets *CYR61* and *CTGF* and diminished rates of cell proliferation [209]. Furthermore, exploring the effects of TAOK2 inactivation on Hippo signaling and cellular activities, including cell proliferation and migration, is also an important area of research. Previous studies indicated that inactivation of tumor suppressor genes involved in the Hippo pathway resulted in elevated cell proliferation rates [115,213]. Our group confirmed this finding by using the CRISPR inhibition (CRISPRi) technique to generate cell lines which stably expressed sgRNAs against TAOK2 (*sgTAOK2i*) to reduce TAOK2 protein amount [209]. Following assays conducted in HEK293_sgTAOK2i cells revealed decreased phosphorylation levels of both LATS1 and YAP1. As YAP1 stimulates the expression of *CYR61* and *CTGF* [118,135], additional RT-qPCR experiments were run to measure *CYR61* and *CTGF* transcript levels. These were significantly increased in TAOK2 depleted HEK293_sgTAOK2i cells, thus confirming that TAOK2 regulates YAP1 transcrip-

tional activity [209]. Collectively, these results reinforce the idea that TAOK2 with its tumor suppressing properties complexes core kinases of the Hippo signaling pathway, influencing YAP1-mediated transcriptional activity and proliferation.

4.1.3 Comparison of TAOK2 with TAOK1 and TAOK3

To contrast the role of TAOK2 on LATS1 phosphorylation with the previously known Hippo pathway activators TAO1 and TAOK3, TAOK1/2/3 were each co-transfected with LATS1 into HEK293 cells and lysed after 20 h incubation time. TAOK1 significantly increased p-LATS1, while TAOK2 and TAOK3 showed a weaker, but still significant effect. These observations aligned with results from the split TEV interaction assay and with previously published research works [126,198,199,209]. As TAOK2 shares close structural and functional similarities with TAOK1 and TAOK3, TAOKs have overlapping functions in different disease contexts, such as cancer, neurodevelopmental disorders, and immune response.

For instance, both TAOK1 and TAOK2 contribute to synapse development in neurons [95], influence neurodevelopmental disorders such as autism [94,107,214], and are involved in the advancement of Alzheimer's disease by phosphorylation tau protein [215,216]. Similarly, TAOKs exhibit overlapping functions in hereditary immunity, with each of the three kinases demonstrating antiviral activity against Influenza A virus infection [217]. Additionally, elevated levels of TAOK1 and TAOK3 are associated with breast cancer [218–220], and heightened expression of TAOK2 and TAOK3 is linked to melanoma [220,221]. On the contrary, there are numerous reports where TAOKs exhibit divergent effects. For example, while TAOK1 is found in increased amounts in lung cancer tissues [218], TAOK2 shows reduced expression in lung tumor samples [222]. Similarly, overexpression of TAOK1 is observed in colorectal cancer tissues [218], whereas TAOK3 levels are diminished in tissues from colorectal cancer patients [223].

Nevertheless, TAOKs have been identified as tumor suppressors due to their involvement in Hippo signaling [126,198,199,209]. Whether TAOKs act as tumor promoters or suppressors depends on varying cellular environments or extracellular stimuli, an area that requires further exploration. In this thesis, interactions between TAOK1, TAOK2, TAOK3 and Hippo pathway components (especially LATS1) were explored according to the results from the split TEV protein-protein interaction screen [209], showing similar effects on LATS1 phosphorylation.

4.1.4 Limitations and future directions

To better characterize the interactions between TAOK2 and Hippo pathway members, a series of experiments testing different environmental conditions such as nutrient depriva-

tion (6 h, 8 h, overnight), metabolic stress induced by 2-DG, two different TAOK2 plasmid variants and transfection of gradual amounts of TAOK2 plasmid was conducted. The experiments using 2-DG were not presented due to inconsistent results, considering the transient nature of the assays which did not turn out to be a suitable cellular system for inducing metabolic stress. For improved quality, these should be repeated using stable cell lines.

Obtaining consistent Western blotting and co-immunoprecipitation results was challenging by reason of probable deviations throughout the procedure, considering the insufficient experience of the experiment conductor. Trying out different antibodies and plasmid constructs has already provided valuable information; however, an extensive trouble shooting could improve efficiency and lead to more accurate results. To optimize TAOK2 expression, it would be of advantage to generate a stable HEK293 cell line using a selection antibiotic like doxycycline or puromycin. Compared to transient transfection, which introduces DNA that remains in the cells for a couple of days, stably integrated and antibiotic-induced expression of TAOK2 would persist long-term and avoid repeated transfections with increased risk of inaccuracy [224]. A stable cell line would also facilitate investigation of physiological effects (growth, proliferation, migration, survival) in cells.

Several attempts were undertaken to examine cell viability and proliferation in transiently transfected cells, e.g., using Crystal Violet Assays or the Celigo Image Cytometer, which were not consistent enough to be integrated in this work. Our group later examined the influence of TAOK2 on cell proliferation by comparison of HEK293 cells containing a stable doxycycline (dox) inducible *TAOK2* gene (TAOK2-dox) to non-inducible control cells. This was measured using a Cell Counting Kit-8 (CCK-8) assay at various timepoints between 8h and 96 h after plating. It was shown that TAOK2-dox cells exhibited slower proliferation compared to the control cells. Also, a scratch wound experiment was conducted to evaluate the impact of TAOK2 on cellular migration, resulting in slower migration of the doxycycline induced TAOK2-dox cells [209]. These results supported the suppressive role of TAOK2 on YAP1-mediated signaling in cancer development.

4.2   TAOK2 regulates synaptic activity

Situated on the 16p11.2 genomic region, TAOK2 has been recognized as a schizophrenia susceptibility gene linked to neurodevelopmental and psychiatric conditions [98–100]. At a cellular and molecular level, TAOK2 plays a a pivotal role in the modulation synaptic plasticity and formation of functional dendritic spines [85,94]. Previous studies showed that TAOK2, which is a MAPKKK, activates p38 MAPK and SAPK/JNK cascades as a response cellular stress [80–82]. Against this background, TAOK2 function was tested by introducing a shRNA via adenoviral vectors into primary cortex neurons to knock down TAOK2 gene expression.

First, a multiparametric phenotypic screening assay called pathwayProfiler (Systasy Bioscience GmbH) was applied on the cells to compare the levels of synaptic activity indicated by the luciferase readout in TAOK2 depleted vs. control cells. The results displayed a strong increase in synaptic activity in TAOK2 depleted cells, indicated by the enhanced activity of the sensors NR4A1p, FOSp, FOSBp, EGR1p, and SARE-MLP. These sensors are involved in signaling pathways associated with neural activity and cellular stress, suggesting that TAOK2 knockdown might upregulate MAPK activity via ERK1/2. The ERK1/2 branch of MAPK signaling is pivotal in controlling cell proliferation and differentiation across various cell types, with a notably high expression in mature and terminally differentiated neurons [63,225]. Activation of ERK1/2 in neurons, triggered by excitatory glutamatergic signals, leads to the phosphorylation of specific targets like RSKs and MSKs [63]. These phosphorylated proteins then migrate to the nucleus, where ERK1/2 further phosphorylate transcription factors like CREB. This cascade is essential for mediating synaptic plasticity and enhancing neuronal function [226]. As shown by Xiao Ma in her PhD thesis, TAOK2 knockout in neurons that underwent stimulation with AMPA and NMDA led to decreased ERK1/2 phosphorylation, thus confirming the results from the pathwayProfiler biochemically [227].

Additionally, the results could be validated by using immunocytochemistry (ICC) to better visualize and localize the interaction between TAOK2 and ERK1/2 in neurons. For this purpose, TAOK2 depleted HEK293 cells (e.g., using CRISPRi) and HEK293 cells with stable integration of doxycycline inducible TAOK2 [209] would be seeded and cultured for up to 24h, followed by immunostaining. This step includes fixation of the cellular proteins, permeabilization of the cell membranes to enable the large antibodies to traverse membranes, and incubation of fluorophore-conjugated primary antibodies against ERK1/2 and TAOK2. After washing and incubation with secondary antibodies, the cells would be visualized using microscopy [228]. To further detect and quantify TAOK2 dependent gene ex-

pression levels, one could conduct real-time quantitative PCR (RT-qPCR), assessing RNA amounts of ERK1/2 downstream transcription targets c-*fos*, c-*jun* or *CREB* [229].

Next, synaptic activity was monitored by the E-SARE assay consisting of a clustered SARE sensor (E-SARE) coupled to a firefly luciferase. The cells were also infected with adenoviral vectors containing two variants of shTAOK2 and with an AAV control. TAOK2 inactivation led to a global increase in synaptic activity, which methodically validated the AAV-induced shRNA knockdown of TAOK2 and the results of the pathway Profiler assay. However, pathwayProfiler results from experiments conducted after this work indicate that a loss-of-function of TAOK2 in neurons isolated from Taok2 (fl/fl) x Emx1-Cre knockout mice reduces sensor activity, which is contrary to the results of this work (personal communication with M. Wehr).

These findings could be explained by the different methodical approaches to inactivate TAOK2 in primary neurons. The introduction of short hairpin RNA (shRNA) into neurons by infection with viral vectors, as applied in this work, has several advantages such as uncomplicated production and efficient long-term knockdown of the targeted gene. Disadvantages of this approach are the inability to adjust suppression levels, impeding the analysis of genes that are implicated in cell survival, development, and regulation of cell cycle. Further, shRNAs can affect the expression of genes other than the intended target, resulting in off-target effects such as down-regulation of other genes and consequent up-regulation of the global synaptic activity (personal communication with M. Wehr). Therefore, using conditional gene knockout to delete TAOK2 might reduce nonspecific effects and give a more accurate picture of TAOK2 function in neurons.

4.2.1 Clinical relevance and therapeutic approaches targeting TAOK2 and the Hippo pathway

Over the past twenty years, extensive research has been devoted to studying the Hippo pathway, classifying it as a pivotal controller of cell growth and proliferation during development and pathogenesis. Notably, the downstream Hippo signaling effectors, YAP1/TAZ, have emerged as significant targets for new cancer therapies due to their role in tumor formation and migration [150,230–232]. Additionally, the Hippo pathway contributes to proper development and connection of the nervous system, being associated with neurological and psychiatric diseases [166,168–170]. It also modulates immune functions and promotes regeneration and wound healing [150].

In their work "Mechanisms of Hippo pathway regulation", Meng et al. suggest broadening the scope of the Hippo pathway and to include proteins that directly influence the activity of LATS1/2 and/or the transcriptional output of YAP1/TAZ as part of Hippo signaling [233]. In

this context, TAOK2 could be perceived not only as a modulator, but as a Hippo pathway member on its own. A recent study about the prognostic effect of Hippo pathway components in lung squamous cell carcinoma cancer identified TAOK 1/2/3 as mutational Hippo pathway core genes with prognostic roles, next to LATS1/2 and WWC1 [234]. However, it is important to acknowledge the significance of Hippo signaling in maintaining physiological homeostasis and regeneration, besides its involvement in pathological processes [235].

Since TAOK2 displays tumor suppressor characteristics, its decreased expression is expected to advance tumor progression. To determine the clinical implications of TAOK2 downregulation, our group examined TAOK2 expression across 28 distinct cancer types and assessed the survival outcomes of individuals with cancer using patient specimens listed in The Cancer Genome Atlas (TCGA) index [209]. The examination revealed a correlation between decreased TAOK2 expression and shorter survival durations across various cancers, including head and neck squamous cell carcinoma, kidney chromophobe, brain glioma, lung and pancreatic adenocarcinoma. This observation was supported by an in vitro model displaying depletion of TAOK2 in human lung cancer (A549) cells and human glioma (U-138) cells using CRISPRi, creating A549_sgTAOK2i and U-138_sgTAOK2i cells. Cell proliferation was measured by CCK-8 assays, being increased in both TAOK2-depleted cell lines. With regard to LATS1, phosphorylation levels were reduced in both cell lines. Conversely, inducing TAOK2 expression in these cells led to lower proliferation but higher p-LATS1 levels. This was confirmed in a cellular model using the stable cell lines A549_TAOK2-dox and U-138_TAOK2-dox, where doxycycline-mediated TAOK2 induction reduced proliferation. Doxycycline alone did not affect wild type A549 and U-138 cell proliferation.

These findings reinforce the concept of TAOK2 controlling cell proliferation via Hippo pathway in the described tumor models. The tumor suppressor quality of TAOK2 is further evidenced by research in mice, which showed that mice with Taok2 depletion on one or both alleles demonstrated expansions in cerebral volume that were dependent on gene dosage [107]. Moreover, TAOK2 has been described as an oncogene in certain contexts, highlighting its cell type or tissue-dependent roles. A study in *BRAF* mutant melanoma cells revealed a link between TAOK2 activity and increased ATP uptake in cells that were resistant to BRAF inhibitor therapy. As TAOK2 is known to activate JNK signaling, it might contribute to drug resistance in these cells [221,236]. This dichotomy in TAOK2's role – as a tumor-suppressor and a tumor-promoter gene alike – adds a layer of complexity to our understanding of its role in cancer biology. Considering the involvement of TAOKs in a variety of pathological processes and diseases such as inflammation, apoptosis, immune regulation, cancer, drug resistance, autism disorder, and Alzheimer's disease [79], creating

targeted inhibitors for TAOK-related pathways could potentially mitigate their impact on the progression of these diseases. Staurosporine, a wide-spectrum inhibitor initially derived from Streptomyces species, was shown to inhibit TAOK2, but also many other serine/threonine protein kinases. Its lack of specificity and high toxicity thereby limit its clinical use [237]. The MST1 (STK4) Inhibitor 9E1 also suppressed TAOK2 activity, but displayed similar properties as staurosporine [238]. Two TAOK inhibitors called com pounds 43 and 63 were identified as ATP-competitive inhibitors with high specificity to TAOK1, TAOK2, and TAOK3 [239]. Moreover, compound 43 selectively targeted and inhibited cancer cells without affecting non-tumor cells, increasing mitotic cell death in cancer cells [239]. Given that reduced TAOK expression enhanced sensitivity to γ-radiation, compound 43 could potentially enhance the responsiveness of tumor cells to anticancer therapies [79,82]. Two additional compounds from a high-throughput screen, SW034538 and SW083688, showed significant inhibition of TAOK2, but their detailed characteristics are yet to be elucidated [240]. The findings presented in our paper highlight the clinical significance of TAOK2 expression levels in cancer prognosis and treatment response, further emphasizing the therapeutic potential of targeting TAOK2 in cancer. Research into developing TAOK-specific inhibitors is a promising field. By focusing on their kinase domains, it's possible to select inhibitors with high specificity that don't affect other MAP kinases [79]. Nevertheless, the effectiveness and safety of these potential drugs must be assessed in vivo. Conducting well-designed animal experiments is crucial to determine the effectiveness of TAOK inhibitors in disease models prior to advancing to human clinical trials.

TAOK2 plays a significant role in the brain, particularly in the regulation of synaptic functions and neuronal circuits, which is crucial for maintaining cognitive and emotional functions. Dysfunctional regulation of these processes is thought to contribute to the cognitive deficits and social impairments seen in schizophrenia and ASD [79]. TAOK2 is expressed in regions of the brain that are important for higher-order functions, such as the prefrontal cortex and hippocampus. Its role in neurodevelopmental processes such as neuronal migration and dendritic spine formation could help explain the structural and functional brain abnormalities often observed in schizophrenia and ASD [107,241]. Targeting pathways that interact with TAOK2 could help restore normal synaptic function and neuronal connectivity in affected patients. As a kinase, TAOK2 could be targeted with specific inhibitors or activators to regulate its activity in the brain. This approach would need to be carefully balanced, as both too much and too little TAOK2 activity could have negative effects on neuronal health and function. It might be particularly useful in a subset of patients who carry specific genetic variants or mutations in the gene. This approach aligns with the emerging field of precision medicine, where treatments are tailored to an individual's genetic and molecular profile. Another possibility would be the usage of TAOK2-targeted therapies in

combination with current antipsychotics or other emerging treatments for schizophrenia, potentially enhancing efficacy or reducing side effects. However, given the polygenic trait of schizophrenia involving approximately 300 identified risk genes [106], as well as the strong influence of environmental factors, it remains a challenging endeavor to fully explore its potential in preclinical and clinical studies and to target it safely in a therapeutic context.

Given its implication in both normal and pathological processes in the central nervous system, as well as its interaction with other signaling pathways, it is not surprising that genes related to the Hippo pathway have recently been linked to various psychiatric disorders. Chlorpromazine (an antipsychotic drug for schizophrenia (SZ)) was shown to suppress YAP1 by modulating Hippo signaling [242], while valproic acid (used to treat bipolar disorder (BD)) activated Hippo pathway via RASSF1a expression induction [172], both leading to apoptosis in cancer cells. Five of eight drugs, which are commonly used in BD and SZ treatment – amisulpride, aripiprazole, clozapine, quetiapine, and risperidone – showed a significant downregulation of Hippo pathway genes such as *NF2* and *WWC1* [166]. Consequently, upregulation of YAP/TAZ leads to reduced activity of pro-inflammatory pathways, including Wnt, Notch and NFκB signaling [244–248]. These effects might indicate the possibility of reversing Hippo-related inflammatory immune responses implicated in the development of affective disorders [166]. However, the implications of regular intake of antipsychotic drugs over many years or potential drug-drug interactions in cases of multiple drug administration represent a significant challenge. Identifying new pathways associated with psychiatric disorders that can be targeted by existing pharmacological treatments presents an opportunity to develop new therapeutic options for these debilitating conditions. This could help improve the mechanistic understanding of schizophrenia, autism and other psychiatric conditions, and also increase research and development efforts by major pharmaceutical companies.

In summary, this thesis supports the notion that TAOK2 regulates YAP1-mediated transcription by activating Hippo core kinases LATS1/2. Considering the tumor suppressor properties and involvement in neurodevelopmental disorders of both TAOK2 and Hippo signaling, amplifying their synergistic effects could be a promising avenue for future drug development strategies.

5. Acknowledgements

First, I would like to express my profound gratitude to my supervisor PD Dr. Michael Wehr for the opportunity to join his research group and to participate in this interesting project. Thank you, Micha, for your continuous support, empathy, patience, and for guiding me towards a more precise and disciplined working attitude.

Further, I am grateful to Prof. Dr. Moritz Rossner and to the entire lab team for the welcoming and familiar atmosphere in the lab, for the interesting Work-in-Progress presentations and their useful suggestions for my experiments. My special thanks go to Barbara Meisel, Monika Rübekeil, Nadia Gabellini and Johanna Zach for their constant technical support and to Beate Kauschat for providing me with primary neuron cultures. In addition, I would like to thank to Dr. Sven Wichert, Dr. Ben Brankatschk, Karin Neumeier, and Stefanie Behrens for helping me throughout the pathwayProlifer and luciferase assays.

Likewise, I am grateful to the German Academic Scholarship Foundation (Studienstiftung des deutschen Volkes) for the generous educational and financial support during my studies, and especially for the possibility to extend my studies to accomplish this thesis.

I also wish to express my eternal gratitude to my mother, Gabriela, for her unconditional love and support throughout my entire life. Finally, I sincerely thank my husband, Gerhard, for the wonderful journey we have had until now and for always encouraging me. Life is so much more beautiful with you.

6.   Affidavit
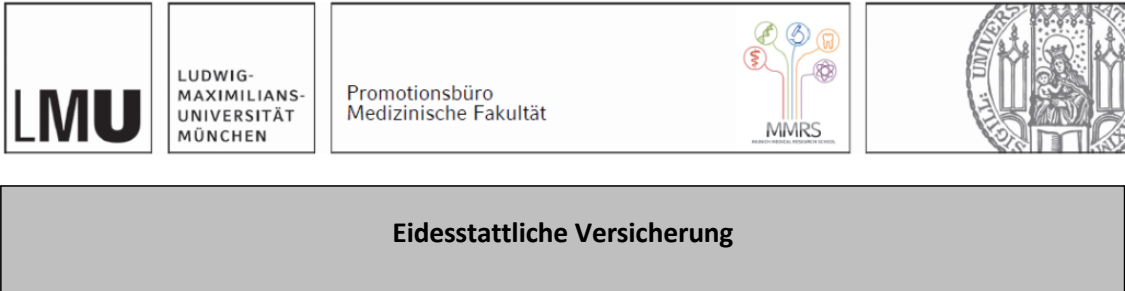
Eidesstattliche Versicherung

Wernigg, Madalina
_____
Name, Vorname

Ich erkläre hiermit an Eides statt, dass ich die vorliegende Dissertation mit dem Titel:

The Serine/Threonine Kinase Thousand and One Amino Acid Kinase 2 (TAOK2)

Regulates Hippo/YAP Signaling and Synaptic Activity

selbständig verfasst, mich außer der angegebenen keiner weiteren Hilfsmittel bedient und alle Erkenntnisse, die aus dem Schrifttum ganz oder annähernd übernommen sind, als solche kenntlich gemacht und nach ihrer Herkunft unter Bezeichnung der Fundstelle einzeln nachgewiesen habe.

Ich erkläre des Weiteren, dass die hier vorgelegte Dissertation nicht in gleicher oder in ähnlicher Form bei einer anderen Stelle zur Erlangung eines akademischen Grades eingereicht wurde.

Zürich, 14.02.2025   Madalina Wernigg
_____   _____
Ort, Datum   Unterschrift Doktorandin bzw. Dokto-
rand

7. Refences

1. Mental disorders [Internet]. [cited 2022 Mar 7]. Available from: https://www.who.int/news-room/fact-sheets/detail/mental-disorders

2. Ashok AH, Baugh J, Yeragani VK. Paul Eugen Bleuler and the origin of the term schizophrenia (SCHIZOPRENIEGRUPPE). Indian J Psychiatry. 2012;54(1):95–6.

3. Rees E, Creeth HDJ, Hwu HG, Chen WJ, Tsuang M, Glatt SJ, et al. Schizophrenia, autism spectrum disorders and developmental disorders share specific disruptive coding mutations. Nat Commun. 2021 Sep 9;12(1):5353.

4. Gogtay N, Vyas NS, Testa R, Wood SJ, Pantelis C. Age of Onset of Schizophrenia: Perspectives From Structural Neuroimaging Studies. Schizophr Bull. 2011 May;37(3):504–13.

5. Kaul D, Schwab SG, Mechawar N, Matosin N. How stress physically re-shapes the brain: Impact on brain cell shapes, numbers and connections in psychiatric disorders. Neurosci Biobehav Rev. 2021 May;124:193–215.

6. Weinberg MS, Johnson DC, Bhatt AP, Spencer RL. Medial prefrontal cortex activity can disrupt the expression of stress response habituation. Neuroscience. 2010 Jul;168(3):744–56.

7. Daftary S, Van Enkevort E, Kulikova A, Legacy M, Brown ES. Relationship between depressive symptom severity and amygdala volume in a large community-based sample. Psychiatry Res Neuroimaging. 2019 Jan;283:77–82.

8. Saleh A, Potter GG, McQuoid DR, Boyd B, Turner R, MacFall JR, et al. Effects of early life stress on depression, cognitive performance and brain morphology. Psychol Med. 2017 Jan;47(1):171–81.

9. Wang S, Zhao Y, Zhang L, Wang X, Wang X, Cheng B, et al. Stress and the brain: Perceived stress mediates the impact of the superior frontal gyrus spontaneous activity on depressive symptoms in late adolescence. Hum Brain Mapp. 2019 Dec;40(17):4982–93.

10. McEwen BS, Morrison JH. Brain On Stress: Vulnerability and Plasticity of the Prefrontal Cortex Over the Life Course. Neuron. 2013 Jul 10;79(1):16–29.

11. Wheelock MD, Rangaprakash D, Harnett NG, Wood KH, Orem TR, Mrug S, et al. Psychosocial stress reactivity is associated with decreased whole brain network efficiency and increased amygdala centrality. Behav Neurosci. 2018 Dec;132(6):561–72.

12. Radley JJ, Rocher AB, Miller M, Janssen WGM, Liston C, Hof PR, et al. Repeated Stress In-

duces Dendritic Spine Loss in the Rat Medial Prefrontal Cortex. Cereb Cortex. 2006 Mar 1;16(3):313–20.

13. Yang C, Shirayama Y, Zhang J chun, Ren Q, Hashimoto K. Regional Differences in Brain-Derived Neurotrophic Factor Levels and Dendritic Spine Density Confer Resilience to Inescapable Stress. Int J Neuropsychopharmacol. 2015 Mar 4;18(7):pyu121.

14. Magariños AM, McEwen BS, Flügge G, Fuchs E. Chronic Psychosocial Stress Causes Apical Dendritic Atrophy of Hippocampal CA3 Pyramidal Neurons in Subordinate Tree Shrews. J Neurosci. 1996 May 15;16(10):3534–40.

15. McLaughlin, K. J., Baran SE, Wright RL, Conrad CD. Chronic stress enhances spatial memory in ovariectomized female rats despite CA3 dendritic retraction: possible involvement of CA1 neurons. Neuroscience. 2005;135(4):1045–54.

16. Duman CH, Duman RS. Spine synapse remodeling in the pathophysiology and treatment of depression. Neurosci Lett. 2015 Aug 5;601:20–9.

17. Kang HJ, Voleti B, Hajszan T, Rajkowska G, Stockmeier C, Licznerski P, et al. Decreased Expression of Synapse-Related Genes and Loss of Synapses in Major Depressive Disorder. Nat Med. 2012 Sep;18(9):1413–7.

18. Berdenis van Berlekom A, Muflihah CH, Snijders GJLJ, MacGillavry HD, Middeldorp J, Hol EM, et al. Synapse Pathology in Schizophrenia: A Meta-analysis of Postsynaptic Elements in Postmortem Brain Studies. Schizophr Bull. 2020 Feb;46(2):374–86.

19. Glantz LA, Lewis DA. Decreased dendritic spine density on prefrontal cortical pyramidal neurons in schizophrenia. Arch Gen Psychiatry. 2000 Jan;57(1):65–73.

20. Forrest MP, Parnell E, Penzes P. Dendritic structural plasticity and neuropsychiatric disease. Nat Rev Neurosci. 2018 Mar 16;19(4):215–34.

21. Koenigs M, Grafman J. The functional neuroanatomy of depression: Distinct roles for ventromedial and dorsolateral prefrontal cortex. Behav Brain Res. 2009 Aug 12;201(2):239–43.

22. Mitra R, Jadhav S, McEwen BS, Vyas A, Chattarji S. Stress duration modulates the spatiotemporal patterns of spine formation in the basolateral amygdala. Proc Natl Acad Sci. 2005 Jun 28;102(26):9371–6.

23. Suvrathan A, Bennur S, Ghosh S, Tomar A, Anilkumar S, Chattarji S. Stress enhances fear by forming new synapses with greater capacity for long-term potentiation in the amygdala. Philos Trans R Soc B Biol Sci. 2014 Jan 5;369(1633):20130151.

24. Czéh B, Varga ZKK, Henningsen K, Kovács GL, Miseta A, Wiborg O. Chronic stress reduces the number of GABAergic interneurons in the adult rat hippocampus, dorsal-ventral and region-specific differences: Reduced Number of Hippocampal Gabaergic Neurons After CMS. Hippocampus. 2015 Mar;25(3):393–405.

25. Markram H, Toledo-Rodriguez M, Wang Y, Gupta A, Silberberg G, Wu C. Interneurons of the neocortical inhibitory system. Nat Rev Neurosci. 2004 Oct;5(10):793–807.

26. Zhang ZJ, Reynolds GP. A selective decrease in the relative density of parvalbumin-immunoreactive neurons in the hippocampus in schizophrenia. Schizophr Res. 2002 May;55(1–2):1–10.

27. Lewis DA, Curley AA, Glausier JR, Volk DW. Cortical parvalbumin interneurons and cognitive dysfunction in schizophrenia. Trends Neurosci. 2012 Jan;35(1):57–67.

28. Karolewicz B, Maciag D, O'Dwyer G, Stockmeier CA, Feyissa AM, Rajkowska G. Reduced level of glutamic acid decarboxylase-67 kDa in the prefrontal cortex in major depression. Int J Neuropsychopharmacol. 2010 May;13(04):411.

29. Page CE, Coutellier L. Prefrontal excitatory/inhibitory balance in stress and emotional disorders: Evidence for over-inhibition. Neurosci Biobehav Rev. 2019 Oct;105:39–51.

30. Birnbaum R, Weinberger DR. Genetic insights into the neurodevelopmental origins of schizophrenia. Nat Rev Neurosci. 2017 Dec;18(12):727–40.

31. Skene NG, Bryois J, Bakken TE, Breen G, Crowley JJ, Gaspar HA, et al. Genetic identification of brain cell types underlying schizophrenia. Nat Genet. 2018 Jun;50(6):825–33.

32. Jahangir M, Zhou JS, Lang B, Wang XP. GABAergic System Dysfunction and Challenges in Schizophrenia Research. Front Cell Dev Biol. 2021 May 14;9:663854.

33. Anderson KM, Collins MA, Chin R, Ge T, Rosenberg MD, Holmes AJ. Transcriptional and imaging-genetic association of cortical interneurons, brain function, and schizophrenia risk. Nat Commun. 2020 Jun 8;11(1):2889.

34. Uhlhaas PJ, Singer W. Abnormal neural oscillations and synchrony in schizophrenia. Nat Rev Neurosci. 2010 Feb;11(2):100–13.

35. Fogaça MV, Duman RS. Cortical GABAergic Dysfunction in Stress and Depression: New Insights for Therapeutic Interventions. Front Cell Neurosci. 2019 Mar 12;13:87.

36. Greer PL, Greenberg ME. From Synapse to Nucleus: Calcium-Dependent Gene Transcription in the Control of Synapse Development and Function. Neuron. 2008 Sep;59(6):846–60.

37. Parra-Damas A, Saura CA. Synapse-to-Nucleus Signaling in Neurodegenerative and Neuro-psychiatric Disorders. Biol Psychiatry. 2019 Jul;86(2):87–96.

38. Ma H, Groth RD, Cohen SM, Emery JF, Li BX, Hoedt E, et al. γCaMKII shuttles Ca2+/CaM to the nucleus to trigger CREB phosphorylation and gene expression. Cell. 2014 Oct 9;159(2):281–94.

39. Cohen SM, Suutari B, He X, Wang Y, Sanchez S, Tirko NN, et al. Calmodulin shuttling mediates cytonuclear signaling to trigger experience-dependent transcription and memory. Nat Commun. 2018 Jun 22;9:2451.

40. de Ligt J, Willemsen MH, van Bon BWM, Kleefstra T, Yntema HG, Kroes T, et al. Diagnostic Exome Sequencing in Persons with Severe Intellectual Disability. N Engl J Med. 2012 Nov 15;367(20):1921–9.

41. de Quervain DJF, Papassotiropoulos A. Identification of a genetic cluster influencing memory performance and hippocampal activity in humans. Proc Natl Acad Sci U S A. 2006 Mar 14;103(11):4270–4.

42. Voineagu I, Wang X, Johnston P, Lowe JK, Tian Y, Horvath S, et al. Transcriptomic Analysis of Autistic Brain Reveals Convergent Molecular Pathology. Nature. 2011 May 25;474(7351):380–4.

43. Zhang Y, Fan M, Wang Q, He G, Fu Y, Li H, et al. Polymorphisms in MicroRNA Genes And Genes Involving in NMDAR Signaling and Schizophrenia: A Case-Control Study in Chinese Han Population. Sci Rep. 2015 Aug 10;5:12984.

44. Zhai S, Ark ED, Parra-Bueno P, Yasuda R. Long-Distance Integration of Nuclear ERK Signaling Triggered by Activation of a Few Dendritic Spines. Science. 2013 Nov 29;342(6162):1107–11.

45. Li C, Götz J. Somatodendritic accumulation of Tau in Alzheimer's disease is promoted by Fyn-mediated local protein translation. EMBO J. 2017 Nov 2;36(21):3120–38.

46. Chong YH, Shin YJ, Lee EO, Kayed R, Glabe CG, Tenner AJ. ERK1/2 Activation Mediates Aβ Oligomer-induced Neurotoxicity via Caspase-3 Activation and Tau Cleavage in Rat Organotypic Hippocampal Slice Cultures. J Biol Chem. 2006 Jul;281(29):20315–25.

47. Sarantos MR, Papanikolaou T, Ellerby LM, Hughes RE. Pizotifen Activates ERK and Provides Neuroprotection in vitro and in vivo in Models of Huntington's Disease. J Huntingt Dis. 2012 Jan 1;1(2):195–210.

48. Rupprecht R, Di Benedetto B. Extracellular Signal–Regulated Kinases: A Role for Mood Disorders and the Emotional Component of Pain? Biol Psychiatry. 2017 Apr;81(8):639–41.

49. Einat H, Yuan P, Gould TD, Li J, Du J, Zhang L, et al. The Role of the Extracellular Signal-Regulated Kinase Signaling Pathway in Mood Modulation. J Neurosci. 2003 Aug 13;23(19):7311–6.

50. Hu Y, Hong W, Smith A, Yu S, Li Z, Wang D, et al. Association analysis between mitogen-activated protein/extracellular signal-regulated kinase (MEK) gene polymorphisms and depressive disorder in the Han Chinese population. J Affect Disord. 2017 Nov;222:120–5.

51. Manning G, Whyte DB, Martinez R, Hunter T, Sudarsanam S. The Protein Kinase Complement of the Human Genome. Science. 2002 Dec 6;298(5600):1912–34.

52. Cohen P. The regulation of protein function by multisite phosphorylation – a 25 year update. Trends Biochem Sci. 2000 Dec 1;25(12):596–601.

53. Miranda-Saavedra D, Barton GJ. Classification and functional annotation of eukaryotic protein kinases. Proteins Struct Funct Bioinforma. 2007 Jun 7;68(4):893–914.

54. Baltussen LL, Rosianu F, Ultanir SK. Kinases in synaptic development and neurological diseases. Prog Neuropsychopharmacol Biol Psychiatry. 2018 Jun;84:343–52.

55. Pearson G, Robinson F, Beers Gibson T, Xu BE, Karandikar M, Berman K, et al. Mitogen-activated protein (MAP) kinase pathways: regulation and physiological functions. Endocr Rev. 2001 Apr;22(2):153–83.

56. Kyosseva SV. Mitogen-Activated Protein Kinase Signaling. In: International Review of Neurobiology [Internet]. Elsevier; 2004 [cited 2022 May 22]. p. 201–20. Available from: https://linkinghub.elsevier.com/retrieve/pii/S0074774204590086

57. Lewis TS, Shapiro PS, Ahn NG. Signal Transduction through MAP Kinase Cascades. In: Advances in Cancer Research [Internet]. Elsevier; 1998 [cited 2022 May 22]. p. 49–139. Available from: https://linkinghub.elsevier.com/retrieve/pii/S0065230X08607654

58. Katz M, Amit I, Yarden Y. Regulation of MAPKs by growth factors and receptor tyrosine kinases. Biochim Biophys Acta. 2007 Aug;1773(8):1161–76.

59. Craig EA, Stevens MV, Vaillancourt RR, Camenisch TD. MAP3Ks as central regulators of cell fate during development. Dev Dyn. 2008;237(11):3102–14.

60. Fulda S, Gorman AM, Hori O, Samali A. Cellular Stress Responses: Cell Survival and Cell Death. Int J Cell Biol. 2010;2010:1–23.

61. Vabulas RM, Raychaudhuri S, Hayer-Hartl M, Hartl FU. Protein Folding in the Cytoplasm and the Heat Shock Response. Cold Spring Harb Perspect Biol. 2010 Dec;2(12):a004390.

62. Asih PR, Prikas E, Stefanoska K, Tan ARP, Ahel HI, Ittner A. Functions of p38 MAP Kinases in the Central Nervous System. Front Mol Neurosci. 2020 Sep 8;13:570586.

63. Thomas GM, Huganir RL. MAPK cascade signalling and synaptic plasticity. Nat Rev Neurosci. 2004 Mar;5(3):173–83.

64. Jordan BA, Fernholz BD, Boussac M, Xu C, Grigorean G, Ziff EB, et al. Identification and Verification of Novel Rodent Postsynaptic Density Proteins. Mol Cell Proteomics. 2004 Sep;3(9):857–71.

65. Peng J, Kim MJ, Cheng D, Duong DM, Gygi SP, Sheng M. Semiquantitative Proteomic Analysis of Rat Forebrain Postsynaptic Density Fractions by Mass Spectrometry. J Biol Chem. 2004 May;279(20):21003–11.

66. Trinidad JC, Thalhammer A, Specht CG, Lynn AJ, Baker PR, Schoepfer R. Quantitative Analysis of Synaptic Phosphorylation and Protein Expression*□S. :13.

67. Coba MP, Komiyama NH, Nithiananantharajah J, Kopanitsa MV, Indersmitten T, Skene NG, et al. TNiK Is Required for Postsynaptic and Nuclear Signaling Pathways and Cognitive Function. J Neurosci. 2012 Oct 3;32(40):13987–99.

68. Ayalew M, Le-Niculescu H, Levey DF, Jain N, Changala B, Patel SD, et al. Convergent functional genomics of schizophrenia: from comprehensive understanding to genetic risk prediction. Mol Psychiatry. 2012 Sep;17(9):887–905.

69. Leberer E, Dignard D, Harcus D, Thomas DY, Whiteway M. The protein kinase homologue Ste20p is required to link the yeast pheromone response G-protein beta gamma subunits to downstream signalling components. EMBO J. 1992 Dec;11(13):4815–24.

70. Ramer SW, Davis RW. A dominant truncation allele identifies a gene, STE20, that encodes a putative protein kinase necessary for mating in Saccharomyces cerevisiae. Proc Natl Acad Sci U S A. 1993 Jan 15;90(2):452–6.

71. Hutchison M, Berman KS, Cobb MH. Isolation of TAO1, a Protein Kinase That Activates MEKs in Stress-activated Protein Kinase Cascades. J Biol Chem. 1998 Nov;273(44):28625–32.

72. Wellcome Trust Case Control Consortium, McCarthy SE, Makarov V, Kirov G, Addington AM, McClellan J, et al. Microduplications of 16p11.2 are associated with schizophrenia. Nat Genet. 2009 Nov;41(11):1223–7.

73. Weiss LA, Shen Y, Korn JM, Arking DE, Miller DT, Fossdal R, et al. Association between Microdeletion and Microduplication at 16p11.2 and Autism. N Engl J Med. 2008 Feb 14;358(7):667–75.

74. Kumar RA, KaraMohamed S, Sudi J, Conrad DF, Brune C, Badner JA, et al. Recurrent 16p11.2 microdeletions in autism. Hum Mol Genet. 2007 Nov 7;17(4):628–38.

75. Niarchou M, Chawner SJRA, Doherty JL, Maillard AM, Jacquemont S, Chung WK, et al. Psychiatric disorders in children with 16p11.2 deletion and duplication. Transl Psychiatry. 2019 Jan 16;9:8.

76. Tassi E, Biesova Z, Di Fiore PP, Gutkind JS, Wong WT. Human JIK, a Novel Member of the STE20 Kinase Family That Inhibits JNK and Is Negatively Regulated by Epidermal Growth Factor. J Biol Chem. 1999 Nov;274(47):33287–95.

77. Yustein JT, Xia L, Kahlenburg JM, Robinson D, Templeton D, Kung HJ. Comparative studies of a new subfamily of human Ste20-like kinases: homodimerization, subcellular localization, and selective activation of MKK3 and p38. Oncogene. 2003 Sep 18;22(40):6129–41.

78. Hu C, Feng P, Yang Q, Xiao L. Clinical and Neurobiological Aspects of TAO Kinase Family in Neurodevelopmental Disorders. Front Mol Neurosci. 2021 Mar 24;14:655037.

79. Fang CY, Lai TC, Hsiao M, Chang YC. The Diverse Roles of TAO Kinases in Health and Diseases. Int J Mol Sci. 2020 Oct 10;21(20):7463.

80. Chen Z, Hutchison M, Cobb MH. Isolation of the Protein Kinase TAO2 and Identification of Its Mitogen-activated Protein Kinase/Extracellular Signal-regulated Kinase Kinase Binding Domain. J Biol Chem. 1999 Oct;274(40):28803–7.

81. Chen Z, Raman M, Chen L, Lee SF, Gilman AG, Cobb MH. TAO (Thousand-and-one Amino Acid) Protein Kinases Mediate Signaling from Carbachol to p38 Mitogen-activated Protein Kinase and Ternary Complex Factors. J Biol Chem. 2003 Jun;278(25):22278–83.

82. Raman M, Earnest S, Zhang K, Zhao Y, Cobb MH. TAO kinases mediate activation of p38 in response to DNA damage. EMBO J. 2007 Apr 18;26(8):2005–14.

83. Boggiano JC, Vanderzalm PJ, Fehon RG. Tao-1 Phosphorylates Hippo/MST Kinases to Regulate the Hippo-Salvador-Warts Tumor Suppressor Pathway. Dev Cell. 2011 Nov;21(5):888–95.

84. Plouffe SW, Meng Z, Lin KC, Lin B, Hong AW, Chun JV, et al. Characterization of Hippo Pathway Components by Gene Inactivation. Mol Cell. 2016 Dec;64(5):993–1008.

85. Yadav S, Oses-Prieto JA, Peters CJ, Zhou J, Pleasure SJ, Burlingame AL, et al. TAOK2 Kinase Mediates PSD95 Stability and Dendritic Spine Maturation through Septin7 Phosphorylation. Neuron. 2017 Jan;93(2):379–93.

86. Runge K, Cardoso C, De Chevigny A. Dendritic Spine Plasticity: Function and Mechanisms.

Front Synaptic Neurosci. 2020 Aug 28;12:36.

87. Peters A, Proskauer CC, Kaiserman-Abramof IR. THE SMALL PYRAMIDAL NEURON OF THE RAT CEREBRAL CORTEX. J Cell Biol. 1968 Dec 1;39(3):604–19.

88. Lai KO, Ip NY. Structural plasticity of dendritic spines: The underlying mechanisms and its dysregulation in brain disorders. Biochim Biophys Acta BBA - Mol Basis Dis. 2013 Dec;1832(12):2257–63.

89. Engert F, Bonhoeffer T. Dendritic spine changes associated with hippocampal long-term synaptic plasticity. Nature. 1999 May;399(6731):66–70.

90. Maletic-Savatic M, Malinow R, Svoboda K. Rapid Dendritic Morphogenesis in CA1 Hippocampal Dendrites Induced by Synaptic Activity. Science. 1999 Mar 19;283(5409):1923–7.

91. Matsuzaki M, Honkura N, Ellis-Davies GCR, Kasai H. Structural basis of long-term potentiation in single dendritic spines. Nature. 2004 Jun 17;429(6993):761–6.

92. Zhou Q, Homma KJ, Poo M ming. Shrinkage of Dendritic Spines Associated with Long-Term Depression of Hippocampal Synapses. Neuron. 2004 Dec;44(5):749–57.

93. MacGillavry HD, Hoogenraad CC. The internal architecture of dendritic spines revealed by super-resolution imaging: What did we learn so far? Exp Cell Res. 2015 Jul;335(2):180–6.

94. de Anda FC, Rosario AL, Durak O, Tran T, Gräff J, Meletis K, et al. An Autism Spectrum Disorder Susceptibility Gene, TAO2, is Important for Basal Dendrite Formation in the Neocortex. Nat Neurosci. 2012 Jun 10;15(7):1022–31.

95. Ultanir SK, Yadav S, Hertz NT, Oses-Prieto JA, Claxton S, Burlingame AL, et al. MST3 Kinase Phosphorylates TAO1/2 to Enable Myosin Va Function in Promoting Spine Synapse Development. Neuron. 2014 Dec 3;84(5):968–82.

96. Yasuda S, Tanaka H, Sugiura H, Okamura K, Sakaguchi T, Tran U, et al. Activity-Induced Protocadherin Arcadlin Regulates Dendritic Spine Number by Triggering N-Cadherin Endocytosis via TAO2β and p38 MAP Kinases. Neuron. 2007 Nov;56(3):456–71.

97. Need AC, Ge D, Weale ME, Maia J, Feng S, Heinzen EL, et al. A Genome-Wide Investigation of SNPs and CNVs in Schizophrenia. McCarthy MI, editor. PLoS Genet. 2009 Feb 6;5(2):e1000373.

98. Vysotskiy M, Zhong X, Miller-Fleming TW, Zhou D, Autism Working Group of the Psychiatric Genomics Consortium^, Bipolar Disorder Working Group of the Psychiatric Genomics Consortium^, et al. Integration of genetic, transcriptomic, and clinical data provides insight into 16p11.2

and 22q11.2 CNV genes. Genome Med. 2021 Dec;13(1):172.

99. Maillard AM, Ruef A, Pizzagalli F, Migliavacca E, Hippolyte L, Adaszewski S, et al. The 16p11.2 locus modulates brain structures common to autism, schizophrenia and obesity. Mol Psychiatry. 2015 Feb;20(1):140–7.

100. Rein B, Yan Z. 16p11.2 Copy Number Variations and Neurodevelopmental Disorders. Trends Neurosci. 2020 Nov;43(11):886–901.

101. Dennison CA, Legge SE, Pardiñas AF, Walters JTR. Genome-wide association studies in schizophrenia: Recent advances, challenges and future perspective. Schizophr Res. 2020 Mar 1;217:4–12.

102. Cardno AG, Gottesman II. Twin Studies of Schizophrenia: From Bow-and-Arrow Concordances to Star Wars Mx and Functional Genomics.

103. Stefansson H, Ophoff RA, Steinberg S, Andreassen OA, Cichon S, Rujescu D, et al. Common variants conferring risk of schizophrenia. Nature. 2009 Aug 6;460(7256):744–7.

104. Schizophrenia Working Group of the Psychiatric Genomics Consortium. Biological insights from 108 schizophrenia-associated genetic loci. Nature. 2014 Jul;511(7510):421–7.

105. Owen MJ, Sawa A, Mortensen PB. Schizophrenia. Lancet Lond Engl. 2016 Jul 2;388(10039):86–97.

106. Trubetskoy V, Panagiotaropoulou G, Awasthi S, Braun A, Kraft J, Skarabis N, et al. Mapping genomic loci implicates genes and synaptic biology in schizophrenia. Nature. 2022 Apr;604(7906):502–8.

107. Richter M, Murtaza N, Scharrenberg R, White SH, Johanns O, Walker S, et al. Altered TAOK2 activity causes autism-related neurodevelopmental and cognitive abnormalities through RhoA signaling. Mol Psychiatry. 2019;24(9):1329–50.

108. Stepan J, Heinz DE, Dethloff F, Bajaj T, Zellner A, Hafner K, et al. Hippo-released WWC1 facilitates AMPA receptor regulatory complexes for hippocampal learning. Cell Rep. 2022 Dec;41(10):111766.

109. Cheng J, Wang S, Dong Y, Yuan Z. The Role and Regulatory Mechanism of Hippo Signaling Components in the Neuronal System. Front Immunol. 2020 Feb 19;11:281.

110. Zygulska AL, Krzemieniecki K, Pierzchalski P. HIPPO PATHWAY - BRIEF OVERVIEW OF ITS RELEVANCE IN CANCER. :25.

111.   Meng Z, Moroishi T, Guan KL. Mechanisms of Hippo pathway regulation. Genes Dev. 2016 Jan 1;30(1):1–17.

112.   Panciera T, Azzolin L, Cordenonsi M, Piccolo S. Mechanobiology of YAP and TAZ in physiology and disease. Nat Rev Mol Cell Biol. 2017 Dec;18(12):758–70.

113.   Boopathy GTK, Hong W. Role of Hippo Pathway-YAP/TAZ Signaling in Angiogenesis. Front Cell Dev Biol [Internet]. 2019 [cited 2022 Oct 29];7. Available from: https://www.frontiersin.org/articles/10.3389/fcell.2019.00049

114.   Moon S, Yeon Park S, Woo Park H. Regulation of the Hippo pathway in cancer biology. Cell Mol Life Sci. 2018 Jul;75(13):2303–19.

115.   Ma S, Meng Z, Chen R, Guan KL. The Hippo Pathway: Biology and Pathophysiology. Annu Rev Biochem. 2019 Jun 20;88(1):577–604.

116.   Snigdha K, Gangwani KS, Lapalikar GV, Singh A, Kango-Singh M. Hippo Signaling in Cancer: Lessons From Drosophila Models. Front Cell Dev Biol. 2019 May 24;7:85.

117.   Fulford A, Tapon N, Ribeiro PS. Upstairs, downstairs: spatial regulation of Hippo signalling. Curr Opin Cell Biol. 2018 Apr;51:22–32.

118.   Mo JS, Yu FX, Gong R, Brown JH, Guan KL. Regulation of the Hippo–YAP pathway by protease-activated receptors (PARs). Genes Dev. 2012 Oct 1;26(19):2138–43.

119.   Zhao B, Wei X, Li W, Udan RS, Yang Q, Kim J, et al. Inactivation of YAP oncoprotein by the Hippo pathway is involved in cell contact inhibition and tissue growth control. Genes Dev. 2007 Nov 1;21(21):2747–61.

120.   Camargo FD, Gokhale S, Johnnidis JB, Fu D, Bell GW, Jaenisch R, et al. YAP1 Increases Organ Size and Expands Undifferentiated Progenitor Cells. Curr Biol. 2007 Dec;17(23):2054–60.

121.   Wang SP, Wang LH. Disease implication of hyper-Hippo signalling. Open Biol. 2016 Oct;6(10):160119.

122.   Mueller KA, Glajch KE, Huizenga MN, Wilson RA, Granucci EJ, Dios AM, et al. Hippo Signaling Pathway Dysregulation in Human Huntington's Disease Brain and Neuronal Stem Cells. Sci Rep. 2018 Jul 27;8:11355.

123.   Totaro A, Panciera T, Piccolo S. YAP/TAZ upstream signals and downstream responses. Nat Cell Biol. 2018 Aug;20(8):888–99.

124.   Li Y, Zhou H, Li F, Chan SW, Lin Z, Wei Z, et al. Angiomotin binding-induced activation

of Merlin/NF2 in the Hippo pathway. Cell Res. 2015 Jul;25(7):801–17.

125. Schlegelmilch K, Mohseni M, Kirak O, Pruszak J, Rodriguez JR, Zhou D, et al. Yap1 acts downstream of α-catenin to control epidermal proliferation. Cell. 2011 Mar 4;144(5):782–95.

126. Poon CLC, Lin JI, Zhang X, Harvey KF. The Sterile 20-like Kinase Tao-1 Controls Tissue Growth by Regulating the Salvador-Warts-Hippo Pathway. Dev Cell. 2011 Nov 15;21(5):896–906.

127. Paramasivam M, Sarkeshik A, Yates JR, Fernandes MJG, McCollum D. Angiomotin family proteins are novel activators of the LATS2 kinase tumor suppressor. Margolis B, editor. Mol Biol Cell. 2011 Oct;22(19):3725–33.

128. Wang W, Huang J, Wang X, Yuan J, Li X, Feng L, et al. PTPN14 is required for the density-dependent control of YAP1. Genes Dev. 2012 Sep 1;26(17):1959–71.

129. Wennmann DO, Schmitz J, Wehr MC, Krahn MP, Koschmal N, Gromnitza S, et al. Evolutionary and Molecular Facts Link the WWC Protein Family to Hippo Signaling. Mol Biol Evol. 2014 Jul;31(7):1710–23.

130. Yu FX, Zhao B, Panupinthu N, Jewell JL, Lian I, Wang LH, et al. Regulation of the Hippo-YAP pathway by G-protein coupled receptor signaling. Cell. 2012 Aug 17;150(4):780–91.

131. Yagi R, Chen LF, Shigesada K, Murakami Y, Ito Y. A WW domain-containing Yes-associated protein (YAP) is a novel transcriptional co-activator. EMBO J. 1999 May 4;18(9):2551–62.

132. Basu S, Totty NF, Irwin MS, Sudol M, Downward J. Akt Phosphorylates the Yes-Associated Protein, YAP, to Induce Interaction with 14-3-3 and Attenuation of p73-Mediated Apoptosis. Mol Cell. 2003 Jan;11(1):11–23.

133. Vassilev A, Kaneko KJ, Shu H, Zhao Y, DePamphilis ML. TEAD/TEF transcription factors utilize the activation domain of YAP65, a Src/Yes-associated protein localized in the cytoplasm. Genes Dev. 2001 May 15;15(10):1229–41.

134. Komuro A, Nagai M, Navin NE, Sudol M. WW Domain-containing Protein YAP Associates with ErbB-4 and Acts as a Co-transcriptional Activator for the Carboxyl-terminal Fragment of ErbB-4 That Translocates to the Nucleus. J Biol Chem. 2003 Aug;278(35):33334–41.

135. Zhao B, Ye X, Yu J, Li L, Li W, Li S, et al. TEAD mediates YAP-dependent gene induction and growth control. Genes Dev. 2008 Jul 15;22(14):1962–71.

136. Yamaguchi H, Taouk GM. A Potential Role of YAP/TAZ in the Interplay Between Metastasis and Metabolic Alterations. Front Oncol. 2020 Jun 11;10:928.

137.   Liu-Chittenden Y, Huang B, Shim JS, Chen Q, Lee SJ, Anders RA, et al. Genetic and pharmacological disruption of the TEAD–YAP complex suppresses the oncogenic activity of YAP. Genes Dev. 2012 Jun 15;26(12):1300–5.

138.   Song S, Xie M, Scott AW, Jin J, Ma L, Dong X, et al. A Novel YAP1 Inhibitor Targets CSC-Enriched Radiation-Resistant Cells and Exerts Strong Antitumor Activity in Esophageal Adenocarcinoma. Mol Cancer Ther. 2018 Feb 1;17(2):443–54.

139.   Kawamoto R, Nakano N, Ishikawa H, Tashiro E, Nagano W, Sano K, et al. Narciclasine is a novel YAP inhibitor that disturbs interaction between YAP and TEAD4. BBA Adv. 2021;1:100008.

140.   Li X, Li K, Chen Y, Fang F. The Role of Hippo Signaling Pathway in the Development of the Nervous System. Dev Neurosci. 2021;43(5):263–70.

141.   Zhao X, Moore D. Neural stem cells: developmental mechanisms and disease modeling. Cell Tissue Res. 2018 Jan;371(1):1–6.

142.   Faigle R, Song H. Signaling mechanisms regulating adult neural stem cells and neurogenesis. Biochim Biophys Acta. 2013 Feb;1830(2):2435–48.

143.   Yao M, Wang Y, Zhang P, Chen H, Xu Z, Jiao J, et al. BMP2-SMAD Signaling Represses the Proliferation of Embryonic Neural Stem Cells through YAP. J Neurosci. 2014 Sep 3;34(36):12039–48.

144.   Cao X, Pfaff SL, Gage FH. YAP regulates neural progenitor cell number via the TEA domain transcription factor. Genes Dev. 2008 Dec 1;22(23):3320–34.

145.   Rojek KO, Krzemień J, Doleżyczek H, Boguszewski PM, Kaczmarek L, Konopka W, et al. Amot and Yap1 regulate neuronal dendritic tree complexity and locomotor coordination in mice. PLoS Biol. 2019 May 1;17(5):e3000253.

146.   Huang Z, Hu J, Pan J, Wang Y, Hu G, Zhou J, et al. YAP stabilizes SMAD1 and promotes BMP2-induced neocortical astrocytic differentiation. Development. 2016 Jul 1;143(13):2398–409.

147.   Yuan Z, Becker E, Merlo P. Activation of FOXO1 by Cdk1 in cycling cells and postmitotic neurons. 2008 Mar 21 [cited 2023 Mar 18]; Available from: https://core.ac.uk/reader/59039739?utm_source=linkout

148.   Yuan Z, Lehtinen MK, Merlo P, Villén J, Gygi S, Bonni A. Regulation of Neuronal Cell Death by MST1-FOXO1 Signaling. J Biol Chem. 2009 Apr 24;284(17):11285–92.

149.   Qu J, Zhao H, Li Q, Pan P, Ma K, Liu X, et al. MST1 Suppression Reduces Early Brain

Injury by Inhibiting the NF-κB/MMP-9 Pathway after Subarachnoid Hemorrhage in Mice. Behav Neurol. 2018 Jun 19;2018:6470957.

150. Dey A, Varelas X, Guan KL. Targeting the Hippo pathway in cancer, fibrosis, wound healing and regenerative medicine. Nat Rev Drug Discov. 2020 Jul;19(7):480–94.

151. Nehme NT, Schmid JP, Debeurme F, André-Schmutz I, Lim A, Nitschke P, et al. MST1 mutations in autosomal recessive primary immunodeficiency characterized by defective naive T-cell survival. Blood. 2012 Apr 12;119(15):10.1182/blood-2011-09–378364.

152. Abdollahpour H, Appaswamy G, Kotlarz D, Diestelhorst J, Beier R, Schäffer AA, et al. The phenotype of human STK4 deficiency. Blood. 2012 Apr 12;119(15):3450–7.

153. Ramjee V, Li D, Manderfield LJ, Liu F, Engleka KA, Aghajanian H, et al. Epicardial YAP/TAZ orchestrate an immunosuppressive response following myocardial infarction. J Clin Invest. 127(3):899–911.

154. Moroishi T, Hayashi T, Pan WW, Fujita Y, Holt MV, Qin J, et al. The Hippo Pathway Kinases LATS1/2 Suppress Cancer Immunity. Cell. 2016 Dec 1;167(6):1525-1539.e17.

155. Lu L, Finegold MJ, Johnson RL. Hippo pathway coactivators Yap and Taz are required to coordinate mammalian liver regeneration. Exp Mol Med. 2018 Jan;50(1):e423.

156. Grijalva JL, Huizenga M, Mueller K, Rodriguez S, Brazzo J, Camargo F, et al. Dynamic alterations in Hippo signaling pathway and YAP activation during liver regeneration. Am J Physiol-Gastrointest Liver Physiol. 2014 Jul 15;307(2):G196–204.

157. Dong J. Differences in Yes-associated protein and mRNA levels in regenerating liver and hepatocellular carcinoma. Mol Med Rep [Internet]. 2011 Oct 19 [cited 2022 Nov 20]; Available from: http://www.spandidos-publications.com/10.3892/mmr.2011.640

158. Hogan BLM, Barkauskas CE, Chapman HA, Epstein JA, Jain R, Hsia CCW, et al. Repair and Regeneration of the Respiratory System: Complexity, Plasticity, and Mechanisms of Lung Stem Cell Function. Cell Stem Cell. 2014 Aug;15(2):123–38.

159. Liu Z, Wu H, Jiang K, Wang Y, Zhang W, Chu Q, et al. MAPK-Mediated YAP Activation Controls Mechanical-Tension-Induced Pulmonary Alveolar Regeneration. Cell Rep. 2016 Aug;16(7):1810–9.

160. Sun T, Huang Z, Zhang H, Posner C, Jia G, Ramalingam TR, et al. TAZ is required for lung alveolar epithelial cell differentiation after injury. JCI Insight. 4(14):e128674.

161. LaCanna R, Liccardo D, Zhang P, Tragesser L, Wang Y, Cao T, et al. Yap/Taz regulate

alveolar regeneration and resolution of lung inflammation. J Clin Invest. 129(5):2107–22.

162.   von Gise A, Lin Z, Schlegelmilch K, Honor LB, Pan GM, Buck JN, et al. YAP1, the nuclear target of Hippo signaling, stimulates heart growth through cardiomyocyte proliferation but not hypertrophy. Proc Natl Acad Sci U S A. 2012 Feb 14;109(7):2394–9.

163.   Xin M, Kim Y, Sutherland LB, Murakami M, Qi X, McAnally J, et al. Hippo pathway effector Yap promotes cardiac regeneration. Proc Natl Acad Sci U S A. 2013 Aug 20;110(34):13839–44.

164.   Lin Z, von Gise A, Zhou P, Gu F, Ma Q, Jiang J, et al. Cardiac-Specific YAP Activation Improves Cardiac Function and Survival in an Experimental Murine MI Model. Circ Res. 2014 Jul 18;115(3):354–63.

165.   Gujral TS, Kirschner MW. Hippo pathway mediates resistance to cytotoxic drugs. Proc Natl Acad Sci [Internet]. 2017 May 2 [cited 2023 Jan 18];114(18). Available from: https://pnas.org/doi/full/10.1073/pnas.1703096114

166.   Panizzutti B, Bortolasci CC, Spolding B, Kidnapillai S, Connor T, Richardson MF, et al. Transcriptional Modulation of the Hippo Signaling Pathway by Drugs Used to Treat Bipolar Disorder and Schizophrenia. Int J Mol Sci. 2021 Jul 2;22(13):7164.

167.   Rivas S, Antón IM, Wandosell F. WIP-YAP/TAZ as A New Pro-Oncogenic Pathway in Glioma. Cancers. 2018 Jun 9;10(6):191.

168.   Tanaka H, Homma H, Fujita K, Kondo K, Yamada S, Jin X, et al. YAP-dependent necrosis occurs in early stages of Alzheimer's disease and regulates mouse model pathology. Nat Commun. 2020 Jan 24;11:507.

169.   Lee JK, Shin JH, Hwang SG, Gwag BJ, McKee AC, Lee J, et al. MST1 functions as a key modulator of neurodegeneration in a mouse model of ALS. Proc Natl Acad Sci U S A. 2013 Jul 16;110(29):12066–71.

170.   Liu Y, Gu HY, Zhu J, Niu YM, Zhang C, Guo GL. Identification of Hub Genes and Key Pathways Associated With Bipolar Disorder Based on Weighted Gene Co-expression Network Analysis. Front Physiol. 2019 Aug 20;10:1081.

171.   Stepan J, Anderzhanova E, Gassen NC. Hippo Signaling: Emerging Pathway in Stress-Related Psychiatric Disorders? Front Psychiatry. 2018 Dec 21;9:715.

172.   Matsumoto H, Murakami Y, Kataoka K, Lin H, Connor KM, Miller JW, et al. Mammalian STE20-like kinase 2, not kinase 1, mediates photoreceptor cell death during retinal detachment. Cell Death Dis. 2014 May;5(5):e1269–e1269.

173.   Mao Y, Chen X, Xu M, Fujita K, Motoki K, Sasabe T, et al. Targeting TEAD/YAP-transcription-dependent necrosis, TRIAD, ameliorates Huntington's disease pathology. Hum Mol Genet. 2016 Sep 12;ddw303.

174.   Hoshino M, Qi M ling, Yoshimura N, Miyashita T, Tagawa K, Wada Y ichi, et al. Transcriptional repression induces a slowly progressive atypical neuronal death associated with changes of YAP isoforms and p73. J Cell Biol. 2006 Feb 13;172(4):589–604.

175.   Papassotiropoulos A, Stephan DA, Huentelman MJ, Hoerndli FJ, Craig DW, Pearson JV, et al. Common Kibra Alleles Are Associated with Human Memory Performance. Science. 2006 Oct 20;314(5798):475–8.

176.   Ma X, Mandausch FJ, Wu Y, Sahoo VK, Ma W, Leoni G, et al. Comprehensive split TEV based protein-protein interaction screening reveals TAOK2 as a key modulator of Hippo signalling to limit growth. Cell Signal. 2023 Oct 7;113:110917.

177.   Wehr MC, Laage R, Bolz U, Fischer TM, Grünewald S, Scheek S, et al. Monitoring regulated protein-protein interactions using split TEV. Nat Methods. 2006 Dec;3(12):985–93.

178.   Genevet A, Tapon N. The Hippo pathway and apico–basal cell polarity. Biochem J. 2011 Jun 1;436(2):213–24.

179.   Couzens AL, Knight JDR, Kean MJ, Teo G, Weiss A, Dunham WH, et al. Protein Interaction Network of the Mammalian Hippo Pathway Reveals Mechanisms of Kinase-Phosphatase Interactions. Sci Signal [Internet]. 2013 Nov 19 [cited 2023 Jan 19];6(302). Available from: https://www.science.org/doi/10.1126/scisignal.2004712

180.   Hauri S, Wepf A, van Drogen A, Varjosalo M, Tapon N, Aebersold R, et al. Interaction proteome of human Hippo signaling: modular control of the co-activator YAP1. Mol Syst Biol. 2013 Dec 20;9:713.

181.   Kwon Y, Vinayagam A, Sun X, Dephoure N, Gygi SP, Hong P, et al. The Hippo Signaling Pathway Interactome. Science. 2013 Nov 8;342(6159):737–40.

182.   Wang Y, Xu X, Maglic D, Dill MT, Mojumdar K, Ng PKS, et al. Comprehensive Molecular Characterization of the Hippo Signaling Pathway in Cancer. Cell Rep. 2018 Oct 30;25(5):1304-1317.e5.

183.   Herholt A. Development of a multiplexed RNAi-coupled sensor assay to study neuronal function on the large-scale [Internet]. Georg-August-University Göttingen; 2017 [cited 2023 Apr 7]. Available from: https://ediss.uni-goettingen.de/handle/11858/00-1735-0000-0023-3EB1-0

184.   McClure C, Cole KLH, Wulff P, Klugmann M, Murray AJ. Production and Titering of

Recombinant Adeno-associated Viral Vectors. J Vis Exp JoVE. 2011 Nov 27;(57):3348.

185.   pathwayProfiler - Systasy [Internet]. [cited 2022 Oct 10]. Available from: https://extassay.com/approach/pathway-profiler/

186.   Johnston GA. Advantages of an antagonist: bicuculline and other GABA antagonists: Bicuculline and other GABA antagonists. Br J Pharmacol. 2013 May;169(2):328–36.

187.   Korb E, Finkbeiner S. Arc in synaptic plasticity: from gene to behavior. Trends Neurosci. 2011 Nov;34(11):591–8.

188.   Wakita M, Kotani N, Akaike N. Tetrodotoxin abruptly blocks excitatory neurotransmission in mammalian CNS. Toxicon. 2015 Sep;103:12–8.

189.   Anderson WW, Swartzwelder HS, Wilson WA. The NMDA receptor antagonist 2-amino-5-phosphonovalerate blocks stimulus train-induced epileptogenesis but not epileptiform bursting in the rat hippocampal slice. J Neurophysiol. 1987 Jan 1;57(1):1–21.

190.   Rodríguez-Tornos FM, San Aniceto I, Cubelos B, Nieto M. Enrichment of Conserved Synaptic Activity-Responsive Element in Neuronal Genes Predicts a Coordinated Response of MEF2, CREB and SRF. Schönbach C, editor. PLoS ONE. 2013 Jan 31;8(1):e53848.

191.   Kawashima T, Okuno H, Nonaka M, Adachi-Morishima A, Kyo N, Okamura M, et al. Synaptic activity-responsive element in the Arc/Arg3.1 promoter essential for synapse-to-nucleus signaling in activated neurons. Proc Natl Acad Sci U S A. 2009 Jan 6;106(1):316–21.

192.   Kawashima T, Kitamura K, Suzuki K, Nonaka M, Kamijo S, Takemoto-Kimura S, et al. Functional labeling of neurons and their projections using the synthetic activity–dependent promoter E-SARE. Nat Methods. 2013 Sep;10(9):889–95.

193.   Herholt A, Brankatschk B, Kannaiyan N, Papiol S, Wichert SP, Wehr MC, et al. Pathway sensor-based functional genomics screening identifies modulators of neuronal activity. Sci Rep. 2018 Dec 4;8:17597.

194.   Mishra P, Pandey CM, Singh U, Gupta A, Sahu C, Keshri A. Descriptive Statistics and Normality Tests for Statistical Data. Ann Card Anaesth. 2019;22(1):67–72.

195.   Button KS, Ioannidis JPA, Mokrysz C, Nosek BA, Flint J, Robinson ESJ, et al. Power failure: why small sample size undermines the reliability of neuroscience. Nat Rev Neurosci. 2013 May;14(5):365–76.

196.   Kühnast C, Neuhäuser M. A note on the use of the non-parametric Wilcoxon-Mann-Whitney test in the analysis of medical studies. GMS Ger Med Sci. 2008 Apr 7;6:Doc02.

197. Benjamini Y, Hochberg Y. Controlling the False Discovery Rate: A Practical and Powerful Approach to Multiple Testing. J R Stat Soc Ser B Methodol. 1995;57(1):289–300.

198. Boggiano JC, Vanderzalm PJ, Fehon RG. Tao-1 Phosphorylates Hippo/MST Kinases to Regulate the Hippo-Salvador-Warts Tumor Suppressor Pathway. Dev Cell. 2011 Nov;21(5):888–95.

199. Plouffe SW, Meng Z, Lin KC, Lin B, Hong AW, Chun JV, et al. Characterization of Hippo Pathway Components by Gene Inactivation. Mol Cell. 2016 Dec;64(5):993–1008.

200. Kim Y, Jho E hoon. Regulation of the Hippo signaling pathway by ubiquitin modification. BMB Rep. 2018 Mar;51(3):143–50.

201. Yang Q, Zhao J, Chen D, Wang Y. E3 ubiquitin ligases: styles, structures and functions. Mol Biomed. 2021 Dec;2(1):23.

202. Pirkmajer S, Chibalin AV. Serum starvation: *caveat emptor*. Am J Physiol-Cell Physiol. 2011 Aug;301(2):C272–9.

203. Nourbakhsh K, Ferreccio AA, Bernard MJ, Yadav S. TAOK2 is an ER-localized kinase that catalyzes the dynamic tethering of ER to microtubules. Dev Cell. 2021 Dec 20;56(24):3321-3333.e5.

204. Simon J, Arthur C, Fong AL, Dwyer JM, Davare M, Reese E, et al. Mitogen- and Stress-Activated Protein Kinase 1 Mediates cAMP Response Element-Binding Protein Phosphorylation and Activation by Neurotrophins. J Neurosci. 2004 May 5;24(18):4324–32.

205. Alboni S, Tascedda F, Corsini D, Benatti C, Caggia F, Capone G, et al. Stress induces altered CRE/CREB pathway activity and BDNF expression in the hippocampus of glucocorticoid receptor-impaired mice. Neuropharmacology. 2011 Jun;60(7–8):1337–46.

206. Hirabayashi S, Nakagawa K, Sumita K, Hidaka S, Kawai T, Ikeda M, et al. Threonine 74 of MOB1 is a putative key phosphorylation site by MST2 to form the scaffold to activate nuclear Dbf2-related kinase 1. Oncogene. 2008 Jul 17;27(31):4281–92.

207. Praskova M, Xia F, Avruch J. MOBKL1A/MOBKL1B Phosphorylation by MST1 and MST2 Inhibits Cell Proliferation. Curr Biol. 2008 Mar;18(5):311–21.

208. Portmann T, Yang M, Mao R, Panagiotakos G, Ellegood J, Dolen G, et al. Behavioral Abnormalities and Circuit Defects in the Basal Ganglia of a Mouse Model of 16p11.2 Deletion Syndrome. Cell Rep. 2014 May;7(4):1077–92.

209. Ma X, Mandausch FJ, Wu Y, Sahoo VK, Ma W, Leoni G, et al. Comprehensive split TEV

based protein-protein interaction screening reveals TAOK2 as a key modulator of Hippo signalling to limit growth. Cell Signal. 2024 Jan 1;113:110917.

210. Cho YS, Jiang J. Hippo-Independent Regulation of Yki/Yap/Taz: A Non-canonical View. Front Cell Dev Biol. 2021 Apr 1;9:658481.

211. Adler JJ, Johnson DE, Heller BL, Bringman LR, Ranahan WP, Conwell MD, et al. Serum deprivation inhibits the transcriptional co-activator YAP and cell growth via phosphorylation of the 130-kDa isoform of Angiomotin by the LATS1/2 protein kinases. Proc Natl Acad Sci U S A. 2013 Oct 22;110(43):17368–73.

212. Zhao B, Li L, Lu Q, Wang LH, Liu CY, Lei Q, et al. Angiomotin is a novel Hippo pathway component that inhibits YAP oncoprotein. Genes Dev. 2011 Jan 1;25(1):51–63.

213. Dong J, Feldmann G, Huang J, Wu S, Zhang N, Comerford SA, et al. Elucidation of a Universal Size-Control Mechanism in Drosophila and Mammals. Cell. 2007 Sep 21;130(6):1120–33.

214. Dulovic-Mahlow M, Trinh J, Kandaswamy KK, Braathen GJ, Di Donato N, Rahikkala E, et al. De Novo Variants in TAOK1 Cause Neurodevelopmental Disorders. Am J Hum Genet. 2019 Jul 3;105(1):213–20.

215. Timm T, Li XY, Biernat J, Jiao J, Mandelkow E, Vandekerckhove J, et al. MARKK, a Ste20-like kinase, activates the polarity-inducing kinase MARK/PAR-1. EMBO J. 2003 Oct 1;22(19):5090–101.

216. Tavares IA, Touma D, Lynham S, Troakes C, Schober M, Causevic M, et al. Prostate-derived Sterile 20-like Kinases (PSKs/TAOKs) Phosphorylate Tau Protein and Are Activated in Tangle-bearing Neurons in Alzheimer Disease. J Biol Chem. 2013 May 24;288(21):15418–29.

217. Pennemann FL, Mussabekova A, Urban C, Stukalov A, Andersen LL, Grass V, et al. Cross-species analysis of viral nucleic acid interacting proteins identifies TAOKs as innate immune regulators. Nat Commun. 2021 Dec 1;12:7009.

218. Capra M, Nuciforo PG, Confalonieri S, Quarto M, Bianchi M, Nebuloni M, et al. Frequent Alterations in the Expression of Serine/Threonine Kinases in Human Cancers. Cancer Res. 2006 Aug 15;66(16):8147–54.

219. Lai TC, Fang CY, Jan YH, Hsieh HL, Yang YF, Liu CY, et al. Kinase shRNA screening reveals that TAOK3 enhances microtubule-targeted drug resistance of breast cancer cells via the NF-κB signaling pathway. Cell Commun Signal CCS. 2020 Oct 21;18:164.

220. Iizuka S, Quintavalle M, Navarro JC, Gribbin KP, Ardecky RJ, Abelman MM, et al. Serine-Threonine Kinase TAO3-Mediated Trafficking of Endosomes Containing the Invadopodia

Scaffold TKS5α Promotes Cancer Invasion and Tumor Growth. Cancer Res. 2021 Mar 15;81(6):1472–85.

221.   Sharma R, Fedorenko I, Spence PT, Sondak VK, Smalley KSM, Koomen JM. Activity-based protein profiling shows heterogeneous signaling adaptations to BRAF inhibition. J Proteome Res. 2016 Dec 2;15(12):4476–89.

222.   Li Y, He CL, Li WX, Zhang RX, Duan Y. Transcriptome analysis reveals gender-specific differences in overall metabolic response of male and female patients in lung adenocarcinoma. PLoS ONE. 2020 Apr 1;15(4):e0230796.

223.   Hennig EE, Mikula M, Rubel T, Dadlez M, Ostrowski J. Comparative kinome analysis to identify putative colon tumor biomarkers. J Mol Med Berl Ger. 2012;90(4):447–56.

224.   Fus-Kujawa A, Prus P, Bajdak-Rusinek K, Teper P, Gawron K, Kowalczuk A, et al. An Overview of Methods and Tools for Transfection of Eukaryotic Cells in vitro. Front Bioeng Biotechnol. 2021 Jul 20;9:701031.

225.   Boulton TG, Nye SH, Robbins DJ, Ip NY, Radzlejewska E, Morgenbesser SD, et al. ERKs: A family of protein-serine/threonine kinases that are activated and tyrosine phosphorylated in response to insulin and NGF. Cell. 1991 May 17;65(4):663–75.

226.   Cristo GD, Berardi N, Cancedda L, Pizzorusso T, Putignano E, Ratto GM, et al. Requirement of ERK Activation for Visual Cortical Plasticity. Science. 2001 Jun 22;292(5525):2337–40.

227.   Ma X. Thousand and one amino acid kinase 2 (TAOK2) modulates Hippo pathway activity and impacts on synaptic plasticity [Internet] [Text.PhDThesis]. Ludwig-Maximilians-Universität München; 2021 [cited 2024 Feb 27]. Available from: https://edoc.ub.uni-muenchen.de/29507/

228.   A Practical Guide to Immunocytochemistry - CH [Internet]. [cited 2024 Mar 2]. Available from: https://www.thermofisher.com/uk/en/home/references/newsletters-and-journals/bioprobes-journal-of-cell-biology-applications/bioprobes-issues-2011/bioprobes-66-october-2011/guide-to-immunocytochemistry.html

229.   Wang Y, Prywes R. Activation of the c-fos enhancer by the Erk MAP kinase pathway through two sequence elements: the c-fos AP-1 and p62TCF sites. Oncogene. 2000 Mar 9;19(11):1379–85.

230.   Pan D. The Hippo Signaling Pathway in Development and Cancer. Dev Cell. 2010 Oct 19;19(4):491–505.

231.   Harvey KF, Zhang X, Thomas DM. The Hippo pathway and human cancer. Nat Rev Cancer. 2013 Apr;13(4):246–57.

232. Kwon H, Kim J, Jho E. Role of the Hippo pathway and mechanisms for controlling cellular localization of YAP/TAZ. FEBS J. 2022 Oct;289(19):5798–818.

233. Meng Z, Moroishi T, Guan KL. Mechanisms of Hippo pathway regulation. Genes Dev. 2016 Jan 1;30(1):1–17.

234. Gu C, Chen J, Dang X, Chen C, Huang Z, Shen W, et al. Hippo Pathway Core Genes Based Prognostic Signature and Immune Infiltration Patterns in Lung Squamous Cell Carcinoma. Front Oncol. 2021 Apr 29;11:680918.

235. Fu M, Hu Y, Lan T, Guan KL, Luo T, Luo M. The Hippo signalling pathway and its implications in human health and diseases. Signal Transduct Target Ther. 2022 Nov 8;7:376.

236. Chen Z, Cobb MH. Regulation of Stress-responsive Mitogen-activated Protein (MAP) Kinase Pathways by TAO2. J Biol Chem. 2001 May;276(19):16070–5.

237. Zhou TJ, Sun LG, Gao Y, Goldsmith EJ. Crystal Structure of the MAP3K TAO2 Kinase Domain Bound by an Inhibitor Staurosporine. Acta Biochim Biophys Sin. 2006 Jun 1;38(6):385–92.

238. Anand R, Maksimoska J, Pagano N, Wong EY, Gimotty PA, Diamond SL, et al. Toward the Development of a Potent and Selective Organoruthenium Mammalian Sterile 20 Kinase Inhibitor. J Med Chem. 2009 Mar 26;52(6):1602–11.

239. Koo CY, Giacomini C, Reyes-Corral M, Olmos Y, Tavares IA, Marson CM, et al. Targeting TAO Kinases Using a New Inhibitor Compound Delays Mitosis and Induces Mitotic Cell Death in Centrosome Amplified Breast Cancer Cells. Mol Cancer Ther. 2017 Nov 1;16(11):2410–21.

240. Piala AT, Akella R, Potts MB, Dudics-Giagnocavo SA, He H, Wei S, et al. Discovery of novel TAOK2 inhibitor scaffolds from high-throughput screening. Bioorg Med Chem Lett. 2016 Aug;26(16):3923–7.

241. Scharrenberg R, Richter M, Johanns O, Meka DP, Rücker T, Murtaza N, et al. TAOK2 rescues autism-linked developmental deficits in a 16p11.2 microdeletion mouse model. Mol Psychiatry. 2022 Nov;27(11):4707–21.

242. Yang CE, Lee WY, Cheng HW, Chung CH, Mi FL, Lin CW. The antipsychotic chlorpromazine suppresses YAP signaling, stemness properties, and drug resistance in breast cancer cells. Chem Biol Interact. 2019 Apr;302:28–35.

243. Davood ZA, Shamsi S, Ghaedi H, Sahand RI, Mojtaba G, Mahdi T, et al. Valproic acid may exerts its cytotoxic effect through rassf1a expression induction in acute myeloid leukemia.

Tumor Biol. 2016 Aug;37(8):11001–6.

244.   Höffken V, Hermann A, Pavenstädt H, Kremerskothen J. WWC Proteins: Important Regulators of Hippo Signaling in Cancer. Cancers. 2021 Jan 15;13(2):306.

245.   Sourbier C, Liao PJ, Ricketts CJ, Wei D, Yang Y, Baranes SM, et al. Targeting loss of the Hippo signaling pathway in NF2-deficient papillary kidney cancers. Oncotarget. 2018 Jan 10;9(12):10723–33.

246.   Deng F, Peng L, Li Z, Tan G, Liang E, Chen S, et al. YAP triggers the Wnt/β-catenin signalling pathway and promotes enterocyte self-renewal, regeneration and tumorigenesis after DSS-induced injury. Cell Death Dis. 2018 Feb 2;9(2):153.

247.   Ouyang T, Meng W, Li M, Hong T, Zhang N. Recent Advances of the Hippo/YAP Signaling Pathway in Brain Development and Glioma. Cell Mol Neurobiol. 2020 May;40(4):495–510.

248.   Wang S, Zhou L, Ling L, Meng X, Chu F, Zhang S, et al. The Crosstalk Between Hippo-YAP Pathway and Innate Immunity. Front Immunol. 2020 Feb 27;11:323.

8.   Publication

This thesis contributed to the following publication:

Ma X, Mandausch FJ, Wu Y, Sahoo VK, Ma W, Leoni G, **Hostiuc M**, Wintgens JP, Qiu J, Kannaiyan N, Rossner MJ, Wehr MC. Comprehensive split TEV based protein-protein interaction screening reveals TAOK2 as a key modulator of Hippo signalling to limit growth. Cell Signal. 2024 Jan;113:110917. doi: 10.1016/j.cellsig.2023.110917. Epub 2023 Oct 7. PMID: 37813295.